

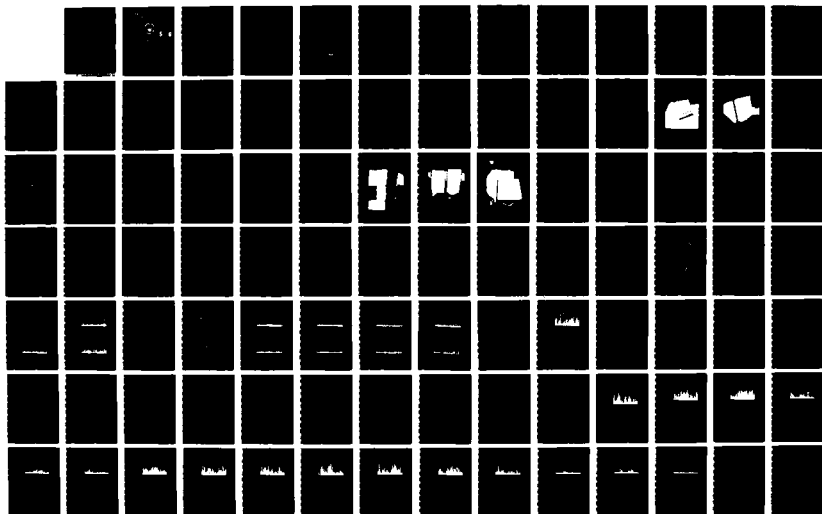
AD-A184 877

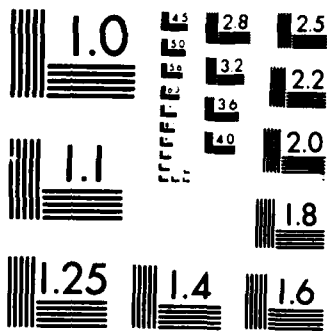
DEVELOPMENT OF AN ACOUSTIC ECHOSOUNDER FOR DETECTION OF 1/2
LOWER LEVEL ATMOSPHERIC TURBULENCE(U) NAVAL
POSTGRADUATE SCHOOL MONTEREY CA F J WEINGARTNER JUN 87

UNCLASSIFIED

F/G 4/2

NL





MICROCOPY RESOLUTION TEST CHART
NATIONAL BUREAU OF STANDARDS-1963-A

AD-A184 877

DTIC FILE COPY

2

NAVAL POSTGRADUATE SCHOOL
Monterey, California



DTIC
ELECTE
OCT 02 1987
S D
D

THESIS

DEVELOPMENT OF AN ACOUSTIC ECHOSOUNDER
FOR DETECTION OF
LOWER LEVEL ATMOSPHERIC TURBULENCE

by

Frank Joseph Weingartner

June 1987

Thesis Advisor:

D. L. Walters

Approved for public release; distribution is unlimited

REPORT DOCUMENTATION PAGE

1a REPORT SECURITY CLASSIFICATION Unclassified			1b RESTRICTIVE MARKINGS		
2a SECURITY CLASSIFICATION AUTHORITY			3 DISTRIBUTION/AVAILABILITY OF REPORT Approved for public release; distribution is unlimited		
2b DECLASSIFICATION/DOWNGRADING SCHEDULE			4 PERFORMING ORGANIZATION REPORT NUMBER(S)		
4 PERFORMING ORGANIZATION REPORT NUMBER(S)			5 MONITORING ORGANIZATION REPORT NUMBER(S)		
6a NAME OF PERFORMING ORGANIZATION Naval Postgraduate School		6b OFFICE SYMBOL (if applicable) 61	7a NAME OF MONITORING ORGANIZATION Naval Postgraduate School		
6c ADDRESS (City, State, and ZIP Code) Monterey, California 93943-5000			7b ADDRESS (City, State, and ZIP Code) Monterey, California 93943-5000		
8a NAME OF FUNDING/SPONSORING ORGANIZATION		8b OFFICE SYMBOL (if applicable)	9 PROCUREMENT INSTRUMENT IDENTIFICATION NUMBER		
8c ADDRESS (City, State, and ZIP Code)			10 SOURCE OF FUNDING NUMBERS		
		PROGRAM ELEMENT NO	PROJECT NO	TASK NO	WORK UNIT ACCESSION NO
11 TITLE (include Security Classification) DEVELOPMENT OF AN ACOUSTIC ECHOSOUNDER FOR DETECTION OF LOWER LEVEL ATMOSPHERIC TURBULENCE					
12 PERSONAL AUTHOR(S) Weingartner, Frank J.					
13a TYPE OF REPORT Master's Thesis		13b TIME COVERED FROM _____ TO _____		14 DATE OF REPORT (Year, Month Day) 1987 June	15 PAGE COUNT 98
16 SUPPLEMENTARY NOTATION					
17 COSATI CODES			18 SUBJECT TERMS (Continue on reverse if necessary and identify by block number)		
FIELD	GROUP	SUB-GROUP	Acoustic Radar, Echosounder, Acoustic Sounder, Acoustic Array, Atmospheric Turbulence Profiles		
19 ABSTRACT (Continue on reverse if necessary and identify by block number)					
<p>Atmospheric density fluctuations induce phase perturbations that degrade the spatial coherence of a laser beam propagating through the atmosphere. These degradations spread the laser beam and alter the centroid and intensity profile stochastically. Turbulent conditions arising from various environmental situations and meteorological phenomena are found at virtually all levels of the atmosphere. A substantial fraction of the optical turbulence along a vertical path arises from the surface heat flux within the first 100-200 meters above the ground.</p> <p>This thesis seeks to measure and analyze these turbulent layers. A high frequency acoustic echosounder was developed to analyze atmospheric turbulence within the first 100-200 meters above the ground with extremely high accuracy. The echosounder design incorporated a 25 element, square, planar array housed within a lead and foam insulated, acoustic shroud. This acoustic echosounder was employed to collect real-time, low level atmospheric data at two sites. This data</p>					
20 DISTRIBUTION/AVAILABILITY OF ABSTRACT <input checked="" type="checkbox"/> UNCLASSIFIED/UNLIMITED <input type="checkbox"/> SAME AS RPT <input type="checkbox"/> DTIC USERS			21 ABSTRACT SECURITY CLASSIFICATION Unclassified		
22a NAME OF RESPONSIBLE INDIVIDUAL Donald L. Walters			22b TELEPHONE (include Area Code) 408-646-2267	22c OFFICE SYMBOL 61We	

19. (continued)

should prove useful in determining whether the performance of laser and electro-optical systems could be increased by raising sensors and transmitters well above the local turbulent layer through the use of towers or other such structures.

f

Approved for public release; distribution is unlimited.

Development of an Acoustic Echosounder for
Detection of Lower Level Atmospheric Turbulence

by

Frank Joseph Weingartner
Lieutenant, United States Navy
B.A., Northwestern University, 1981

Submitted in partial fulfillment of the
requirements for the degree of

MASTER OF SCIENCE IN PHYSICS


from the

NAVAL POSTGRADUATE SCHOOL
June 1987


Author:

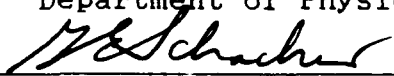

Frank J. Weingartner

Approved by:


Donald L. Walters, Thesis Advisor


Edmund A. Milne, Second Reader


Karlheinz E. Woehler, Chairman,
Department of Physics


Gordon E. Schacher, Dean of Science and
Engineering

ABSTRACT

Atmospheric density fluctuations induce phase perturbations that degrade the spatial coherence of a laser beam propagating through the atmosphere. These degradations spread the laser beam and alter the centroid and intensity profile stochastically. Turbulent conditions arising from various environmental situations and meteorological phenomena are found at virtually all levels of the atmosphere. A substantial fraction of the optical turbulence along a vertical path arises from the surface heat flux within the first 100-200 meters above the ground.

This thesis seeks to measure and analyze these turbulent layers. A high frequency acoustic echosounder was developed to analyze atmospheric turbulence within the first 100-200 meters above the ground with extremely high accuracy. The echosounder design incorporated a 25 element, square, planar array housed within a lead and foam insulated, acoustic shroud. This acoustic echosounder was employed to collect real-time, low level atmospheric data at two sites. This data should prove useful in determining whether the performance of laser and electro-optical systems could be increased by raising sensors and transmitters well above the local turbulent layer through the use of towers or other such structures.

TABLE OF CONTENTS

I.	INTRODUCTION.....	7
II.	BACKGROUND.....	10
III.	SYSTEM DESIGN AND EQUIPMENT DEVELOPMENT.....	15
	A. SPEAKERS.....	15
	B. ACOUSTIC ARRAY.....	18
	C. ENCLOSURE.....	24
	D. ADDITIONAL HARDWARE.....	35
	E. SOFTWARE.....	40
IV.	DATA ANALYSIS.....	41
	A. ECHOSOUNDER PERFORMANCE.....	41
	B. SITE EVALUATION.....	49
V.	CONCLUSIONS AND RECOMMENDATIONS.....	64
	APPENDIX A LINEAR ARRAY PROGRAM.....	66
	APPENDIX B LCDR BUTLER'S BEAM PATTERN PROGRAM.....	68
	APPENDIX C ECHOSOUNDER SOFTWARE.....	72
	APPENDIX D ECHOSOUNDER OUTPUT.....	78
	LIST OF REFERENCES.....	94
	INITIAL DISTRIBUTION LIST.....	97



Accession For	
NTIS CRA&I	<input checked="" type="checkbox"/>
DTIC TAB	<input type="checkbox"/>
Unannounced	<input type="checkbox"/>
Justification	
By _____	
Distributor /	
Availability Codes	
Dist	Avail and/or Special
A-1	

ACKNOWLEDGEMENTS

I would like to express my deepest gratitude and heartfelt thanks to those who, through their assistance and encouragement, made this work possible. First to Dr. Donald Walters, my thesis advisor who was always available for guidance, advice and direction. Additionally, I would like to express sincere thanks and appreciation to LT. Michael Wroblewski, my very good friend and colleague in the joint development of this high speed, computer controlled and monitored echosounder. I would also like to thank my fiancée, Karen and parents, Frank and Sara who provided unending support and encouragement throughout the past two and one quarter years.

I. INTRODUCTION

A coherent laser beam propagating through the atmosphere is very susceptible to numerous turbulent-dependent processes. As electromagnetic waves transit the turbulent regions, atmospheric irregularities randomize the amplitude and phase of the wave. A high resolution acoustic profiler was designed and developed to quantify the altitude dependence of these atmospheric disturbances. Acoustic energy is more susceptible to these irregularities than electromagnetic waves. Historically acoustic sounders have proven to be the best means of providing high resolution atmospheric turbulence profiles within the first 500 to 1000 meters above the ground. Acoustic echosounders are frequently used to detect and measure atmospheric density and velocity fluctuations resulting from wind shears, convection, and temperature inversions.

Presently two optical parameters, the spatial coherence length (r_0) and the isoplanatic angle (θ_0) are measures of the perturbation of electromagnetic waves propagating through the atmosphere, and are measured very reliably by optical systems developed by Walters [Refs. 1 and 2]. Although these systems measure a line integral of the atmospheric optical turbulence with high accuracy, a major drawback of each system is that no provision is provided

for determining the height of the atmospheric disruptions. If these disturbances are found to exist very near the surface, it may be possible to negate their effect by elevating sensors and transmitters or altering the surface heat flux to suppress the generation of turbulence.

This thesis deals with the design, construction and implementation of a high frequency, acoustic echosounder which will accurately analyze the atmospheric density fluctuations within approximately the first 200 meters of the atmosphere. As this project is a product of the research and efforts of two students, the work was appropriately divided. My particular task was concentrated in the actual design and hardware development of the echosounder. My colleague, LT. Michael Wroblewski [Ref. 3], dedicated his efforts toward software development and data display, analysis and storage.

The echosounder developed and discussed herein utilizes a 25 speaker, square, planar antenna array enclosed within an acoustically absorbent shroud comprised of lead and foam insulation inside a sturdy plywood framework. This antenna array was employed as both the transmitter and receiver of the acoustic signal. A computer controlled function generator transmits an acoustic pulse through the antenna array. Additional electronic components incorporated within the overall echosounder system are used to amplify, digitize, display, analyze and ultimately store the return

signal. Over time the received signal data is used to produce a quantitative, three dimensional map of the atmospheric turbulence.

Acoustic echosounders have been developed and in use for many years and have proven to be a valuable probe for analyzing the structure and dynamics of the lower atmosphere [Refs. 4 through 7]. Devices similar to ours have been used to obtain profiles of the atmospheric density and temperature fluctuations [Refs. 8 and 9]. Our device excels by utilizing a high speed HP217 computer to control and monitor the echosounder. This enables us to obtain real-time data collection and analysis with the ability to store and reproduce the atmospheric profile plots at will. This information should help quantify the effects of low level turbulence on electro-optical systems performance. It may then be possible to negate these turbulent effects by simply mounting sensors and transmitters well above the turbulent layers or by adaptive optics.

This thesis discusses the development of a high frequency, 5KHz, acoustic echosounder, the criteria involved in the actual designs of both the acoustic array and the acoustically absorbent enclosure, and the selection and function of all the associated component parts of the echosounder system. Finally the operational success of the system will be discussed and the output data analyzed.

II. BACKGROUND

Acoustic echosounders probe the atmosphere by transmitting a pulse of acoustic power which is subsequently scattered back from the atmosphere by temperature and velocity inhomogeneities. The echosounder (echosonde) equation, often referred to as the radar equation in meteorology, is used to determine the backscattered acoustic power. This equation is summarized by Neff in Reference 10 and is based upon the work of Tatarski [Ref. 11] and Little [Ref. 5].

$$P_R = E_R [P_T E_T] [\exp(-2\alpha R)] [\sigma_0(R, f)] [\frac{1}{2} c \tau] [A G R^{-2}]$$

where

P_R is the electrical power returned from a range R .

P_T is the electrical power transmitted at frequency f .

E_R is the efficiency of conversion from acoustic power to electrical power by the transducer.

E_T is the efficiency of conversion from electrical power to acoustic power by the transducer.

$\exp(-2\alpha R)$ is the round trip power loss due to attenuation where α is the average attenuation (meters⁻¹) to the scattering volume at the range R (meters).

$\sigma_0(R, f)$ is the scattering cross section per unit volume at a distance R and frequency f ,

c is the local speed of sound (meters/second),

τ is the pulse length (seconds),

A is the aperture area of the antenna (meters²),

R is the range (meters), and

G is the effective-aperture factor of the antenna.

Empirically measuring or calculating the values for all other terms, one can use this equation to determine $\sigma(R, f)$, the scattering cross section per unit volume; that is, the fraction of incident power backscattered per unit distance into a unit solid angle at a frequency f. Based upon experimental results, Tatarski [Ref. 11] expresses the acoustic backscatter cross section per unit volume, $\sigma(R, f)$, by,

$$\sigma(R, f) = 0.0039 k^{1/3} \frac{C\tau^2}{T_0^2},$$

where

$k = 2\pi/\lambda$ is the incident acoustic wavenumber at wavelength λ ,

T_0 is the local mean temperature in degrees Kelvin, and

$C\tau^2$ is the temperature structure parameter.

Combining this equation with the echosonde equation, one obtains a volume-averaged measure of $C\tau^2$.

$$C\tau^2 = \frac{1}{0.0039} \frac{1}{ERET} T_0^2 k^{-1/3} \frac{2}{c\tau} \frac{1}{AG} \frac{P_R}{P_T} R^2 \exp(2\alpha R)$$

Hall and Wescott [Ref. 12] calculated a beam-shape compensation factor of 0.40 for a piston source antenna with a uniformly illuminated square aperture. This value is the same as the effective-aperture factor, G and can be substituted into the above equation. Approximating the aperture area of the antenna to be equivalent to 25 times the aperture area of a single speaker having a diameter of 7.620 centimeters, we get a value of 0.1140 square meters. Combining these values with the numerical constants in the above equation, we can simplify the equation for C_T^2 .

$$C_T^2 = 11245 \frac{1}{E_R E_T} T_0^2 k^{-1/3} \frac{1}{c\tau} \frac{P_R}{P_T} R^2 \exp(2\alpha R)$$

The efficiency of conversion factors for our echosounder were determined with the use of an IVIE Electronics IE-30A Audio Analyzer Sound Level Meter, a HP3314A Function Generator, a HP3561A Dynamic Signal Analyzer, a reference speaker, the acoustic array and the Naval Postgraduate School anechoic chamber. The function generator was used to transmit a 1.0 volt, 5.0 KHz, sinusoidal signal through the reference speaker. The acoustic array was employed as a receiver and was aligned along the centroid of the main lobe of the reference speaker signal. With the acoustic array in position, the sound level meter was used to determine the total power

available for reception by the acoustic array; that is, the total power actually ensounded within the solid angle of the acoustic array. Ten independent measurements were made with the sound level meter and then averaged to yield a power value of 73.7 dB. Using a conversion factor and the array aperture area determined above, the total acoustical power, P_a , available at the acoustic array is given by the equation below.

$$P_a = 107.37 \cdot (1 \cdot 10^{-12} \text{ Watts / m}^2) \cdot (0.11401 \text{ m}^2)$$

or,

$$P_a = 2.67 \cdot 10^{-6} \text{ Watts}$$

The dynamic signal analyzer was then used to measure the actual power received by the acoustic array and converted into electrical power. Four independent measurements were recorded and averaged to yield a value of 4.035 mV_{rms}. The acoustic array impedance was previously measured and determined to be 12.1 ± 0.4 Ω. These values were used in the following equation to determine P_e , the total electrical power converted by the acoustic array.

$$P_e = \frac{(4.035 \cdot 10^{-3} \text{ V}_{rms})^2}{12.1 \Omega} = 1.34 \cdot 10^{-6} \text{ Watts}$$

The efficiency of conversion factor for acoustic to

electrical power is the ratio of P_a to P_e , or,

$$E_R = \frac{1.34 \cdot 10^{-6} \text{ Watts}}{2.67 \cdot 10^{-6} \text{ Watts}} = 0.503 \quad .$$

The value for the efficiency of conversion for electrical to acoustic power, E_R , is not readily calculatable with the equipment at hand. However, based upon the design of the speakers used, the values for E_R and E_T should be approximately equal. Furthermore, allowing for experimental error especially in the reading of the sound level meter, the best accuracy for the values of E_R and E_T is 0.5 ± 0.1 . Substituting conversion factor values of 0.5 into the above equation, we can further simplify the equation for C_T^2 .

$$C_T^2 = 44980 \text{ k}^{-1/3} \frac{T_0^2}{c\tau} \frac{P_R}{P_T} R^2 \exp(2\alpha R)$$

The above equation was incorporated into a computer program that provides the system control, data acquisition and data processing techniques [Ref. 3]. The reduced data was then used to measure the temperature structure parameter as a function of time of day and altitude for various sites.

III. SYSTEM DESIGN AND EQUIPMENT DEVELOPMENT

A. SPEAKERS

In the design of our echosounder, it was determined that a rapid decay time was required to obtain accurate short range information. Weight restrictions involved with equipment transportation plus high efficiency in the 2KHz to 5KHz range led to our decision to use piezo ceramic speakers. The Motorola KSN 1005A speaker was selected based on these requirements and the specifications charted in the Motorola catalog [Ref. 13] and reproduced below in Figures 1 through 3.

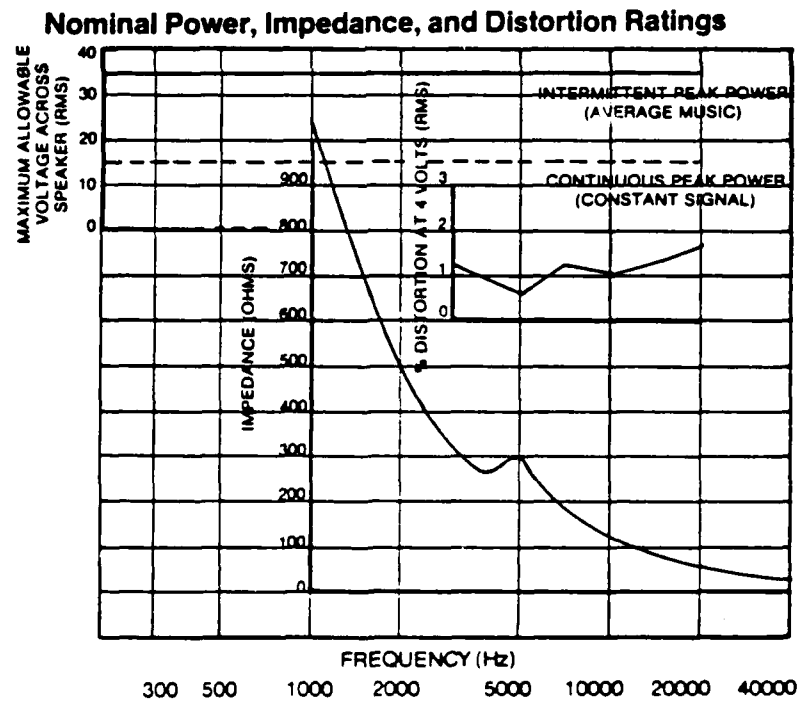


Fig. 1. Speaker Ratings

Typical Frequency Response

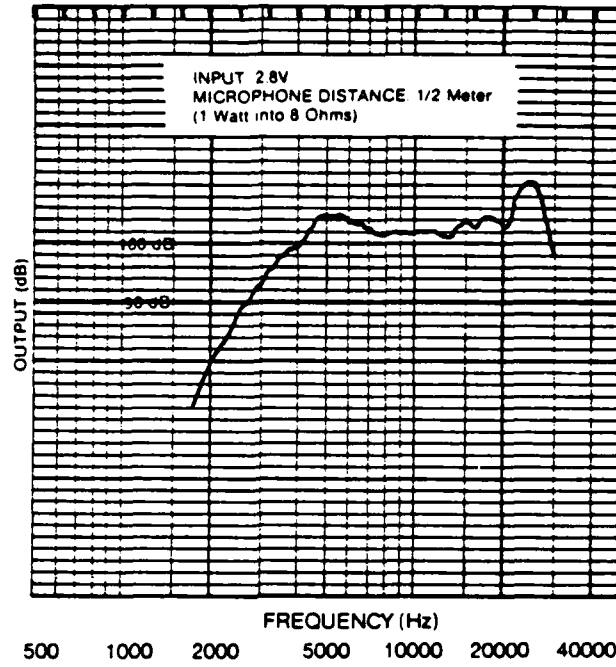


Fig. 2. Speaker Frequency Response

Dimensions: KSN 1005A, KSN 1003A

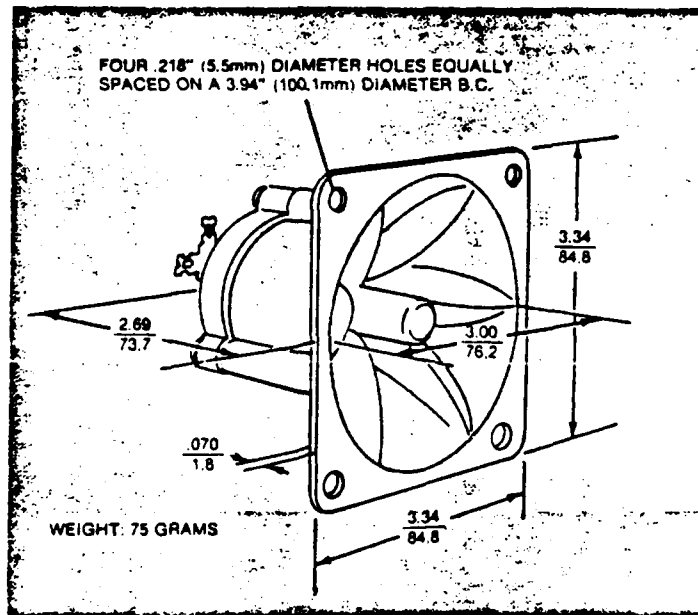


Fig. 3. Speaker Dimensions

These charts indicate that a maximum response for our speakers occurs at a resonant frequency of 5000 Hertz. This frequency was used as the baseline from which all our measurements were made.

Using the speakers in an anechoic chamber, the average e^{-1} voltage decay time was measured to be approximately 900 μ sec (Fig. 4). This decay time translates into a sound propagation distance of just over 15.0 centimeters (at STP) from the speakers. Considering our requirements, this speaker was ideally suited to serve our purpose.

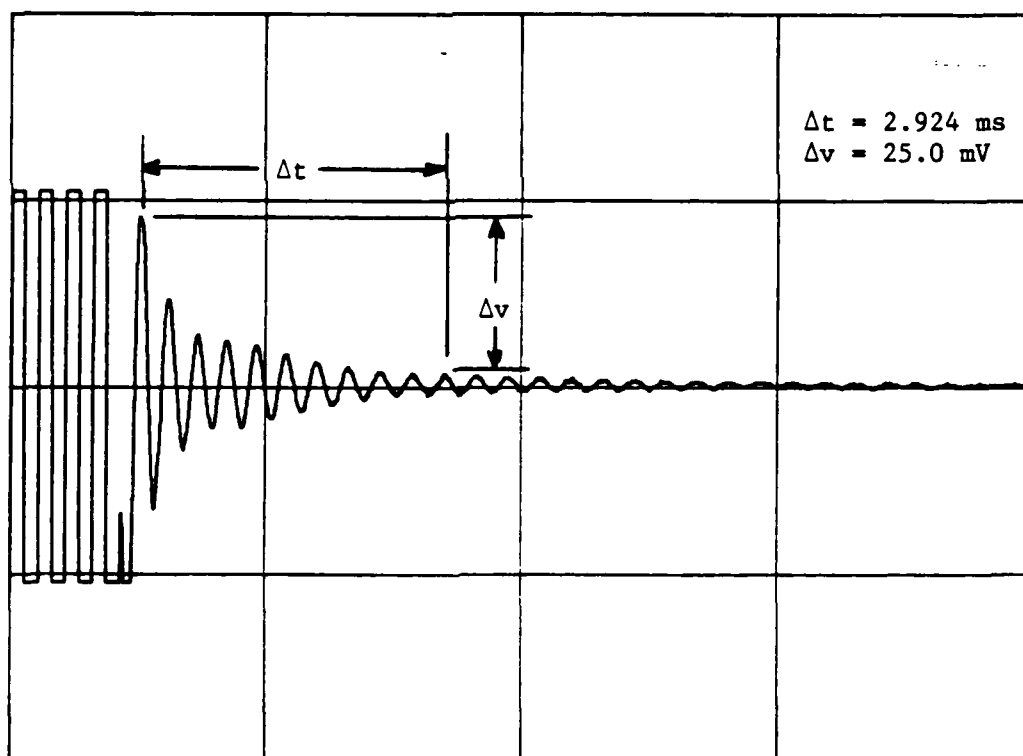


Fig. 4. Speaker Decay Time Trace

B. ACOUSTIC ARRAY

Our next consideration was the echosounder array pattern. Ideally, the acoustic sources should be placed exactly one half wavelength apart. At a frequency of 5000 Hertz, this would require spacings of 3.4 centimeters (at STP) which is physically impossible for the speakers we have chosen. The closest possible spacing was 7.62 centimeters between sources after shaving off the flange of the horn (Fig. 3).

From Kinsler, et al. [Ref. 14: p. 195], the equation for the directionality factor of a simple line array is derived as:

$$H(N, \theta) = \left| \frac{1}{N} \frac{\sin \left(\frac{N}{2} kd \sin \theta \right)}{\sin \left(\frac{1}{2} kd \sin \theta \right)} \right| ,$$

where

k is the wave number ($2\pi/\lambda$),

d is the distance between sources,

N is the number of sources, and

θ is the angle measured from a line perpendicular to the array to the direction of interest.

However, this equation assumes simple point sources which does not accurately describe the speakers we have chosen. It was necessary to couple this equation to the

directionality factor for a piston source which is also identified in Kinsler, et al. [Ref. 14: p. 108].

$$D(\theta) = \left| \frac{2 J_1 (ka \sin \theta)}{ka \sin \theta} \right| ,$$

where

k is the wave number,

a is the radius of the piston source,

θ is the angle measured from a line perpendicular to the array to the direction of interest, and

J_1 is a first order Bessel function.

These two equations were combined to produce the equation of directionality for a linear array of piston sources, $L(N,\theta)$, by simple multiplication.

$$L(N,\theta) = H(N,\theta) \cdot D(\theta) ,$$

This equation was incorporated into a computer program [Appendix A] and used to generate linear array patterns for varying numbers of piston sources (Figs. 5 through 9).

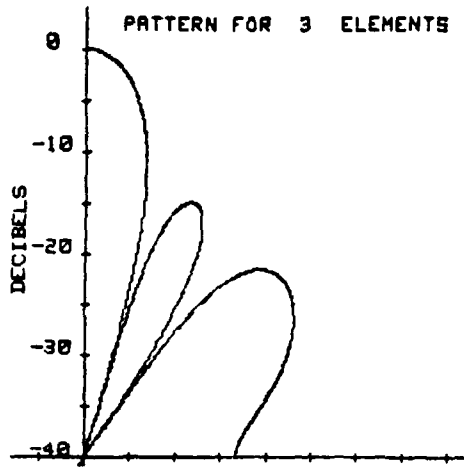


Fig. 5. Three Element Array

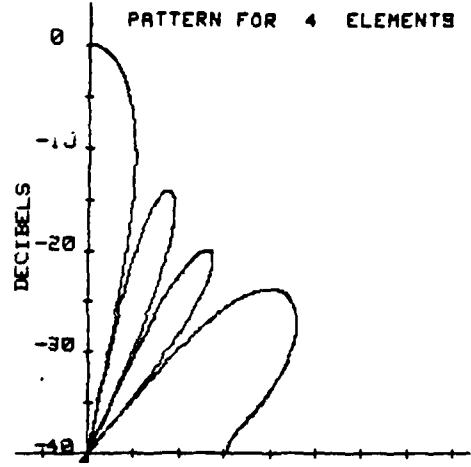


Fig. 6. Four Element Array

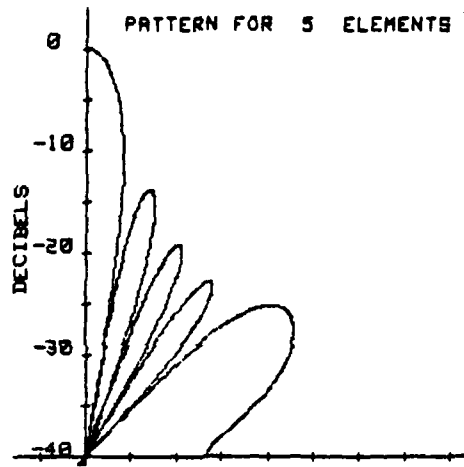


Fig. 7. Five Element Array

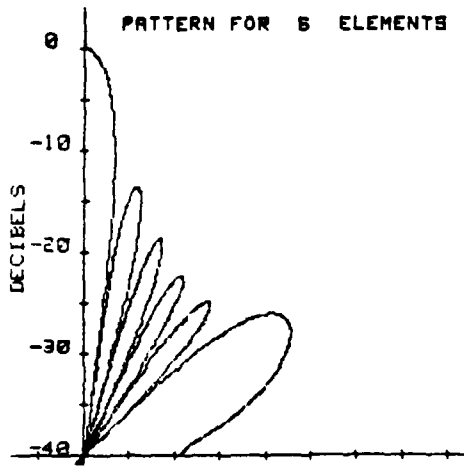


Fig. 8. Six Element Array

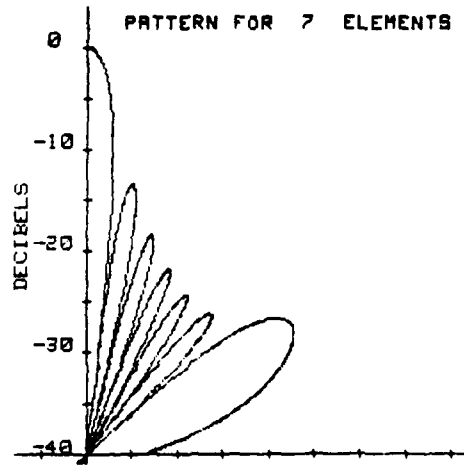


Fig. 9. Seven Element Array

It was concluded from these plots of the linear array beam patterns for varying numbers of piston sources that five linear elements would provide the best combination of forward directionality, sidelobe suppression, physical size, and a relatively low cost. Then, in order to enhance both array efficiency and symmetry, we settled on a five by five element array design with 7.62 centimeter spacing between speakers in both the vertical and horizontal directions.

After we verified the manufacturer's polarity designation for 35 speakers and inspected each of these speakers for physical defects and loose wiring connections, we obtained Lissajous plots for each individual speaker. Figure 10 represents a typical Lissajous plot for one of the speakers incorporated into the five by five element array. Based upon the speaker's output to input voltage ratios as illustrated by these Lissajous plots, we were able to rank all of our speakers by signal efficiency. It was based upon this criteria that we selected the 25 most efficient speakers for use in the five by five element array, placing the best speakers at the center and subsequent ranking speakers further toward the sides and corners.

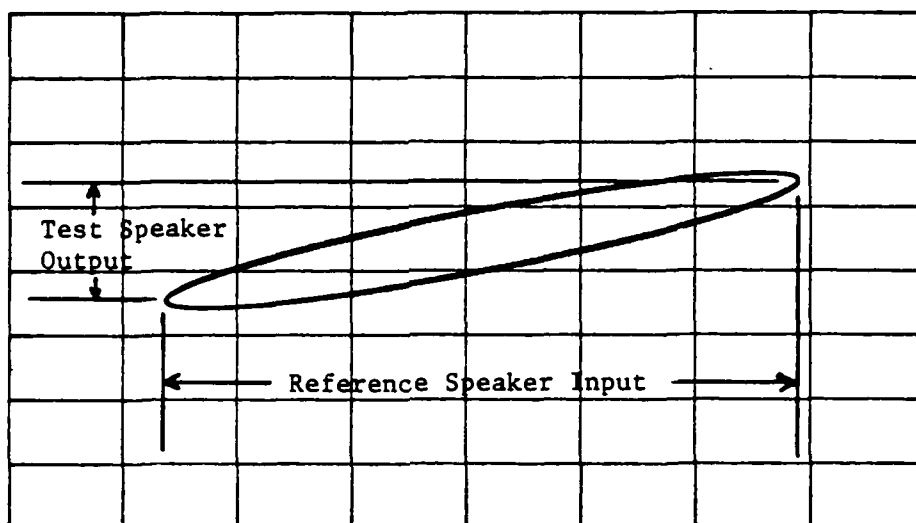


Fig. 10. Lissajous Plot

The 25 selected speakers were mounted in a five by five planar array on a balsa wood insulated bilayered sheet metal board. After wiring all the speakers in series, we surrounded all the electrical connections and speaker backs with two 3.0 centimeter layers of foam insulation sandwiching a 1.0 millimeter lead sheet. Then the entire array mounting was enclosed in a 44 by 44 by 5 centimeter sheet metal box. This design was chosen to suppress virtually all acoustic energy propagating out the rear hemisphere of the array, while shielding the array from any external electrical interference (Figs. 11 and 12).

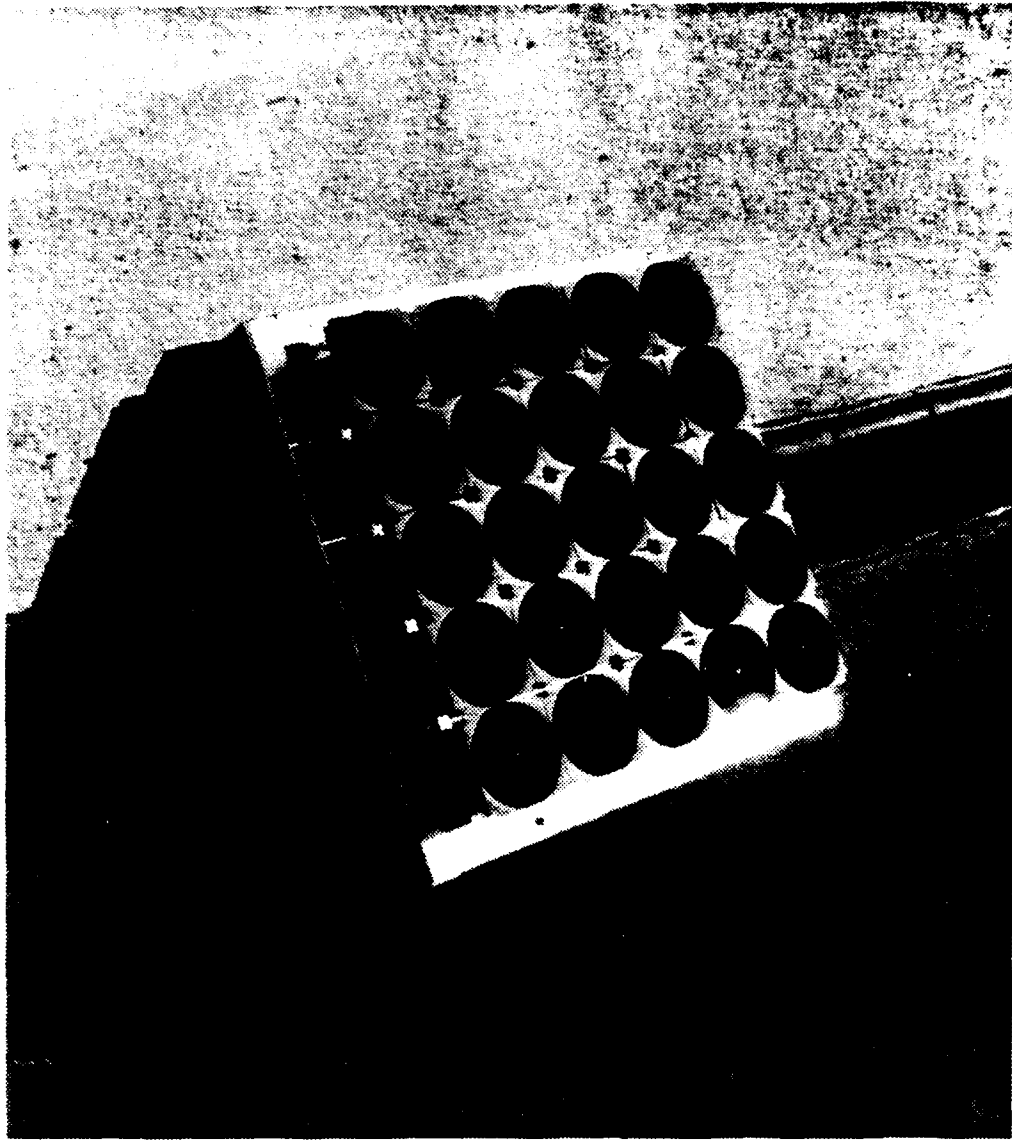


Fig. 11. Array Photograph

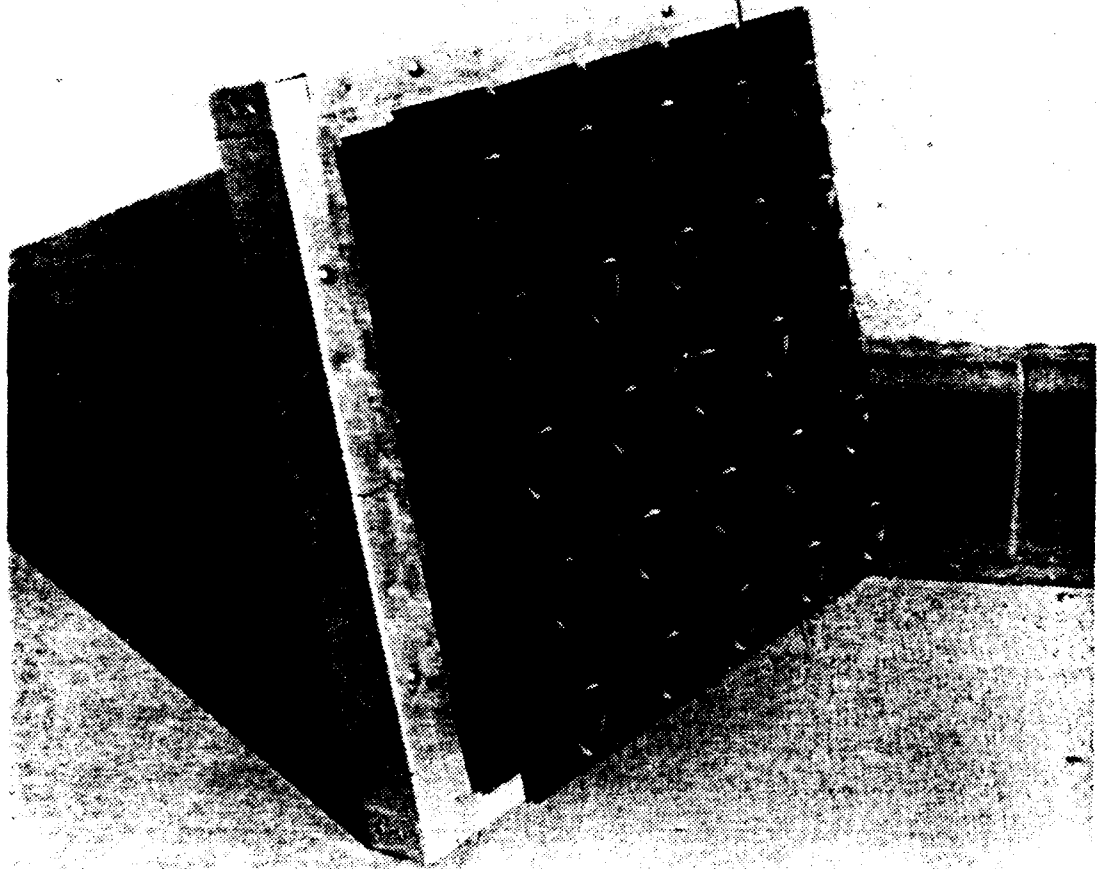


Fig. 12. Array Photograph

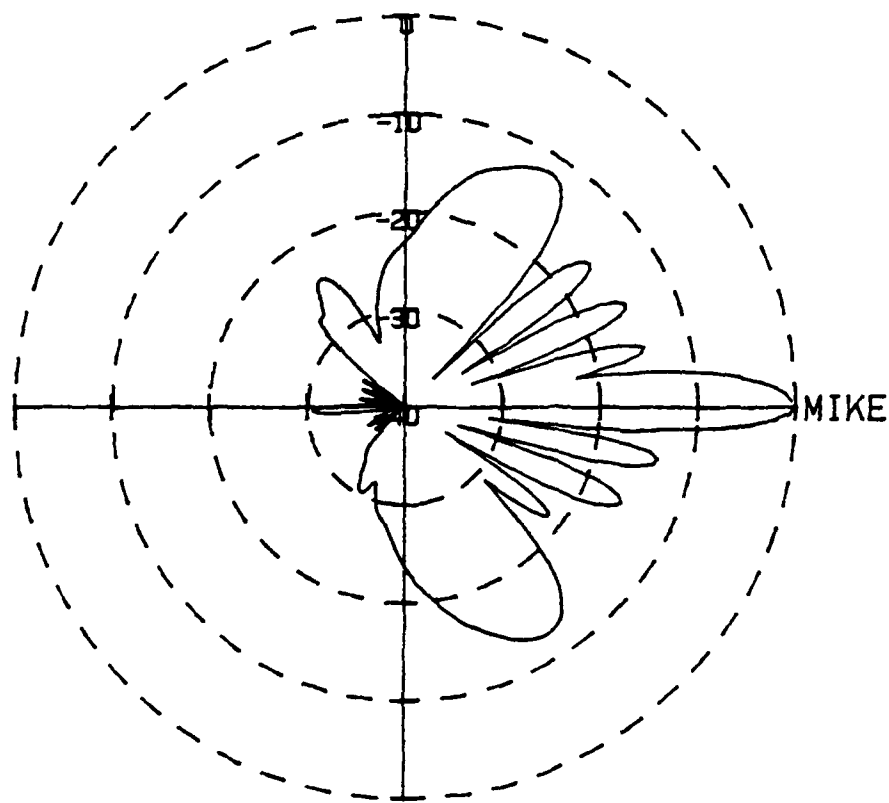
C. ENCLOSURE

Acoustic echosounding has proven to be an extremely useful technique for probing and analyzing the lower

atmosphere. In order to utilize the acoustic waves transmitted and later received by this remote sensing method efficiently, it is essential to have an efficient antenna with highly directive beams and strongly suppressed sidelobes. Antenna design becomes increasingly more important in a noisy environment where noise pollution within the sidelobes may dominate the desired signal within the main lobe. Hall and Wescott [Ref. 12] showed that sidelobe suppression improved with higher frequencies. Their studies showed that the measured 90 degree sidelobe suppression ranged from 38 dB at 1 KHz to 50 dB at 5 KHz. Furthermore, any significant improvement in sidelobe suppression could only be obtained by surrounding the antenna with an acoustic energy absorbing cuff or shroud.

In an effort to maximize our antenna main lobe to sidelobe power ratio, we intend to operate at 5KHz. Additionally, we have designed an acoustic energy absorbing enclosure. Many designs were considered based upon previous research in the field of echosounding [Refs. 15 through 18]. In addition, we obtained the actual acoustic beam patterns for our array using a computer program written by LCDR Butler [Ref. 19] which we modified for our purposes. This modified version of LCDR Butler's computer program is in Appendix B. By rotating the array in an anechoic chamber, we were able to produce highly accurate polar plots of the array beam patterns (Figs. 13 and 14).

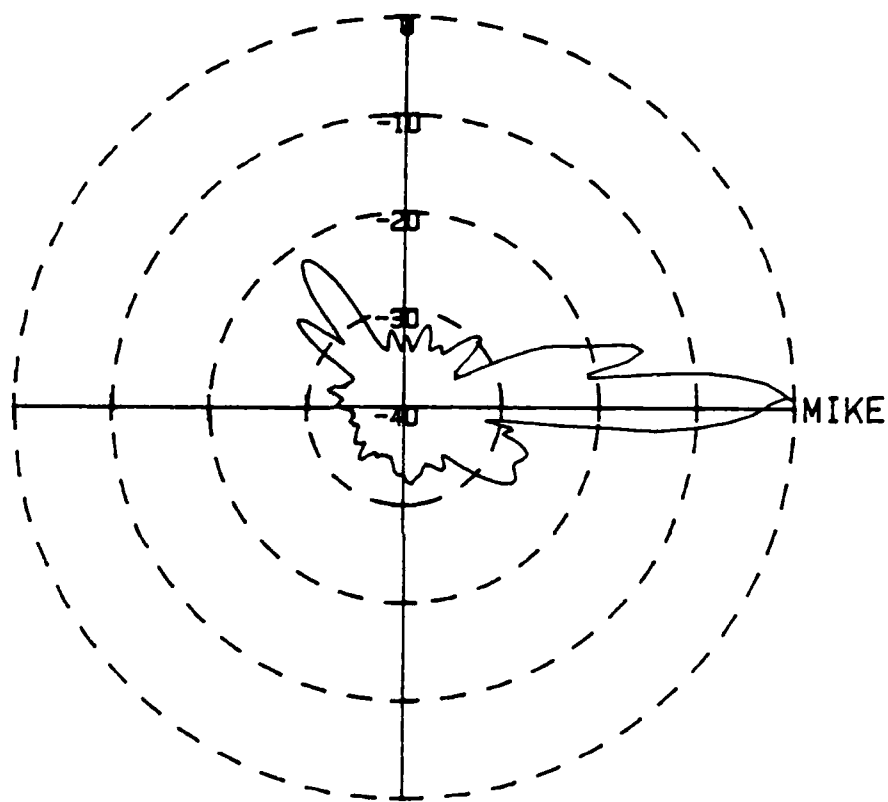
5 X 5 ACOUSTIC ARRAY BEAM PATTERN



R=3.60 M MIKE VT= 8.2465 INPUT=5.0 V FREQ=5.0 KHZ

Fig. 13. Polar Plot of 5 X 5 Array Beam Pattern

DIAGONAL 5 X 5 ACOUSTIC ARRAY BEAM PATTERN



R=3.60 M MIKE VT= 3.9497 INPUT=2.5 V FREQ=5.0 KHZ

Fig. 14. Polar Plot of 5 X 5 Array Beam Pattern
at a 45° Aspect

A comparison of the theoretical beam pattern for the five element, piston source array in Figure 7 with the experimentally measured polar plot of the 5 X 5 acoustic array in Figure 13 and the associated coordinates corresponding to the individual data points illustrate significant agreement. As predicted by our computer model [Appendix A], the actual acoustic beam pattern is comprised of nine distinct lobes in the forward hemisphere. Both the positions of these lobes and their relative amplitudes are within 2.0 percent of their predicted values. The computer modeled main lobe full width angle of 19.5 degrees very closely predicted the experimentally measured main lobe full width angle of 19.0 degrees. Reflected, scattered, diffracted and electronic noise all contribute to the clutter near the origin of Figure 13. This is the primary reason why the minima don't actually go to zero as predicted by our model. Additional reasons include mechanical noise in the device used to rotate the acoustic array and vibrational noise in the array itself. The apparent lobe in the upper left hand quadrant is an anomaly seen in all polar plots herein, and corresponds to acoustic energy reflected off the door and window of the anechoic chamber. Figure 14 represents the acoustic array mounted at a 45° aspect. A computer model for this orientation is a very complicated task and was not performed at this time. However, this polar plot of the acoustic array beam

pattern, and in particular, the appreciable sidelobe suppression strongly support the need for further array design studies.

Since it was our aim to suppress all sidelobes and utilize the main lobe, we chose not to taper our enclosure as most previous researchers had. Rather we designed the enclosure based upon the dimensions of the array itself and the acoustic beams it generated. The height of the enclosure is 160 cm. Allowing for the base foam and lead insulation, the array housing and the base framework itself, the actual array piston sources are positioned 143 cm from the mouth of the enclosure. The length and width of the enclosure are both 65 cm. Again allowing for construction materials, the inner dimensions are both 48 cm. Hence, the position of the center speaker is 24 cm from any of the four sides. These dimensions produce the unobstructed 19.0 degree path into which the main lobe is transmitted.

$$2 \cdot \tan^{-1} (24 \text{ cm} / 143 \text{ cm}) = 19.05^\circ \approx 19.0^\circ$$

Plywood was used for the construction of the enclosure and provided not only a rigid, inexpensive framework, but also provided an impedance mismatch which helped to attenuate external noise interference. Anticipating all kinds of weather conditions during data collection, the plywood enclosure was first waterproofed with four coats of

marine varnish. Grooved joints, caulking and weather stripping were also design considerations.

A millimeter layer of lead can suppress an acoustic signal by reflection as much as 40 dB (Figs. 15 and 16). About 7.0 centimeters of convoluted foam can suppress a signal another 3 to 4 dB (Figs. 15 and 17). The primary purpose of the convoluted foam is to attenuate the sidelobes which repeatedly reflect off the enclosure interior at glancing incident angles. Together the lead and convoluted foam make an extremely efficient absorbing material for use in our enclosure.

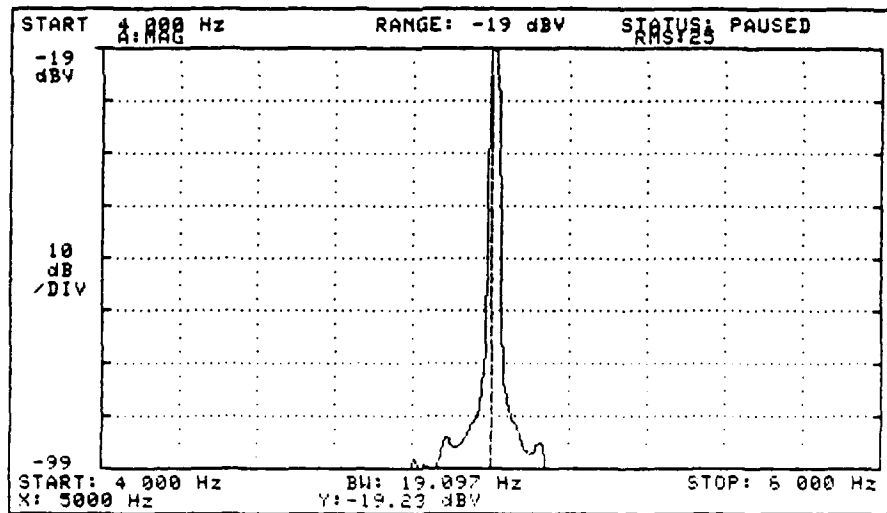


Fig. 15. Signal Response Reference, No Insulation

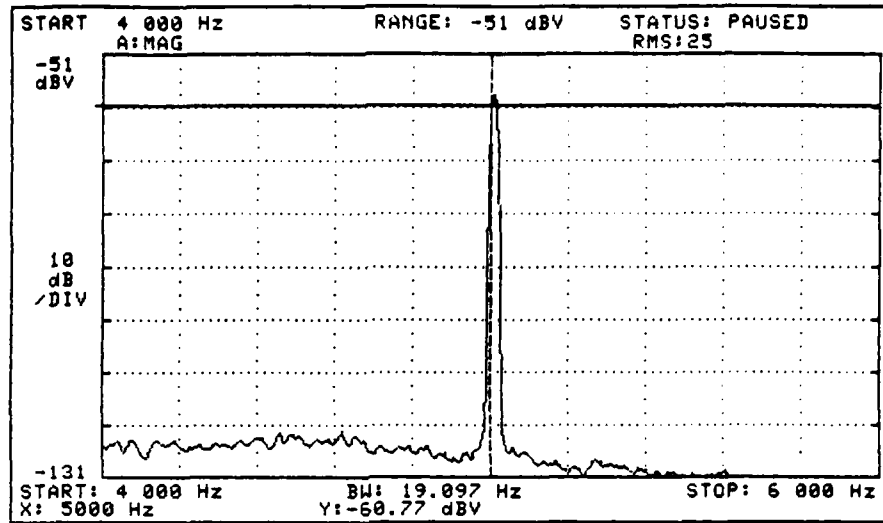


Fig. 16. Signal Suppression by Lead

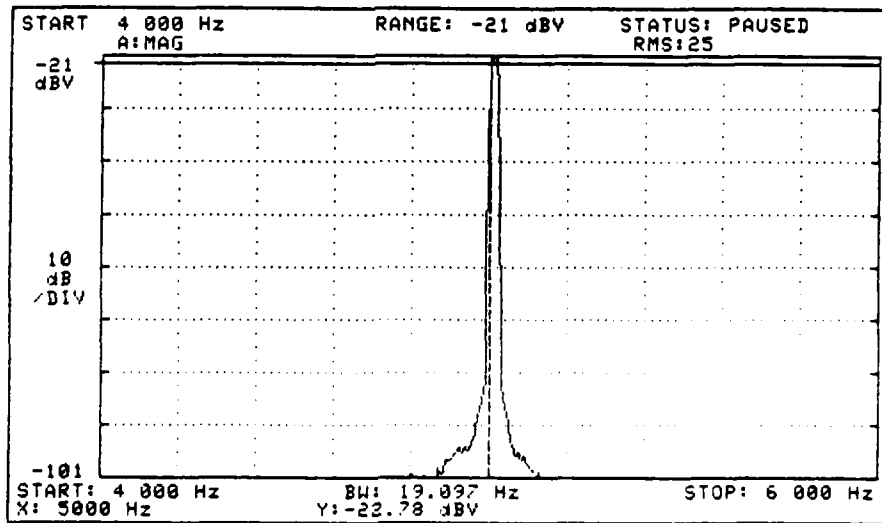


Fig. 17. Signal Suppression by Foam

Lead-lined absorbing foam was glued to all inner surfaces of the enclosure with two 1.0 millimeter layers of lead overlapping at all corners. Strong aluminum brackets were used to connect the four side panels to each other as well as to the enclosure base (Figs. 18 through 20).

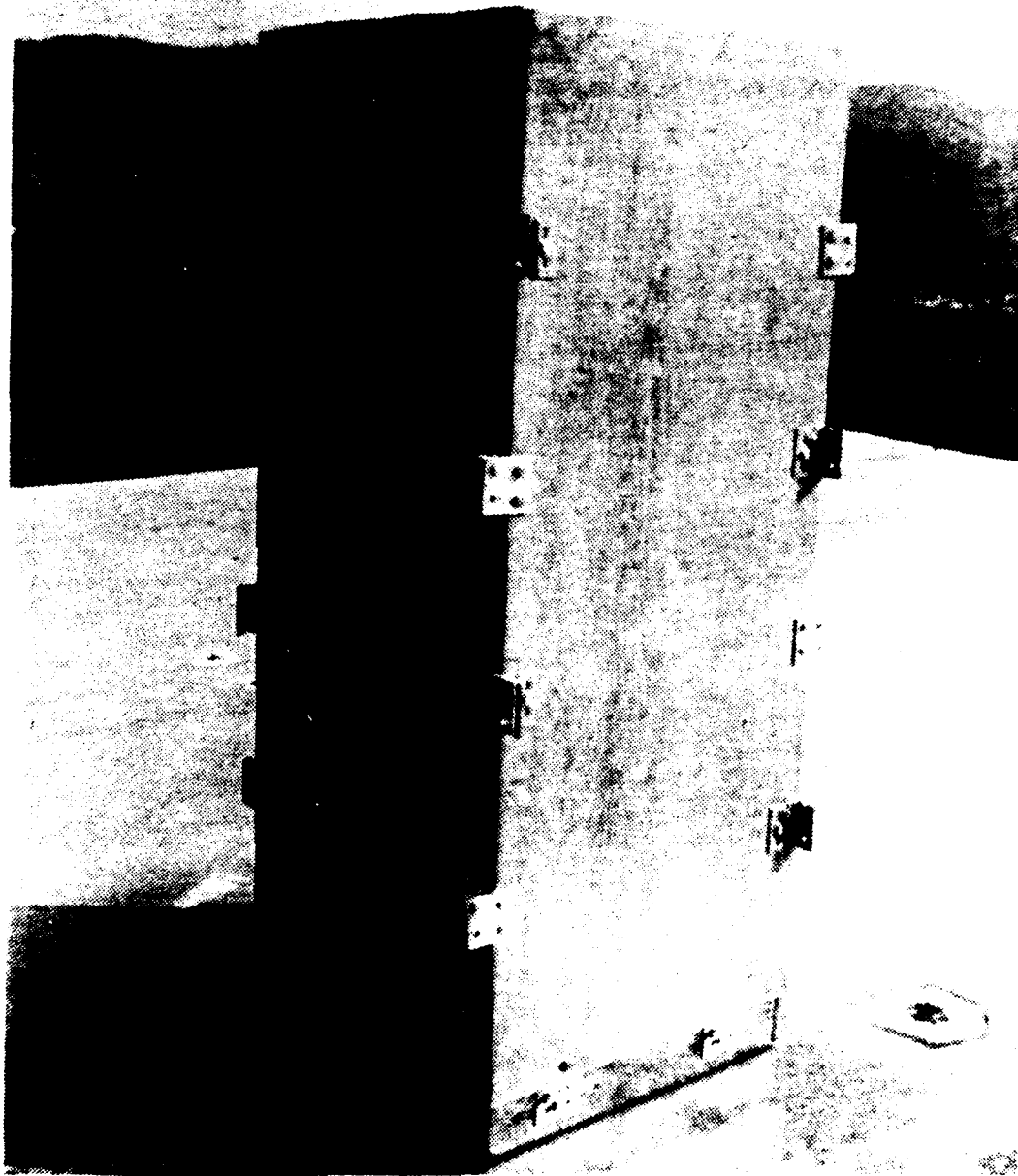


Fig. 18. Enclosure Photograph, Fully Assembled

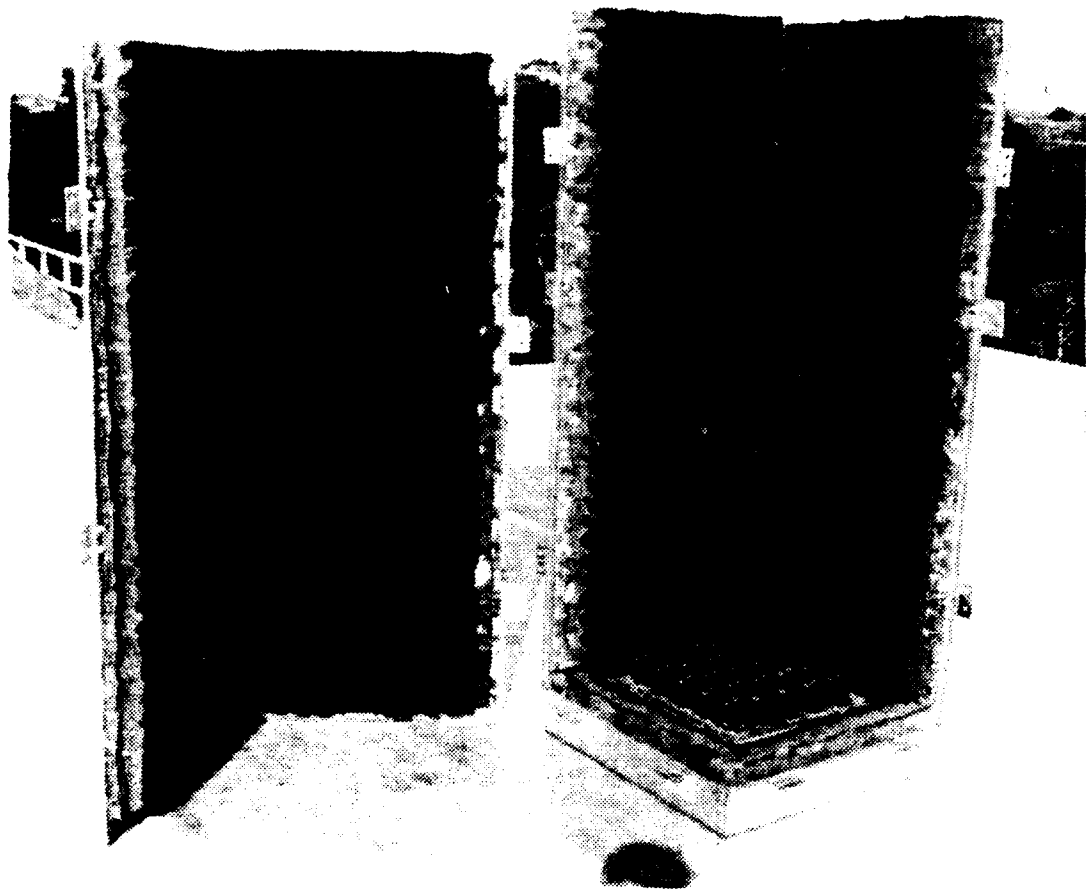


Fig. 19. Enclosure Photograph, Interior

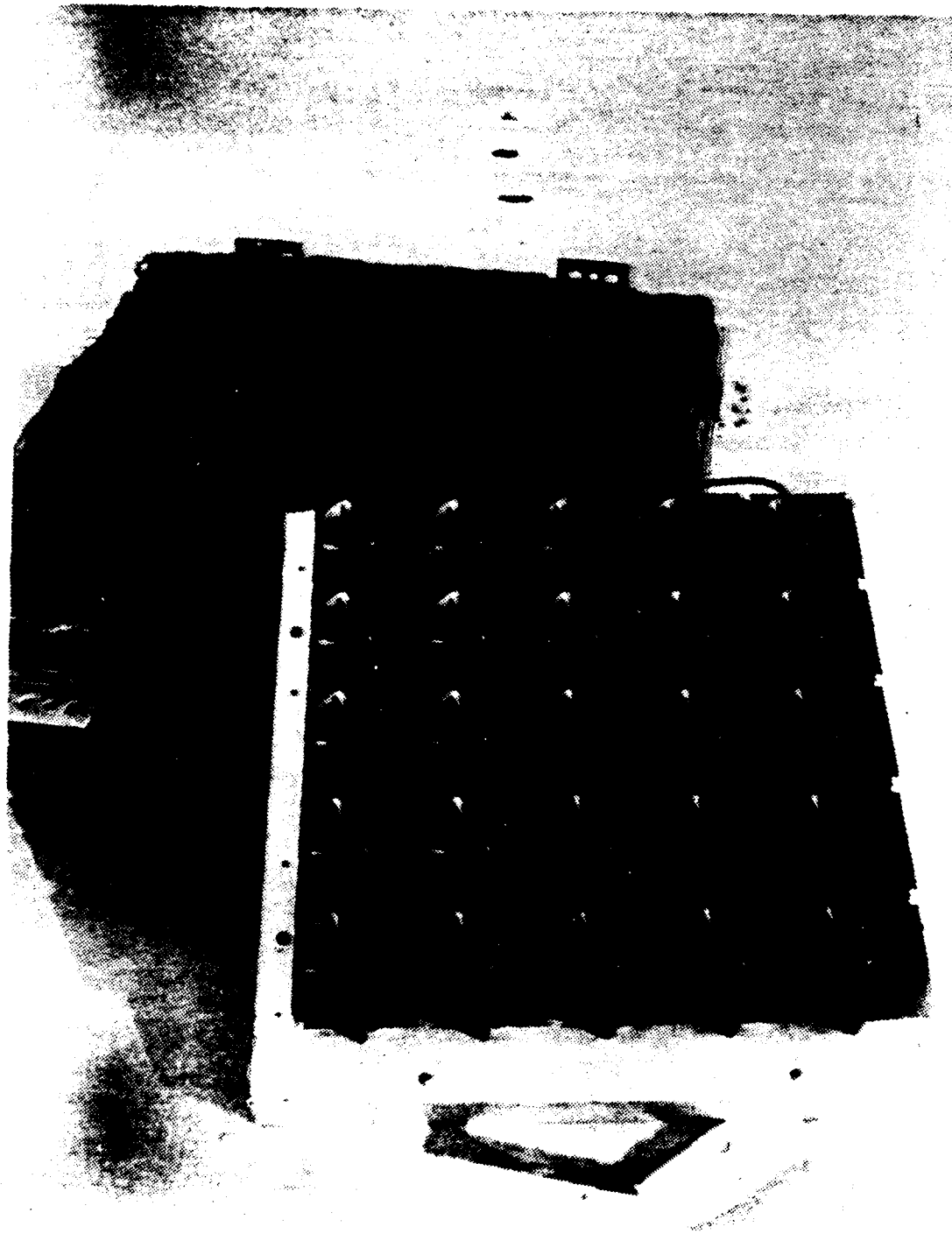


Fig. 20. Enclosure Photograph, Base with Array

D. ADDITIONAL HARDWARE

In addition to the acoustic array and enclosure discussed in the previous sections, there are primarily six more pieces of equipment essential to the function of the echosounder. Below is a brief description of these additional components.

1. HP200 Series Computer

The Hewlett-Packard (HP) 200 Series Computer includes a 20 megabyte hard disk drive, a floppy disk drive and an associated printer and monitor. The HP200 Series Computer is the central control component for the entire echosounder arrangement. The computer used is an HP217 programmed in Basic 3.0 and equipped with an Infotek BC203 Basic Compiler and an Infotek FP210 Floating Point Accelerator to enhance the speed of program execution. The computer is used to maintain timing and process control, to define all parameters for the HP3314A Function Generator as well as to execute the trigger command that produces the echosounder transmitted acoustic pulse. The computer also processes the data from the acoustic array via the pre-amplifier, bandpass filter and analog to digital converter. The computer then conducts data reduction routines to produce and display a high resolution atmospheric profile.

2. HP3314A Function Generator

The Hewlett-Packard (HP) 3314A Function Generator is a multimode function generator capable of providing

sine, square and triangular wave functions as well as any desired waveform ranging in frequency from 0.001 Hertz to 19.999 Megahertz. The HP3314A Function Generator was used to supply a pulse of an integer number of sinusoidal cycles of constant amplitude to the QSC Model 1700 Audio Amplifier. Typically a pulse of 100 sinusoidal cycles was used. A constant frequency setting of 5000 Hertz was used for all data runs.

3. QSC Model 1700 Audio Amplifier

The QSC Model 1700 Audio Amplifier is a high power amplifier which can supply 350 watts over an 8 ohm load. This amplifier was used to boost the output voltage of the function generator by a factor of 20 from 1.5 volts to 30 volts. The power supplied to each speaker in the array during operation was then 37.1 watts as indicated in the equation below.

$$\text{Power} = \frac{(\text{Voltage}_{\text{rms}})^2}{\text{Impedance}} = \frac{(30)^2}{2 \cdot 12.1} = 37.1 \text{ Watts}$$

4. Pre-amplifier

The pre-amplifier was designed and constructed by Walters [Ref. 20] to supply a gain of 1000 to the returned signal and isolate the data acquisition system from the transmitted pulse. The pre-amplifier may be thought of as a safety and switching mechanism for the system. An LT 1007 and an LT 1037 Operational Amplifier were selected for

use in the pre-amplifier based upon their low noise properties which were evaluated by physically incorporating them into the device and measuring their noise and gain characteristics with a HP3561A Dynamic Signal Analyzer. The IN 4000 Series Rectifiers isolate the power amplifier from the receiver between pulses and limit the voltage applied to the operational amplifiers. The electrical diagram of this device is outlined in Figure 21.

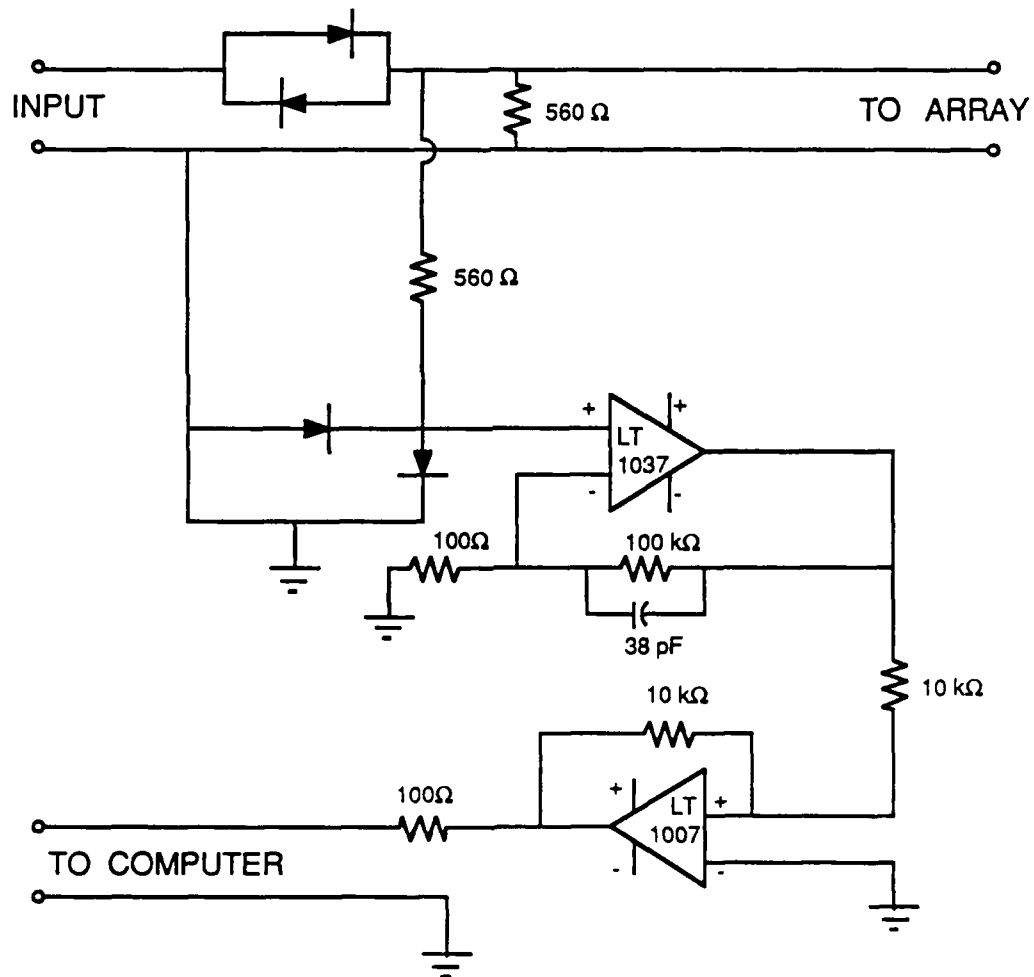


Fig. 21. Schematic of Pre-amplifier

5. Rockland Wavetek Model 852 Bandpass Filter

The Rockland Wavetek Model 852 Filter operates as a 48 dB per octave bandpass filter that suppresses broadband noise in the system. High and low bandpass settings of 5500 Hertz and 4500 Hertz respectively were used with a roll off of 48 dB per octave. The filter response at these settings is illustrated in Figure 22.

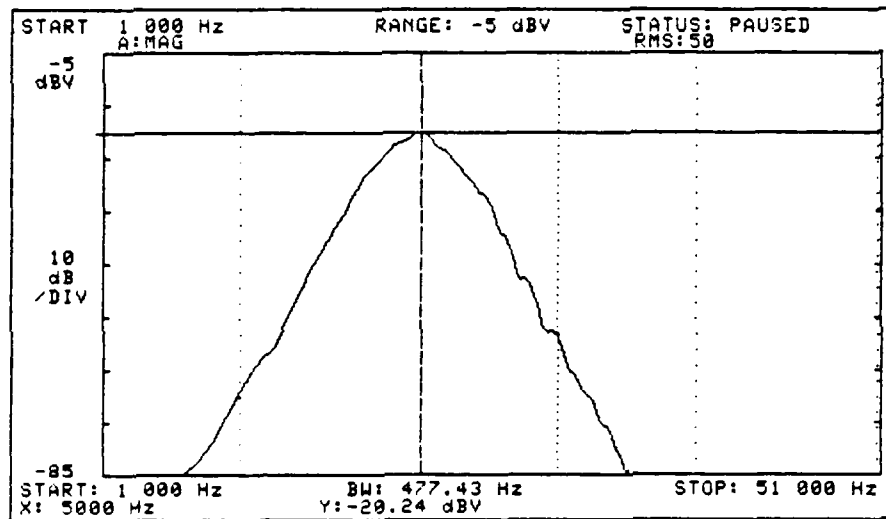


Fig. 22. Bandpass Filter Response

The 3dB (half power) bandwidth was approximately 1 KHz wide. Although it would have been desirable to reduce the bandpass interval to between 50 and 100 Hertz without impairing signal response, the Rockland Wavetek Model 852

Bandpass Filter was the best filter available. It performed adequately despite the large 1 KHz bandpass.

6. Infotek AD200 Analog to Digital Converter

An Infotek AD200 12 bit Analog to Digital Converter was used to sample the amplified signal voltage and digitize it for the computer system. A typical sampling frequency used was 20000 Hertz.

The arrangement of the above equipment is illustrated in Figure 23.

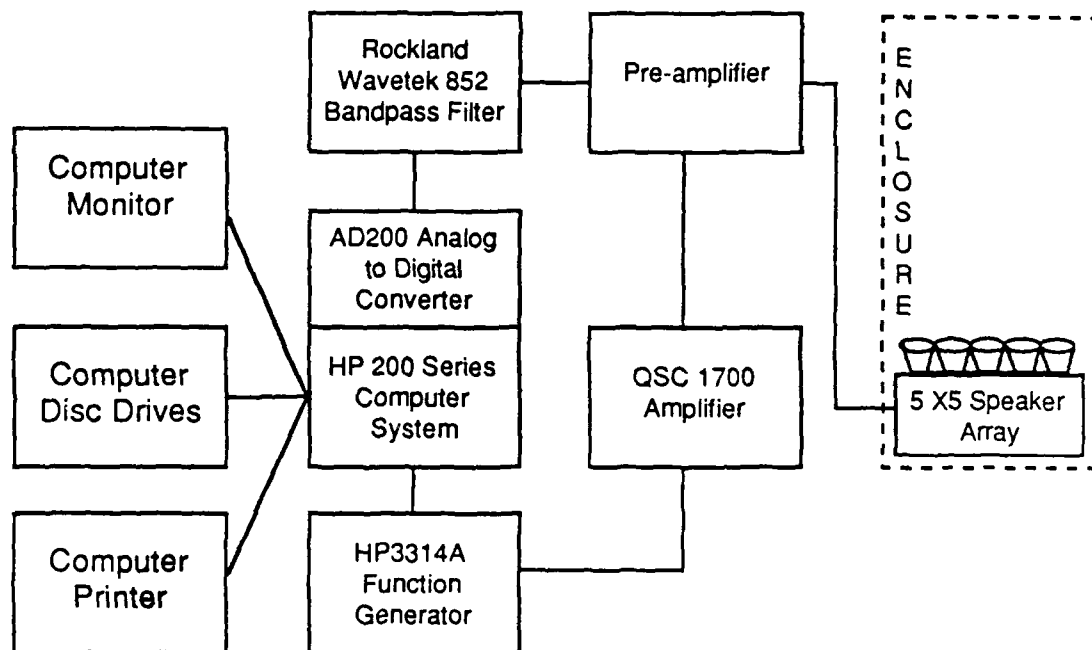


Fig. 23. Echosounder Equipment Arrangement

E. SOFTWARE

The software and the HP217 Computer were responsible for controlling and monitoring every operational aspect of the system. LT Wroblewski [Ref. 3] provides an in-depth discussion of the echosounder software which is also summarized in Appendix C.

IV. DATA ANALYSIS

A. ECHOSOUNDER PERFORMANCE

An analysis of the acoustic echosounder output was conducted to determine the validity of previously determined echosounder parameters. The e^{-1} decay time constant for the applied voltage of a single speaker was previously calculated to be 900 μ s which corresponds to a distance of 15.3 cm. The e^{-1} decay time constant for the applied voltage of the entire acoustic array was determined by the same experimental procedure to be 1060 μ s which corresponds to a distance of 18.0 cm. Although the 25 speakers in the acoustic array transmitting in unison should have approximately the same e^{-1} decay time constant as the single speaker, it is not surprising that the array e^{-1} decay time constant is larger. Using ten time intervals, an expectation of 99.99 percent decay of the transmitted signal should occur within a distance of 180.0 cm or just under 2.0 meters. Reviewing typical echosounder traces and Cr^2 plots [Appendix D], it is evident that such a short recovery time is actually quite accurate. The recovery distance is typically found to be on the order of 9 meters or 53 ms. This "blind zone" is not uncommon in most radar systems and is in part a return signal from ground clutter surrounding the acoustic array and its

enclosure immediately following pulse transmission. An analog to digital intensity factor of 4000 is assigned to the heavily shaded region of the recovery zone. Since the computer software has generated this value as the product of the actual analog to digital "count" value and the range from the acoustic echosounder, this value of 4000 must be divided by the range at the recovery zone boundary to give us an actual analog to digital "count" value. This result is then multiplied by an experimentally measured conversion factor of $3.34 \cdot 10^{-8}$ volts_{ms}/count. This result may then be used in the determination of the total electrical power received and converted by the acoustic array. The value for the total electrical power received by the acoustic array is calculated in the equations below.

$$\text{Voltage}_{\text{ms}} = (3.34 \cdot 10^{-8} \text{ v/count}) (4000 \text{ m} \cdot \text{counts}) (9 \text{ m})^{-1}$$

$$\text{Voltage}_{\text{ms}} = 1.48 \cdot 10^{-5} \text{ volts}$$

$$\text{Power} = (\text{Voltage}_{\text{ms}})^2 \cdot (\text{Array Impedance})^{-1}$$

$$\text{Power} = (1.48 \cdot 10^{-5} \text{ volts})^2 \cdot (12.1 \Omega)^{-1}$$

$$\text{Power} = 1.82 \cdot 10^{-11} \text{ Watts}$$

Using this received electrical power value and the known transmitted acoustic power value of 37.1 Watts, we can

solve for the e^{-1} decay time constant of the applied voltage. The product of the total acoustic power received and the efficiency of conversion factor ($E_R = 0.50$), yields the total electrical power received. Hence, the total acoustic power received is $3.64 \cdot 10^{-11}$ Watts. Although the distance of 9 meters corresponds to a time interval of 53 ms, this value is actually inflated by the system pulse length of 20 ms. Compensating for this, the actual recovery zone time interval is 33 ms. The e^{-2} decay time constant of the power is equal to the e^{-1} decay time constant of the applied voltage. These values are calculated below.

$$\frac{3.64 \cdot 10^{-11} \text{ Watts}}{37.1 \text{ Watts}} = e^{-2t/\tau} \text{ or,}$$

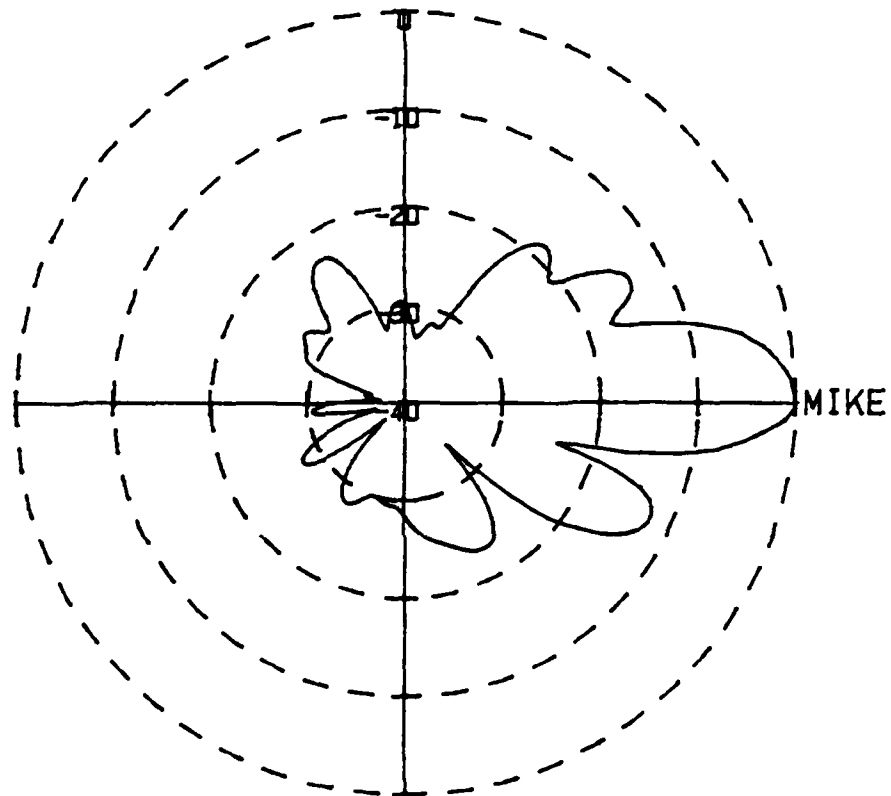
$$\tau = \frac{-2 \cdot 33 \text{ ms}}{\ln(6.37 \cdot 10^{-12})} = 2.56 \text{ ms} ,$$

This e^{-1} decay time constant of the applied voltage corresponds to a distance of 43.5 cm and is about twice the previously determined value.

Consideration was also given to the construction of a hexagonal planar array rather than a square planar array

based upon the astounding sidelobe suppression for the five by five element, square array at a 45° orientation as illustrated in Figure 14. To investigate the potential of such a close packed design, two small seven element hexagonal arrays were constructed. The first array design utilized a close packed spacing of 7.62 cm, while the second array design employed a $3/2$ wavelength or 10.2 cm spacing. Polar plots of the beam patterns for both these hexagonal array designs were made by rotating the arrays in an anechoic chamber with the main diagonal both horizontal and vertical. In both cases the first sidelobe suppression for both close packed orientations was down by nearly 15 dB, while the first sidelobe suppression for both $3/2$ wavelength spacing orientations was only down by about 7 dB. Furthermore, the ratios of the size of the main lobe to those of the sidelobes is much greater for the close packed design than they are for the $3/2$ wavelength spacing arrangement for both the vertical and horizontal orientations. The polar plots of the array beam patterns for both close packed and $3/2$ wavelength spacing hexagonal designs are illustrated in Figures 24 through 27. These figures strongly warrant further study of the hexagonal close packed array design.

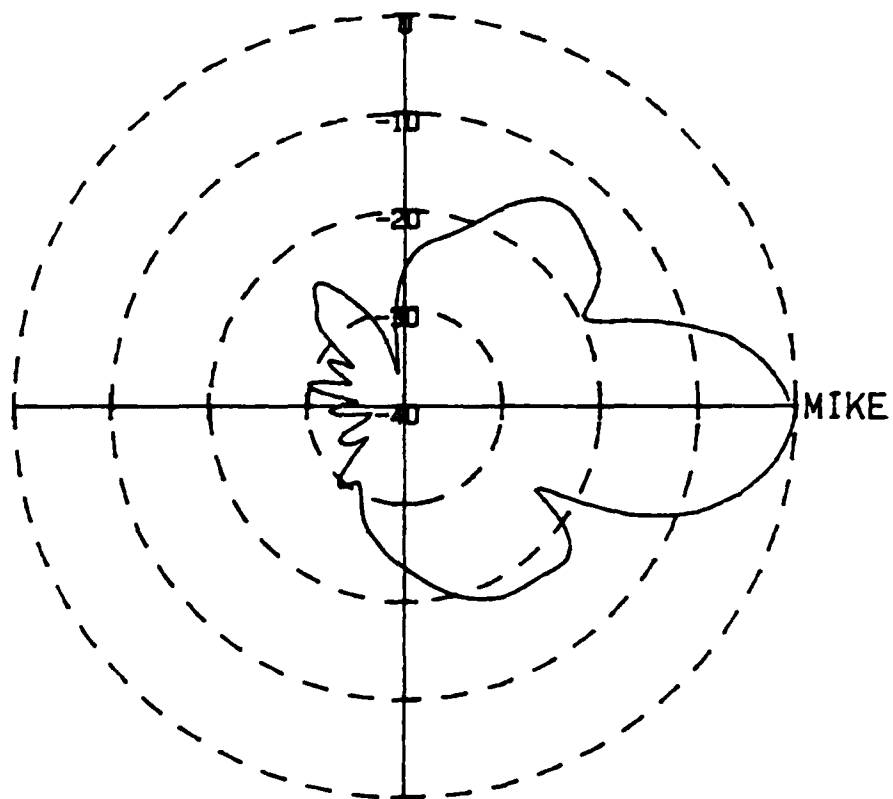
HORIZONTAL DIAGONAL, CLOSE PACKED, 7 SPEAKER HEXAGONAL ARRAY



R=3.60 M MIKE VT= 5.6364 INPUT=5.0 V FREQ=5.0 KHZ

Fig. 24. Polar Plot of Close Packed Hexagonal Array
(Horizontal Diagonal)

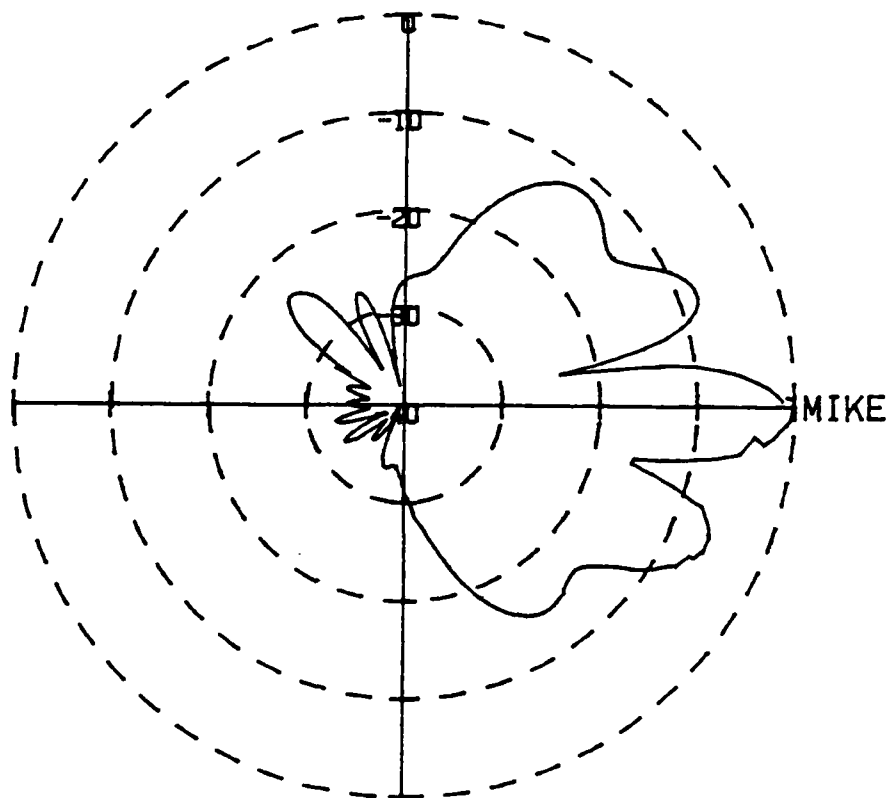
VERTICAL DIAGONAL, CLOSE PACKED, 7 SPEAKER HEXAGONAL ARRAY



R=3.60 M MIKE VT= 5.1559 INPUT=5.0 V FREQ=5.0 KHZ

Fig. 25. Polar Plot of Close Packed Hexagonal Array
(Vertical Diagonal)

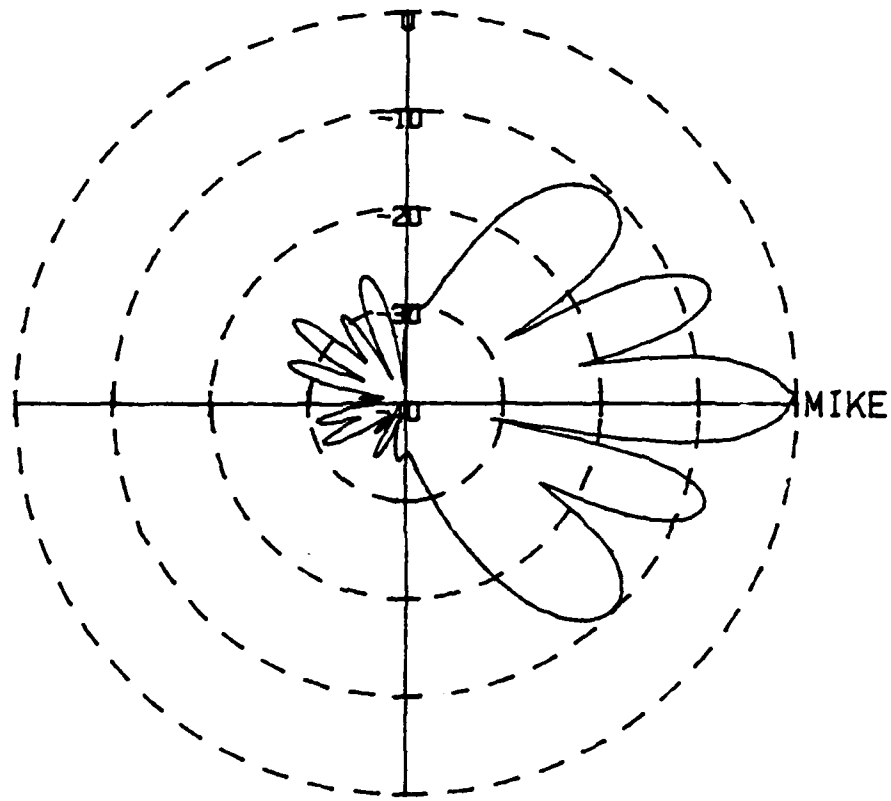
HORIZONTAL DIAGONAL, 3/2 WAVELENGTH SPACING, 7 SPEAKER HEXAGONAL ARRAY



R=3.60 M MIKE VT= 5.18 INPUT=5.0 V FREQ=5.0 KHZ

Fig. 26. Polar Plot of 3/2 Wavelength Hexagonal Array (Horizontal Diagonal)

VERTICAL DIAGONAL, 3/2 WAVELENGTH SPACING, 7 SPEAKER HEXAGONAL ARRAY



R=3.60 M MIKE VT= 6.0215 INPUT=5.0 V FREQ=5.0 KHZ

Fig. 27. Polar Plot of 3/2 Wavelength Hexagonal Array
(Vertical Diagonal)

B. SITE EVALUATION

Echosounder data was collected at two different locations. The primary data collection site was the upper roof of Spanagel Hall at the Naval Postgraduate School, Monterey, California. This site was chosen simply for convenience of data collection. Data gathered at this location is believed to represent the California coast during the spring near sea level. The second data collection site chosen was in the vicinity of the 24 inch telescope at Lick Observatory, San Jose, California. This site is located atop Mt. Hamilton at an altitude of approximately 5700 feet and nearly 20 miles inland from the coast.

These two data collection sites represent areas of differing atmospheric air pressures, water vapor pressures, local temperature ranges, and local wind velocity ranges. These characteristics all play important roles in effecting the local atmospheric turbulent conditions and thereby the atmospheric structure parameter, C_t^2 .

In addition to collecting echosounder data at Lick Observatory, simultaneous measurements of the isoplanatic angle (θ_0) and spatial coherence length (r_0) were made with systems developed by Walters [Refs. 1 and 2]. A basic knowledge of these two systems is necessary to understand the correlation procedures made. The isoplanatic angle

(θ_0) is primarily an upper atmospheric measurement which indicates atmospheric disruptions at a range of two to 15 kilometers above the Earth's surface. On the otherhand, the spatial coherence length (r_0) is a uniform measure of the effects of the entire atmospheric blanket on coherent light transmission. A close comparison of the acoustic echosounder data, the isoplanatic angle (θ_0) measurements and the spatial coherence length (r_0) measurements should give us an indication of the turbulent contributions from the lower and upper troposphere as well as the stratosphere above.

Based upon isoplanatic angle (θ_0) and spatial coherence length (r_0) measurements at Mt. Wilson near Los Angeles, California, a strong correlation between the isoplanatic angle (θ_0) and spatial coherence length (r_0) measurements occurs if the low altitude boundary layer contribution is sufficiently small. This strong correlation helps to reinforce the overall description of the atmosphere at the time of data collection. Figures 28 and 29 graphically illustrate the atmospheric measurements made at Mt. Wilson on 2 April 1987 by Walters. The strong correlation between the isoplanatic angle (θ_0) and the spatial coherence length (r_0) is especially evident between the hours of 0700 and 1300 universal time. The close tracking of these two measurements during this time interval indicate that the

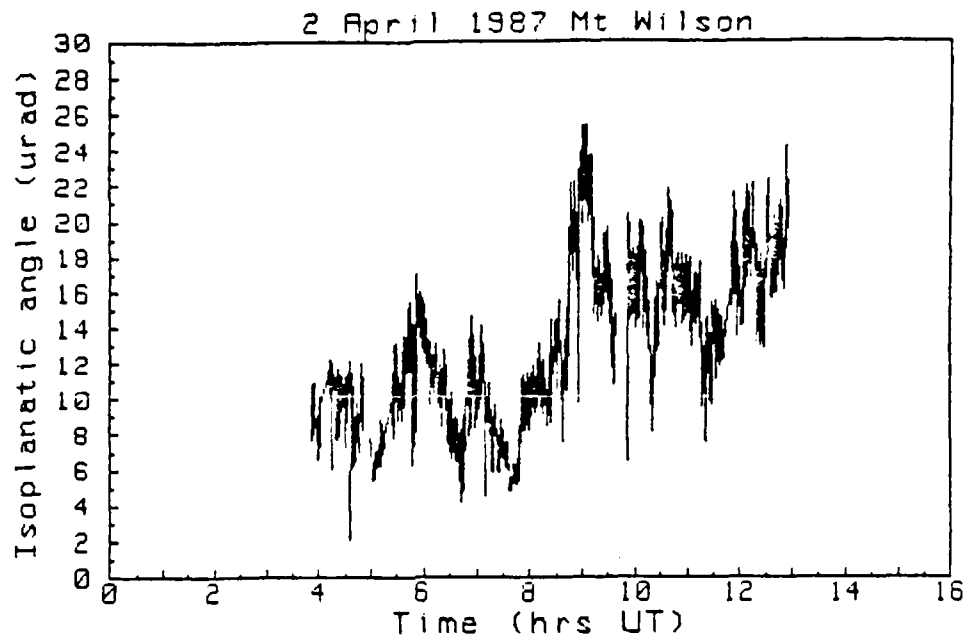


Fig. 28. Isoplanatic Angle Measurements, Mt. Wilson

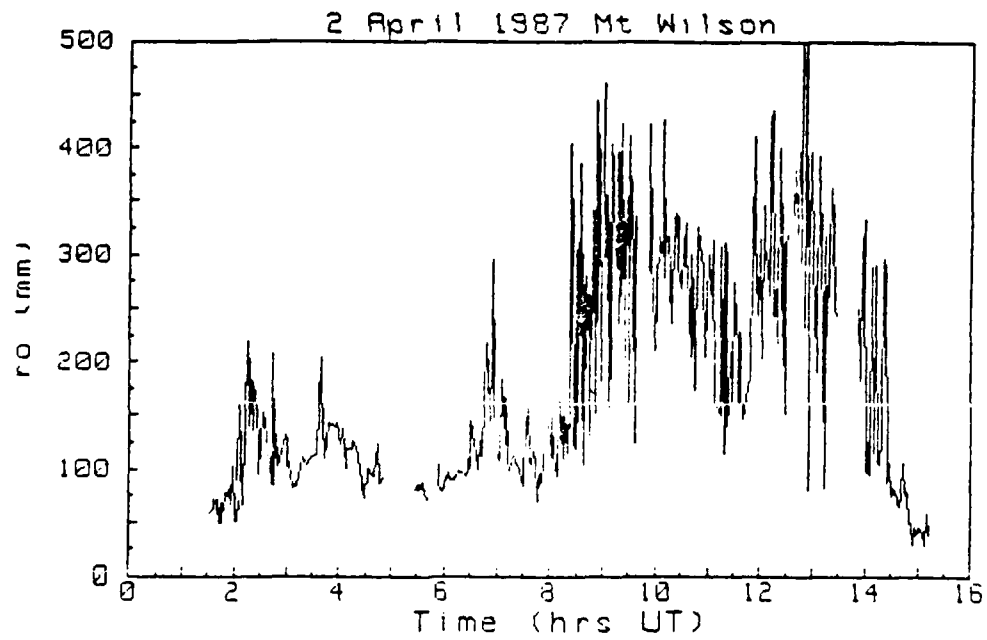


Fig. 29. Spatial Coherence Length Measurements, Mt. Wilson

upper atmospheric conditions, as measured by the isoplanatic angle (θ_0), are dominating the entire atmospheric profile as measured by the spatial coherence length (r_0). Unfortunately, the existence or non-existence of any turbulent surface effects cannot be ascertained by the employment of the above two systems alone. However, employment of these two systems together with the acoustic echosounder should enable us to produce a complete atmospheric profile with strong correlation between all three atmospheric measurements.

On 9 and 10 April 1987, all three systems were operated at Lick Observatory. Again good correlation between the isoplanatic angle (θ_0) and the spatial coherence length (r_0) measurements was noted. In addition, strong correlation between the spatial coherence length (r_0) measurements and the acoustic echosounder data was conclusively present. A comparison of the isoplanatic angle (θ_0) and the spatial coherence length (r_0) measurements in Figures 30 and 31 shows good correlation between the two atmospheric parameters especially during the 0930 to 1130 time interval on 9 April 1987. However, during subsequent hours the isoplanatic angle (θ_0) measurements remain high (approximately 12 μ rad) indicating relatively calm turbulent conditions in the upper atmosphere, while the spatial coherence length (r_0) values

drop sharply after 1100 universal time indicating dominant and increasing lower atmospheric turbulence. This increase in the low level turbulence should be evident in the echosounder data commencing around 1200 universal time (0400 local standard time) on 9 April 1987. A comparison of the echosounder data in Figures 32 through 34 illustrates this increase in the local surface turbulence.

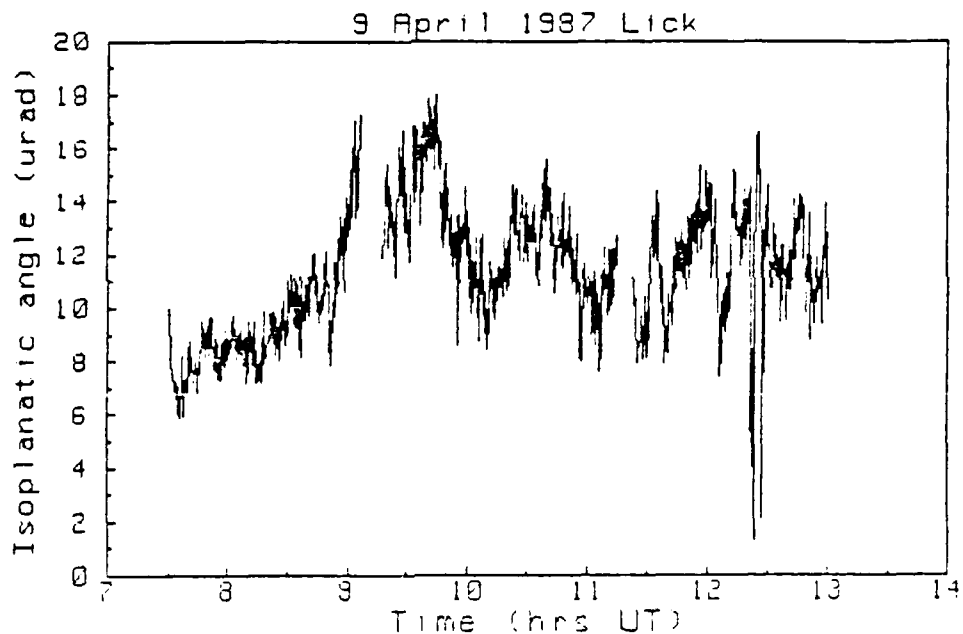


Fig. 30. Isoplanatic Angle Measurements, Lick Observatory

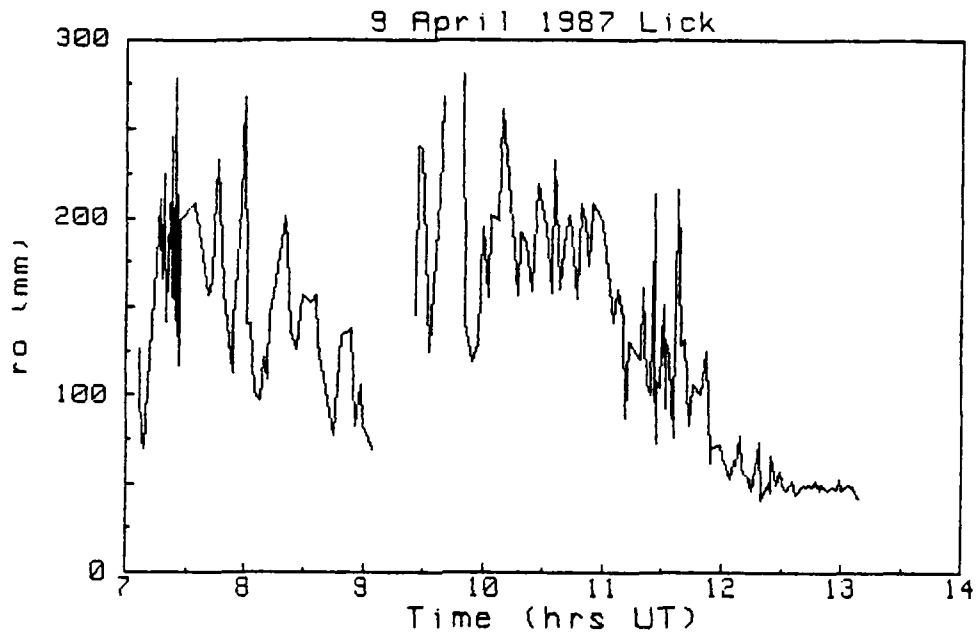


Fig. 31. Spatial Coherence Length Measurements, Lick Observatory

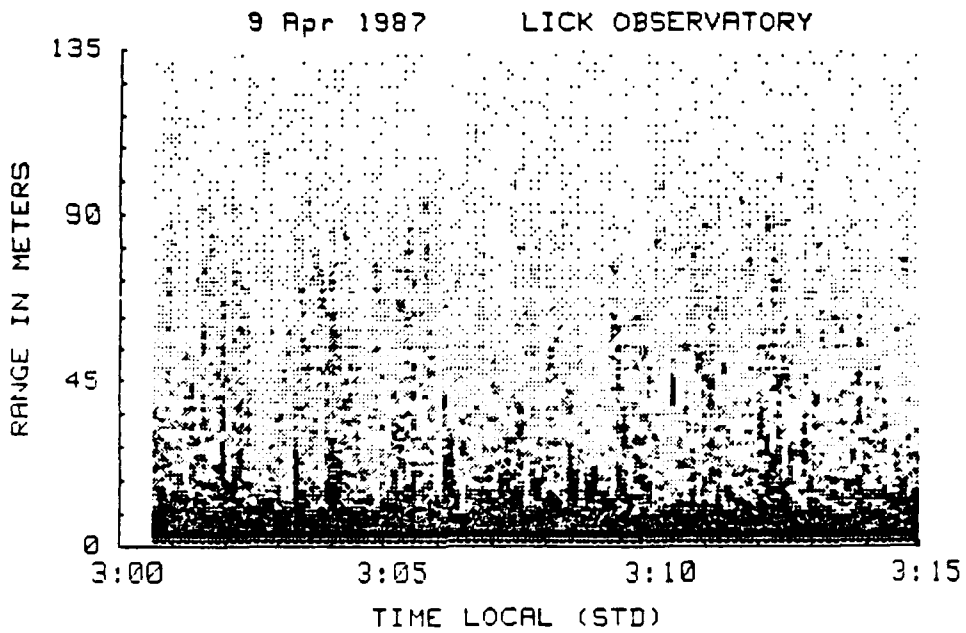


Fig. 32. Echosounder Trace, Lick Observatory

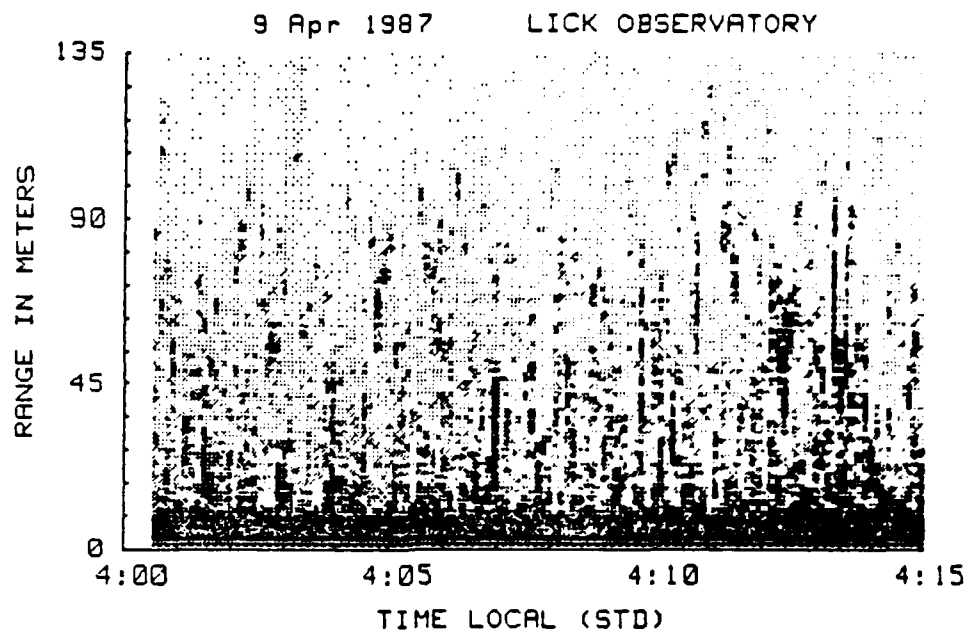


Fig. 33. Echosounder Trace, Lick Observatory

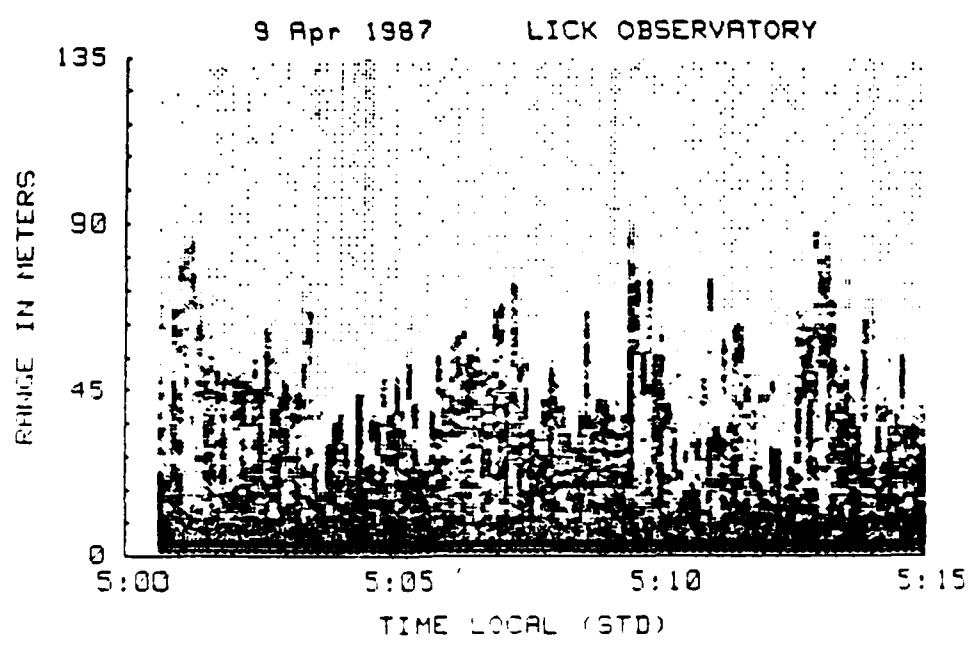


Fig. 34. Echosounder Trace, Lick Observatory

The strong correlation between the echosounder data around 0400 to 0500 local standard time and the spatial coherence length (r_0) measurements at 1200 universal time, combined with the lack of correlation between the isoplanatic angle (θ_0) and the spatial coherence length (r_0) measurements indicate that the lower atmospheric and surface turbulent layers are dominating the atmospheric profile during this time period.

Data collected on 10 April 1987, again illustrate the strong correlation between the three atmospheric measurements made. A comparison of the isoplanatic angle (θ_0) and the spatial coherence length (r_0) measurements during the time interval of 0700 and 1300 universal time indicate steady turbulent conditions in the upper atmosphere and greatly varying turbulent conditions at lower atmospheric levels. This is evident in Figures 35 and 36 by the consistent values of the isoplanatic angle (θ_0) during the time period compared with the steady increase and eventual decline of the spatial coherence length (r_0) values during the same time interval. The trace variations in Figure 36 during the hours of 0800 and 1200 universal time are indicative of a period of diminishing lower atmospheric or surface turbulence followed by the onset of an increasingly turbulent period around 1200. This turbulent trend is distinctively supported by the echosounder data in Figures 37 through 44.

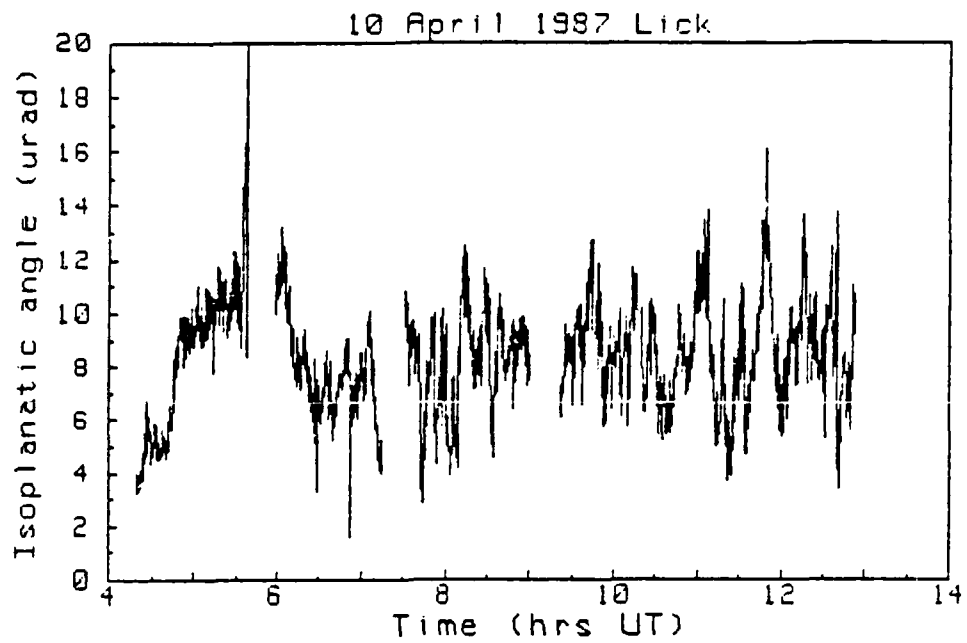


Fig. 35. Isoplanatic Angle Measurements, Lick Observatory

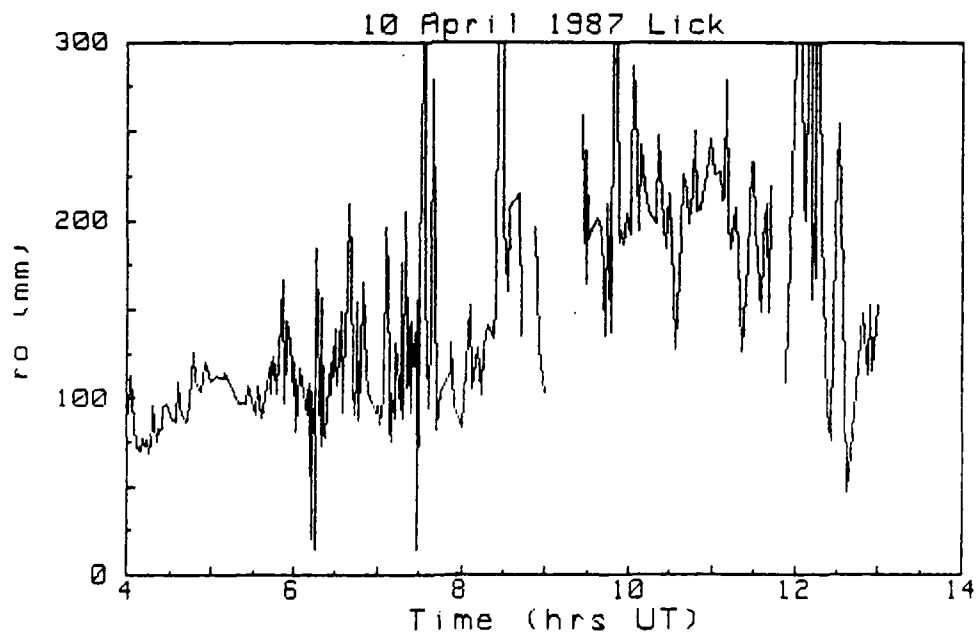


Fig. 36. Spatial Coherence Length Measurements, Lick Observatory

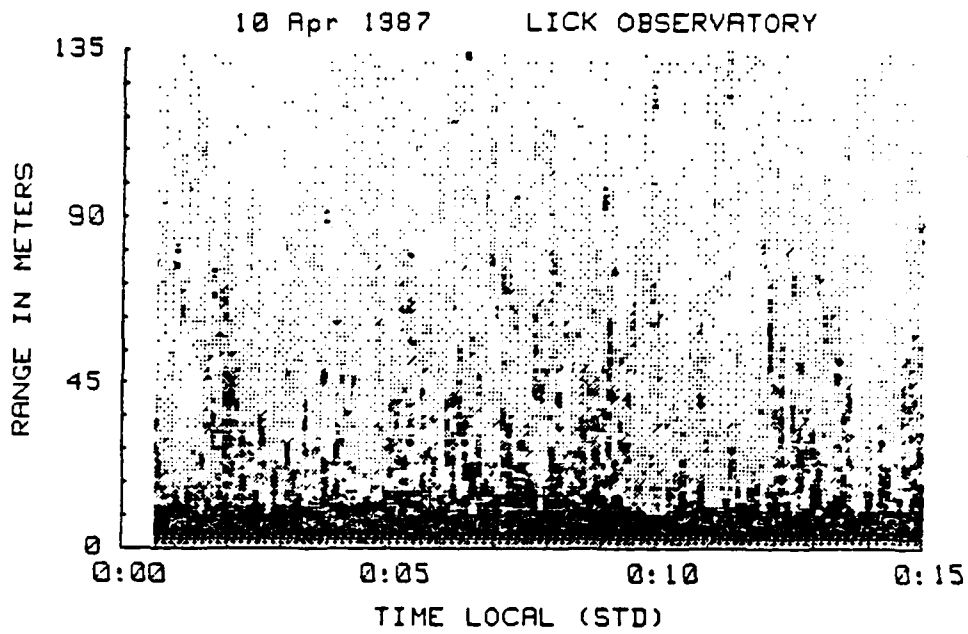


Fig. 37. Echosounder Trace, Lick Observatory

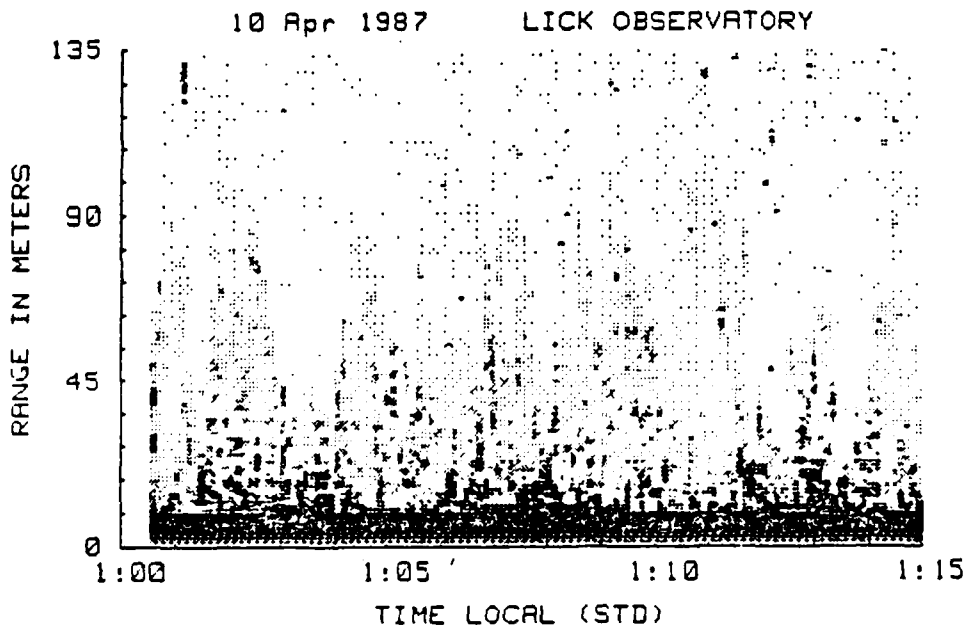


Fig. 38. Echosounder Trace, Lick Observatory

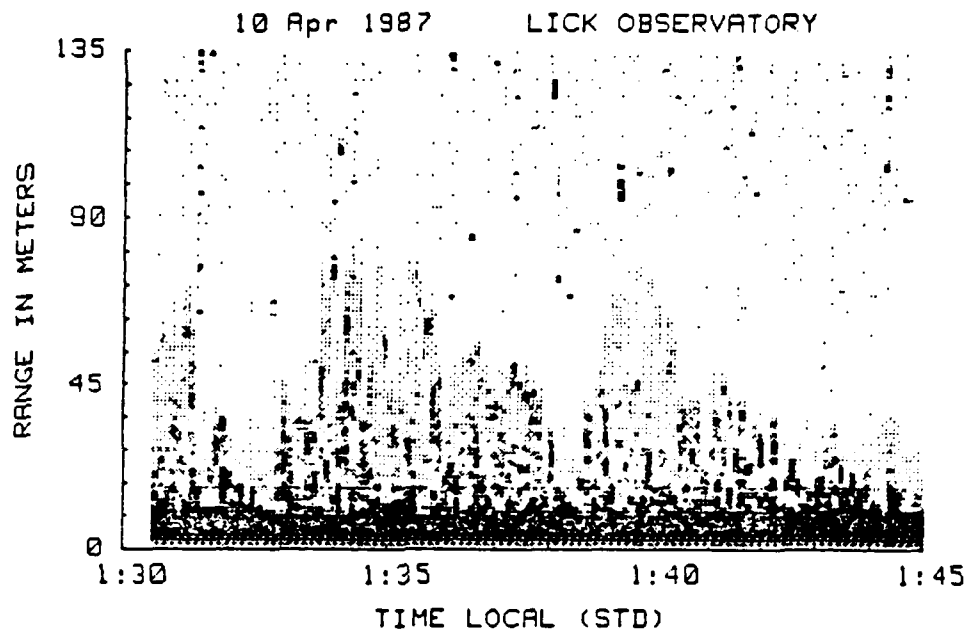


Fig. 39. Echosounder Trace, Lick Observatory

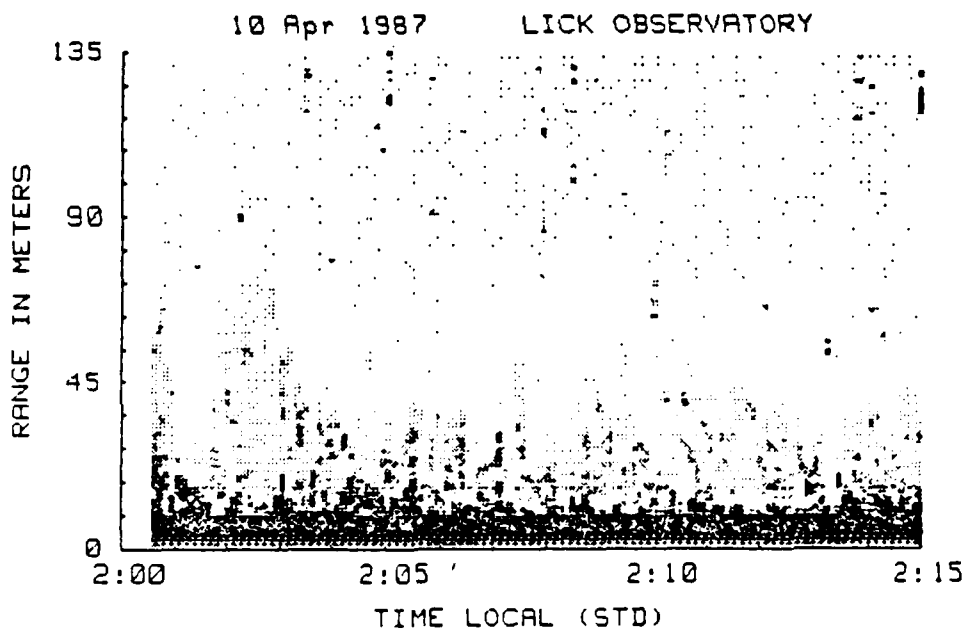


Fig. 40. Echosounder Trace, Lick Observatory

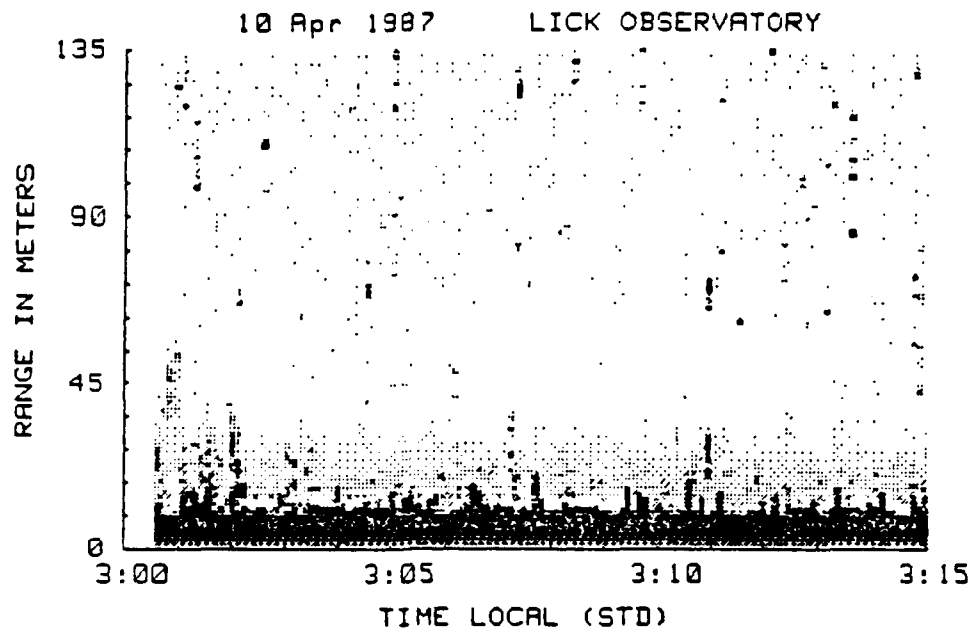


Fig. 41. Echosounder Trace, Lick Observatory

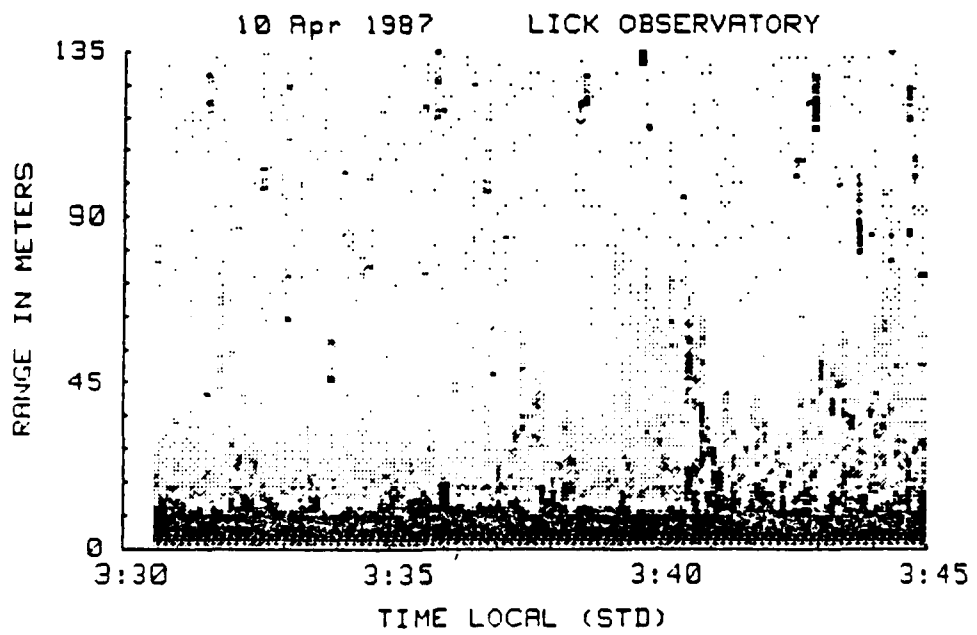


Fig. 42. Echosounder Trace, Lick Observatory

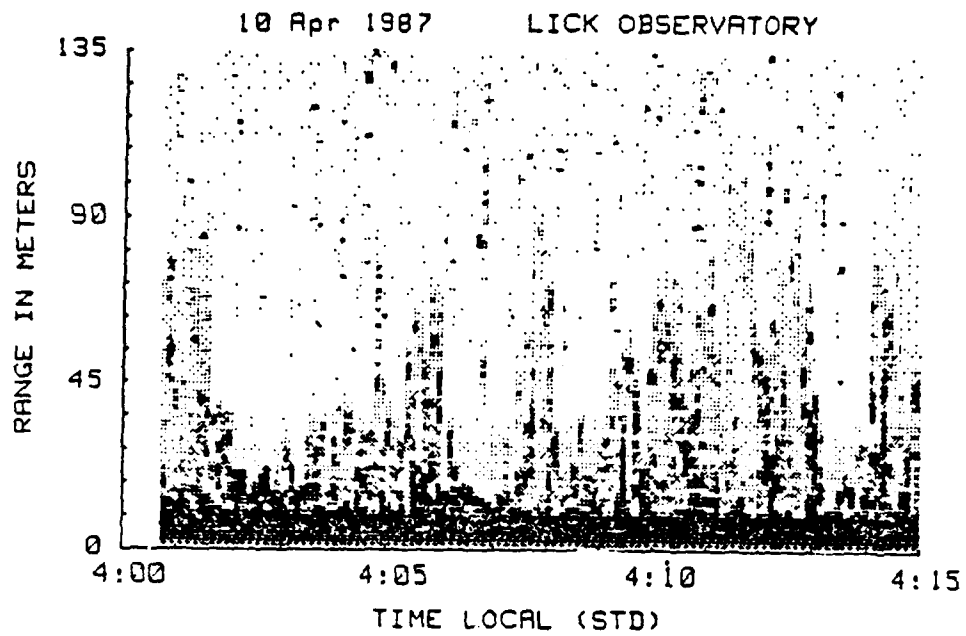


Fig. 43. Echosounder Trace, Lick Observatory

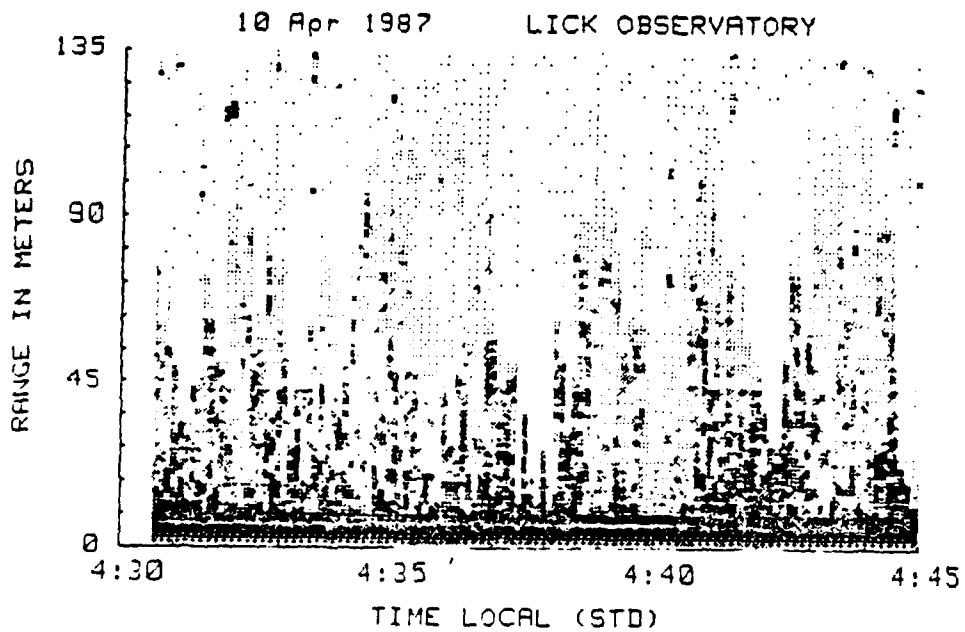


Fig. 44. Echosounder Trace, Lick Observatory

The large 200 mm spatial coherence lengths around 1100 universal time are consistent with the low turbulence evident in the echosounder profiles around 0300 local standard time.

Only acoustic echosounder measurements were made on the upper roof of Spanagel Hall at the Naval Postgraduate School. Data runs on 26 and 27 April 1987, include both echosounder data and the associated Ct^2 plots. Of particular interest is the plot of 11:30 on the 27th of April in Figure 45, which shows the maritime boundary inversion layer around 100 m being perturbed by convective plumes at lower altitudes. Sixteen additional echosounder output traces were included in Appendix D to exhibit typical atmospheric activity. Many of the plots, such as the 14:45, 15:30, and the 17:30 of 26 April and the 10:00, 11:15, 13:00, 14:15, 15:15, 16:15, and the 17:15 of 27 April, have convective plumes which are prevalent whenever a heat flux between the surface and atmosphere exists. The plots of 18:15 and 19:15 on the 26th of April and of 13:00, 18:45, and 20:00 on the 27th of April clearly show the passage of the neutral event which is encountered when the atmospheric and surface temperature difference becomes negligible. Finally, the plot of 16:30 on 26 April can be associated with strong winds which exhibit a somewhat uniform return for all altitudes across the entire 15 minute interval of the trace.

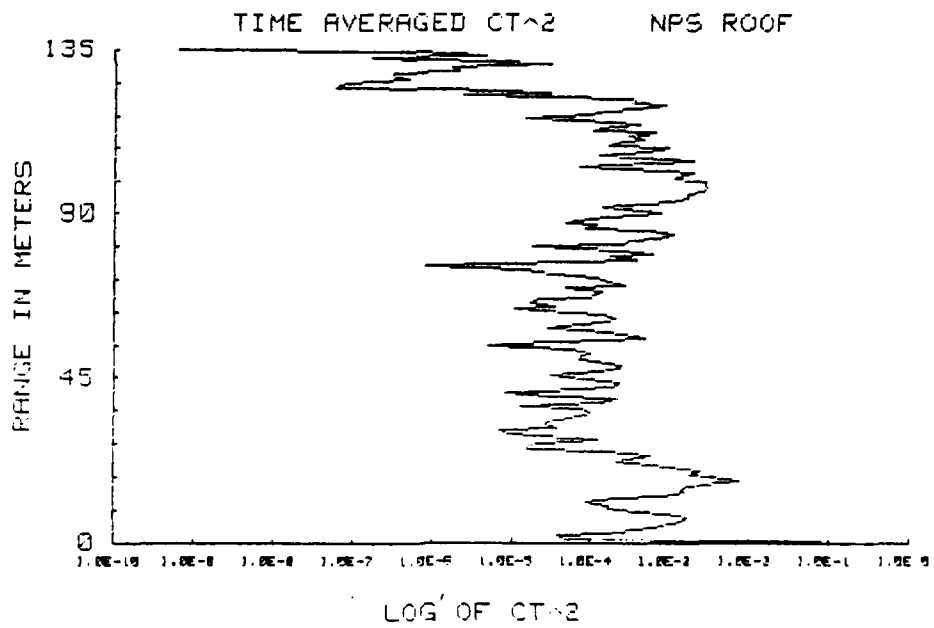
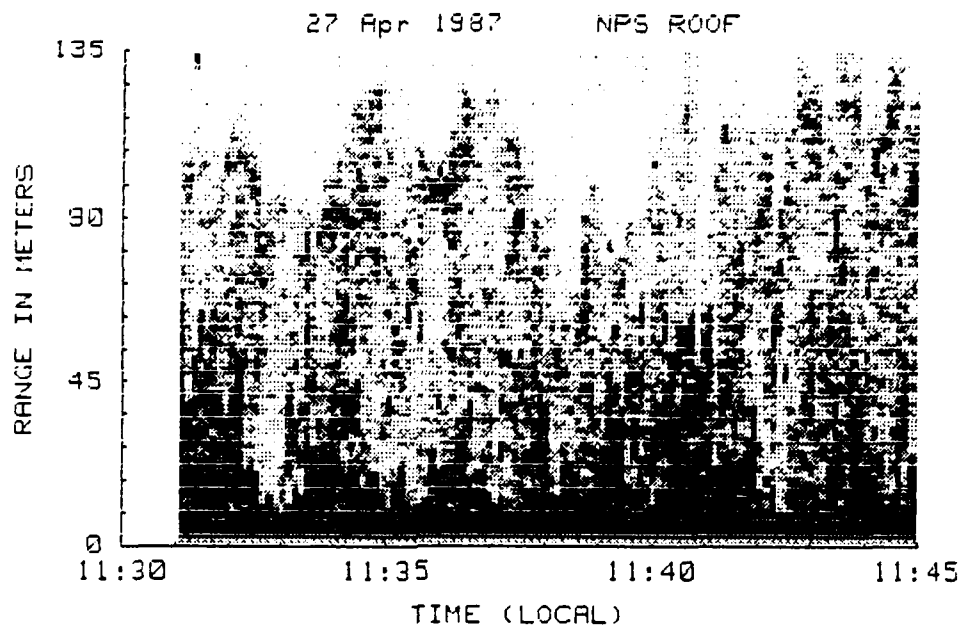


Fig. 45. Echosounder Trace and Cr² Plot, NPS Roof

V. CONCLUSIONS AND RECOMMENDATIONS

A high frequency, 5kHz, phased array echosounder constructed to measure low level turbulence appears to work within the 10 to 135 meter altitude range. When using the device, detailed profiles of the short range atmospheric density fluctuations were obtained. The profiles were found to correlate very well with the measurements of the isoplanatic angle (θ_0) and the spatial coherence length (r_0) during periods of simultaneous operation. This short range echosounder, when used in conjunction with the other atmospheric measuring devices, is an invaluable tool. The graphical output provides us with a more complete description of the atmosphere that can be used to calculate C_n^2 , the atmospheric index of refraction structure parameter.

Further software developments such as the incorporation of Doppler and Fast Fourier Transform routines into the echosounder program will determine the radial velocity profile of the return signal. Such an improvement will determine the velocity of the probed air masses and plot these echosounder traces as a function of color intensity.

Other areas of further research include the design and testing of different array patterns. One such pattern, the hexagonal array, is already undergoing tests. As the

speaker array evolves, it is also evident that the enclosure must follow suit to accommodate the new array design and associated beam patterns. Further improvements in software routines are also inevitable. It is always desirable to store on a disc all data collected at a site. Presently, the floppy disc capacity is inadequate for the storage of more than two hours of data. Furthermore, if FFT and Doppler routines are to be added, the computational speed of the computer will inhibit the pulse repetition rate. A special data acquisition technique called "Direct Memory Access" may then have to be introduced into the HP computer to allow simultaneous data collection and processing.

Finally, this product may be used in various applications not already addressed. One such use may be to measure windshear at airports. Other researchers have expressed interest in using the echosounder to measure arctic atmospheric conditions during meteorological surveys. Assuredly, as the device evolves into a more compact and highly efficient instrument, its range of application will continue to expand.

APPENDIX A
LINEAR ARRAY PROGRAM

```

10  1 ANTENNA BEAM PATTERN FOR AN N ELEMENT LINEAR ARRAY
20  GCLEAR
30  Ri=.0381
40  Fr=5000
50  Ka=(Ri*2*PI*Fr)/343
60  INPUT "ENTER THE # OF DRIVERS ",N
70  D=.0762
80  Kd=(2*PI*D*Fr)/343
90  Kd2=Kd/2.
100 Num_decades=4
110 Scale=10^Num_decades
120 Thetastep=.001
130 GCLEAR
140 VIEWPORT 20,80,20,80
150 WINDOW -20,105,-2,110
160 AXES 100/(2*Num_decades),100/(2.*Num_decades),0,0,20,20
170 MOVE 10,103
180 LABEL "PATTERN FOR ";N;" ELEMENTS"
190 CSIZE 3
200 FOR I=1 TO 5
210     MOVE -15,(25*(I-1))-1
220     M=(10-((6-I)*10))
230     LABEL M
240 NEXT I
250 LDIR PI/2
260 MOVE -15,40
270 LABEL "DECIBELS"
280 LDIR 0
290 FOR Theta=Thetastep TO PI/2 STEP Thetastep
300     Arg=Ka*SIN(Theta)
310     Arg2=2*FNJ1(Arg)
320     Arg2=Arg2/Arg
330     Kds=Kd2*SIN(Theta)
340     Htheta=SIN(Kds*N)/(N*SIN(Kds))
350     Htheta=Htheta*Arg2
360     Htheta=Scale*Htheta*Htheta
370     Htheta=LGT(Htheta)/Num_decades
380     X=Htheta*SIN(Theta)
390     Y=Htheta*COS(Theta)
400     PLOT X*100,Y*100
410     !PRINT Theta,Htheta
420 NEXT Theta
430 END
440 I

```

```

450 DEF FNJ1(X)
460 ! J1 BESSEL FUNCTION 10 MAY,1984; DLW
470 IF X>3. THEN GOTO Xgt3
480 X3=X/3.
490 X3=X3*X3
500 Fx=.5+X3*(-.56249985+X3*(.21093573+X3*(-.03954289+X3*
(.00443319+X3*(-.00031761+X3*.00001109))))))
510 J1=Fx*X
520 RETURN J1
530 Xgt3: X3=3./X
540 Fx=.79788456+X3*(.00000156+X3*(.01659667+X3*(.00017105+X3*
(-.00249511+X3*(.00113653-X3*.00020033))))))
550 Tx=X-2.35619449+X3*(.12499612+X3*(.0000565+X3*(-.00637879+
X3*(.00074348+X3*(.00079824-X3*.00029166))))))
560 J1=Fx*COS(Tx)/SQR(X)
570 RETURN J1
580 FNEND

```

APPENDIX B

LCDR BUTLER'S BEAM PATTERN PROGRAM

```

10 PRINT "** BEAM PATTERN COMPUTATION AND PLOT PROGRAM **"
20 PRINT "*****"
30 !
40 !
50 PRINT "***** SET_UP *****"
60 !
70 !
80 PRINT CHR$(10)
90 PRINT "THIS PROGRAM CONTROLS THE FOLLOWING APPARATUS"
100 PRINT "TO MEASURE, DISPLAY, PLOT AND STORE THE"
110 PRINT "DIRECTIONAL CHARACTERISTICS OF A SINGLET,"
120 PRINT "DOUBLET, TRIPLET, AND QUADRUPLLET ARRAY."
130 !
140 PRINT " INSTRUMENT                ADDRESS "
150 PRINT " "
160 PRINT " HP_3478 MULTIMETER (VOLTS)      724    "
170 PRINT " HP_3478 MULTIMETER (RES)         723    "
180 PRINT " DATA AQUISITION/CONTROL        709    "
190 !
200 DISP "INITIALIZE INSTRUMENTS"
210 !
220 REM *** PRESET AND INITIALIZE INSTRUMENTS ***
230 OUTPUT 709 ;"RS" ! RESET
240 OUTPUT 723 ;"F3R5T1" ! FREE RUN 30KOHMS
250 OUTPUT 724 ;"F2RAT1" ! FREE RUN AUTORANGE AC VOLT
260 !
270 DISP "INITIALIZE PROGRAM"
280 !
290 OPTION BASE 1
300 COM ANGLE(150),CALC_ANGLE(150),NAME$(10)
310 DEG
320 PRINTER IS 701
330 INTEGER I,C,L,N
340 DIM R(360),VOLT(360),OHMS(DATA(360)),C(10),L(10),N(10)
350 MVOLT=0
360 MASS STORAGE IS ".DATA1"
370 DISP "NUMBER OF DATA POINTS DESIRED"
380 BEEP 10,300
390 INPUT N
400 DISP "ENTER DISC DATA FILE NAME"
410 INPUT NAME$
420 DISP "WANT NEW DATA (Y/N)?"

```

```

430 BEEP 10.300
440 INPUT QS
450 IF QS="Y" THEN GOTO 480
460 IF QS="N" THEN GOTO 920
470 GOTO 430
480 REM *** DEFAULT PARAMETERS ***
490 !
500 ! MUST INSERT FOR LINES 390, 400, 410 AND 810
510 ! PRIOR TO START OF RUN
520 !
530 CREATE NAMES$.360.16
540 ASSIGN# 1 TO NAMES$
550 NAMES$="RUN 1"
560 FULLSCALE=500 ! LOCK IN MVA
570 CONV=360/10000 ! CONVERT OHMS TO DEGREES
580 SET UP: ! *** SET UP MEASUREMENT PARAMETERS ***
590 PRINT "HRS (10)"
600 PRINT " ".GRAPH TITLE:";NAMES$
610 REM *** MODIFY IN PRECEDING LINE WHEN NECESSARY ***
620 DISP "MANUALLY ENTER DESIRED FREQ FOR SPEAKER DRIVER"
630 DISP "ENTER 0 IF NO CHANGE"
640 DISP "ENTER 1 TO CHANGE TITLE"
650 BEEP 10.500
660 INPUT " ".CHG:
670 IF CHG THEN GOTO 640
680 IF CHG THEN GOTO 630
690 PRINT "HRS (10)"
700 GOTO 430
710 REM ***
720 REM ***
730 REM ***
740 REM ***
750 REM ***
760 REM ***
770 REM ***
780 REM ***
790 REM ***
800 REM ***
810 REM ***
820 REM ***
830 REM ***
840 REM ***
850 REM ***
860 REM ***
870 REM ***
880 REM ***
890 REM ***
900 REM ***
910 REM ***
920 REM ***

```



```

910 END
920 DISP "WHAT IS DATA RUN DESIRED?"
930 BEEP 10,500
940 INPUT NAMES$
950 ASSIGN# 1 TO NAMES$
960 FOR I=1 TO N
970 READ# 1 ; OHMS_DATA(I),VOLT(I)
980 NEXT I
990 ASSIGN# 1 TO *
1000 GOTO 860
1010 !
1020 !
1030 PLOT_ROUTINE: ! *** PLOTS POLAR DATA ***
1040 !
1050 !
1060 PLOTTER IS 705
1070 GRAPH
1080 GCLEAR
1090 PEN 1
1100 LIMIT 50,210,20,180
1110 SCALE -60,60,-60,60
1120 XAXIS 0,10,-40,40
1130 YAXIS 0,10,-40,40
1140 CSIZE 3
1150 LINE TYPE 1
1160 FOR L=0 TO 40 STEP 10
1170 MOVE 0,L
1180 CORG 5
1190 LABEL 1,40
1200 NEXT L
1210 LINE TYPE 1
1220 CSIZE 5
1230 MOVE 0,50
1240 !
1250 ! POINTS ARE AT 10 AND 20 PRIOR TO START OF RUN
1260 !
1270 ! POINTS ARE AT 10 AND 20 PRIOR TO START OF RUN
1280 !
1290 ! POINTS ARE AT 10 AND 20 PRIOR TO START OF RUN
1300 !
1310 ! POINTS ARE AT 10 AND 20 PRIOR TO START OF RUN
1320 !
1330 ! POINTS ARE AT 10 AND 20 PRIOR TO START OF RUN
1340 !
1350 ! POINTS ARE AT 10 AND 20 PRIOR TO START OF RUN
1360 !
1370 ! POINTS ARE AT 10 AND 20 PRIOR TO START OF RUN
1380 !
1390 ! POINTS ARE AT 10 AND 20 PRIOR TO START OF RUN
1400 !
1410 ! POINTS ARE AT 10 AND 20 PRIOR TO START OF RUN
1420 !
1430 ! POINTS ARE AT 10 AND 20 PRIOR TO START OF RUN
1440 !
1450 ! POINTS ARE AT 10 AND 20 PRIOR TO START OF RUN
1460 !
1470 ! POINTS ARE AT 10 AND 20 PRIOR TO START OF RUN
1480 !
1490 ! POINTS ARE AT 10 AND 20 PRIOR TO START OF RUN
1500 !

```

```
1370 MOVE L,0
1380 FOR I=0 TO 360 STEP 5
1390 DRAW L*COS (I),L*SIN (I)
1400 NEXT I
1410 NEXT L
1420 LINE TYPE 1
1430 PEN UP
1440 PEN 2
1450 FOR I=1 TO N ! BEGINS BEAM PATTERN COMPUTATION
1460 IF VOLT(I)>MVOLT THEN MVOLT=VOLT(I)
1470 NEXT I
1480 FOR I=1 TO N
1490 K=OHMS_DATA(I)/10000*360
1500 K1=K
1510 IF OHMS_DATA(I)<10 THEN K=K1+360/295
1520 IF OHMS_DATA(I)>10500 THEN GOTO 1610
1530 VECTOR=20*LGT (VOLT(I)/MVOLT)+40
1540 LINE TYPE 1
1550 IF VECTOR<1 THEN VECTOR=0
1560 PRINT I,K,VECTOR
1570 X(I)=VECTOR*COS (K)
1580 Y(I)=VECTOR*SIN (K)
1590 PLOT X(I),Y(I)
1610 NEXT I
1615 PEN UP
1620 RETURN
```

APPENDIX C

ECHOSOUNDER SOFTWARE

The driving force of this system is found within the HP200 Series Computer. The software and computer system were responsible for controlling and monitoring every operational phase of the hardware components. The program which accomplishes this task was entitled "ACRDR" and is listed in Reference 3. This program was modeled after a program written by Walters [Ref. 20], but each program performs a distinctly different computational task. This program was written in HP Basic 4.0 and was compiled by an Infotek BC203 Basic Compiler to enhance the speed of execution.

The program "ACRDR" is easily broken down into a number of blocks and subroutines which perform specific operations. These sections are outlined in a flowchart (Fig. 46). Each block is straightforward in its purpose and the program is designed to be as helpful to the user as possible. As a prologue to the actual program code, there is a listing of all the program variables with a brief description of their use. Such a listing familiarizes the user with the computations to be made and also provides quick references for any future modifications to be implemented.

The initialization procedures which set all the parameters necessary for data collection follow the variable definition section. These parameters control such things as the contrast between background and return signal and the setting of the computer's internal clock. All options of the HP3314A Function Generator are decided by the user at this phase. Another initialization involves preparing the Infotek AD200 Analog to Digital Converter for operation. Finally, internal arrays are dimensioned, integer variables are defined and the computer function keys are redefined to suit the "ACRDR" program.

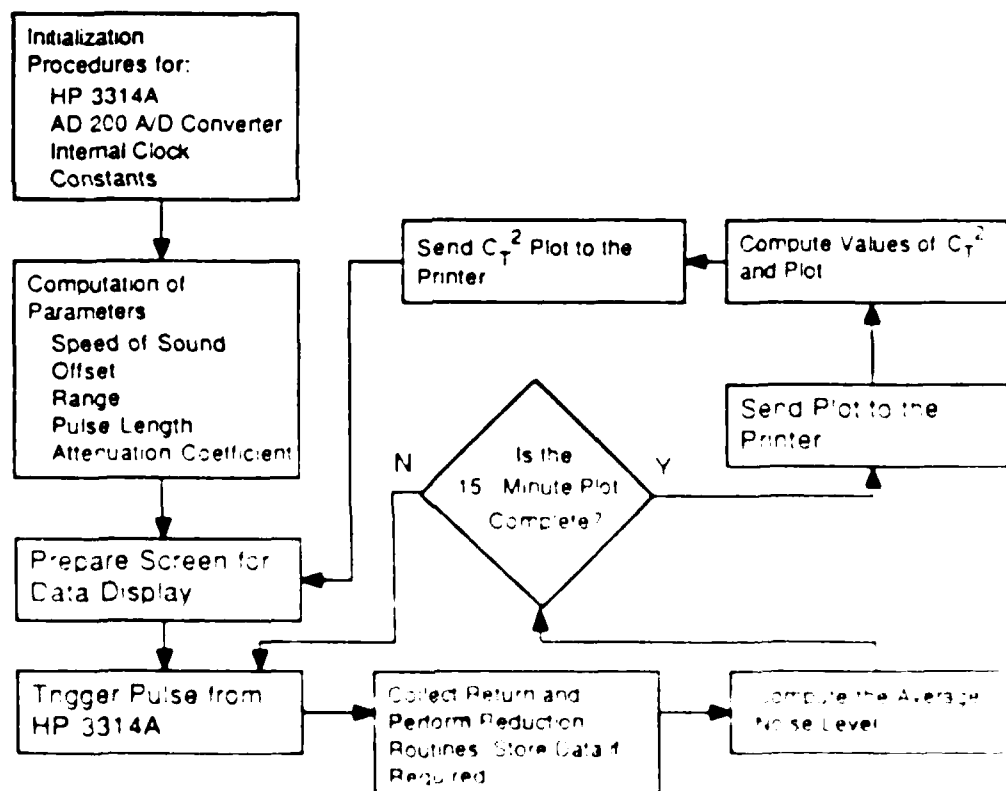


Fig. 4. Flowchart of fundamental program operations.

Now that the system is ready to operate, certain constants must be determined based upon atmospheric conditions at the time of data collection. From the ambient temperature, a speed of sound in air is determined by the equation in Kinsler, et al. (Ref. 14, p. 106).

$$c = c_0 [1 + (T/273)]^{1/2}$$

where

c is the local speed of sound,

c_0 is the speed of sound in air at 0°C Celsius, 331.5 m/s, and

T is the local temperature in degrees Celsius.

For this value and a user defined sampling frequency, the total number of samples, the maximum range of the travel time, and the time resolution are determined.

$$N = \frac{2R}{\Delta t} \cdot \frac{1}{\text{SAMPLING FREQUENCY}} \cdot \frac{1}{2}$$

where

N is the number of samples, R is the maximum range,

Δt is the time resolution, and $\text{SAMPLING FREQUENCY}$ is the sampling frequency.

For this value

the total number of samples, the maximum range,

the time resolution, and the time resolution are determined.

where

the allowed maximum of 16301 data points and the speed of sound can be safely estimated to be 340 m/s at room temperature. By defining a typical sampling frequency of 20000 Hz, a range of approximately 135 meters is obtained.

Another parameter determined is the atmospheric attenuation coefficient. This calculation is done in a subroutine obtained from Reference 21 and is necessary in this program for the calculation of the temperature structure parameter, C_n^2 . Other computations made prior to program execution include the pulse length, wavenumber, and the 10 dB offset of the equipment.

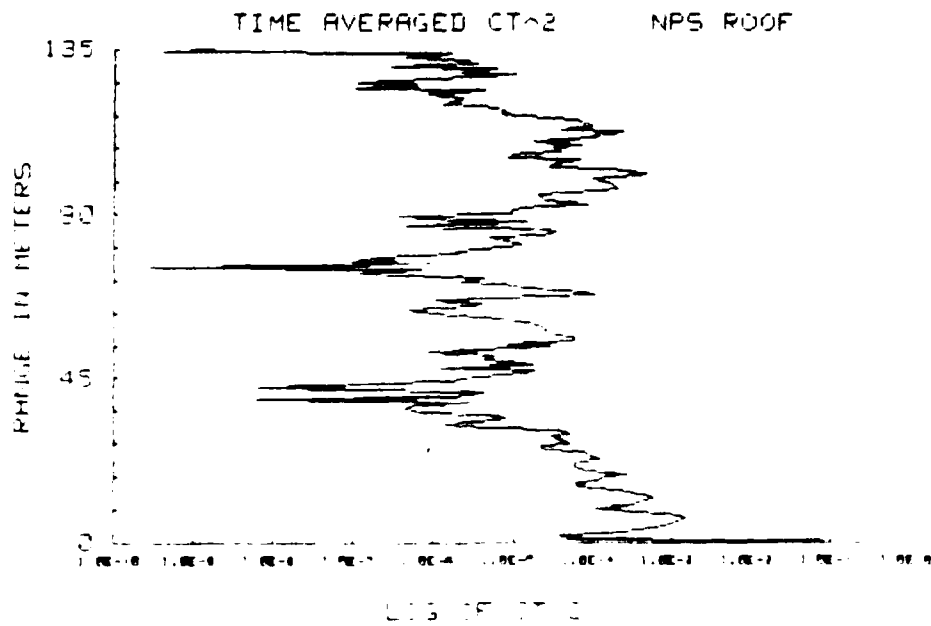
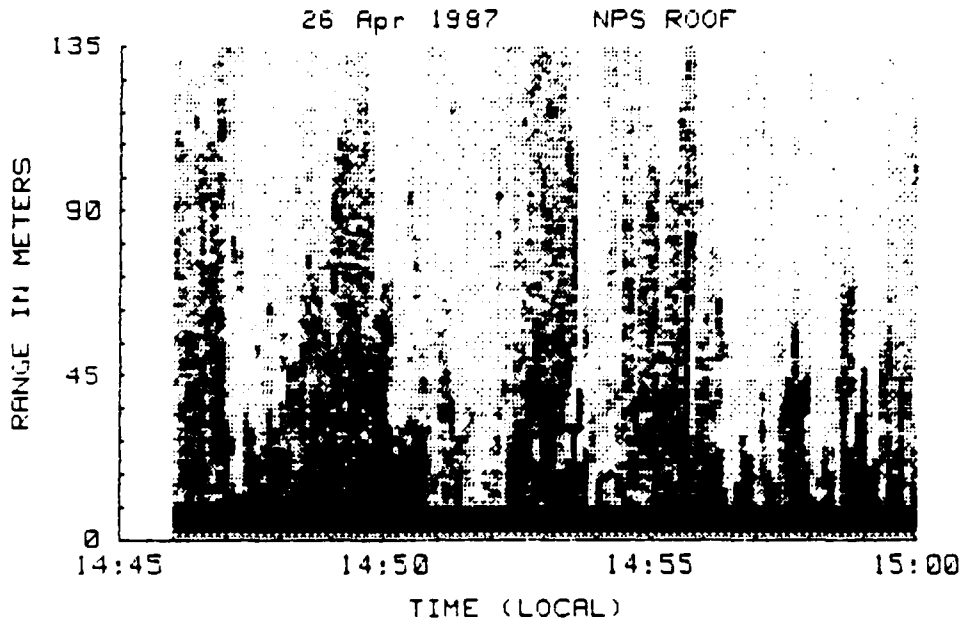
At this point, the computer is finally ready for data collection. The screen setup displays a distance versus time plot and the internal clock of the computer is synchronized with the pulse from the HP 6014A Function Generator. Following transmission of the pulse, the return signal is received, digitized, stored in an array and the data is averaged. A track averaging technique is used to average the data points. The size of the number of averages is determined and changed by keyboard operation. The program then displays the averaged data on the screen. The data is then stored in a file and the program returns to the start of the data collection process. The program is designed to be run on a computer with a minimum of 128K bytes of memory and a hard disk of 10MB. The program is written in Fortran 77 and runs on a VAX/VMS system. The program is available on request from the author.

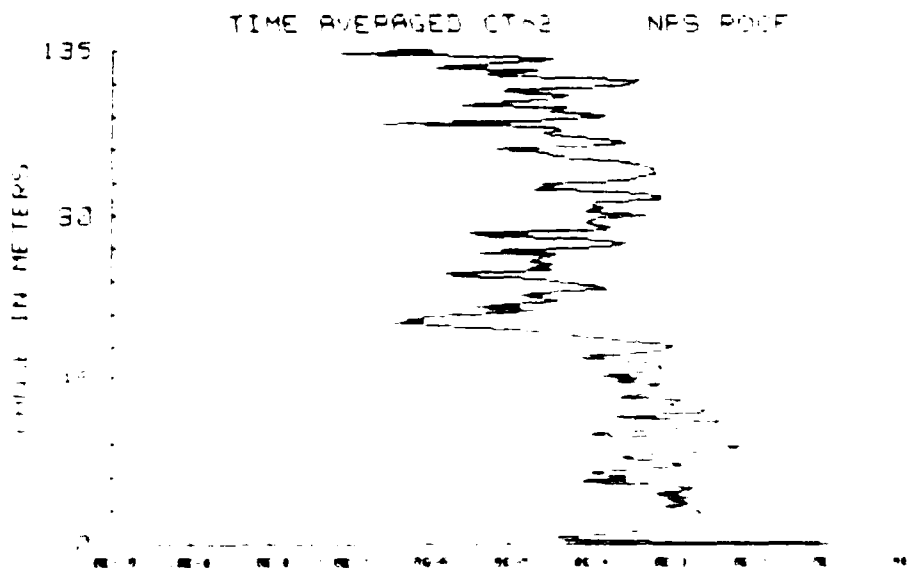
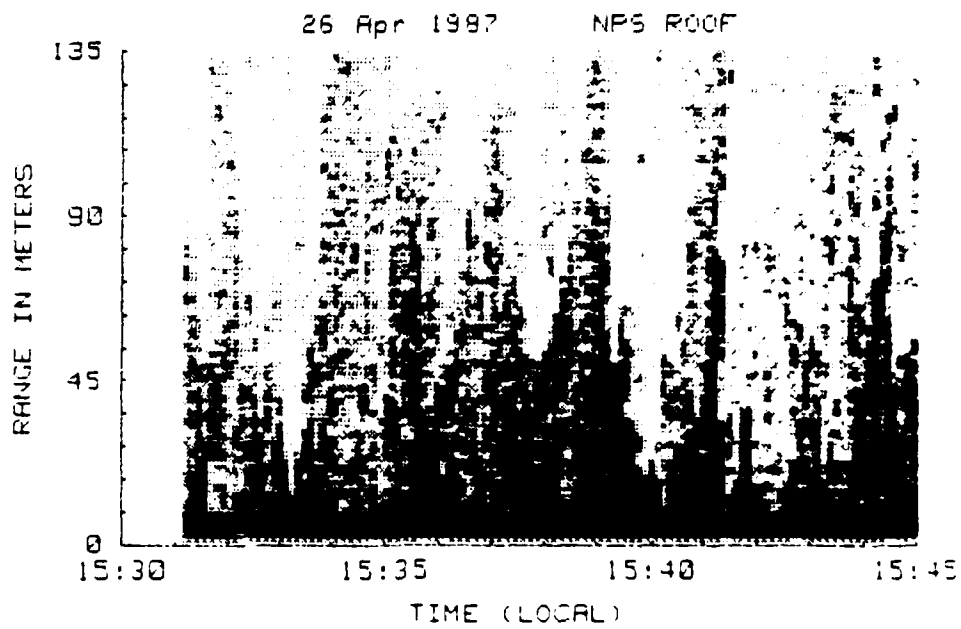
the ratio of power returned to power transmitted, the efficiency of the speakers as transmitters and receivers, the area of the speaker array, the atmospheric attenuation, the pulse length, the temperature, the scattering cross section per unit volume at a specific range and frequency and finally the effective aperture factor of the antenna. Additionally, $C\tau^2$ (Range) is averaged for a particular altitude over 15 minute intervals. Finally, after each pulse is reduced, a corresponding mean square noise level is determined. This is done by averaging each block average at maximum range until at least ten values have been used in the average. An upper limit of five over the average noise level (this corresponds to voltage fluctuations on the order of 100% volts) is set on the routine to avoid averaging any strong return signals or clutter such as passing aircraft. After the ten values are averaged, every subsequent pulse is averaged into the preceding noise level and removed from each subsequent return scan.

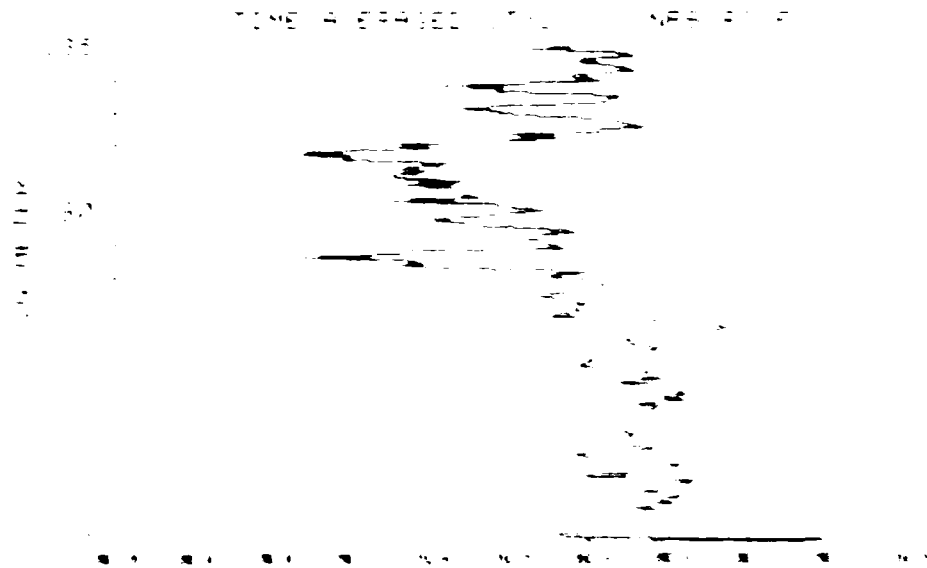
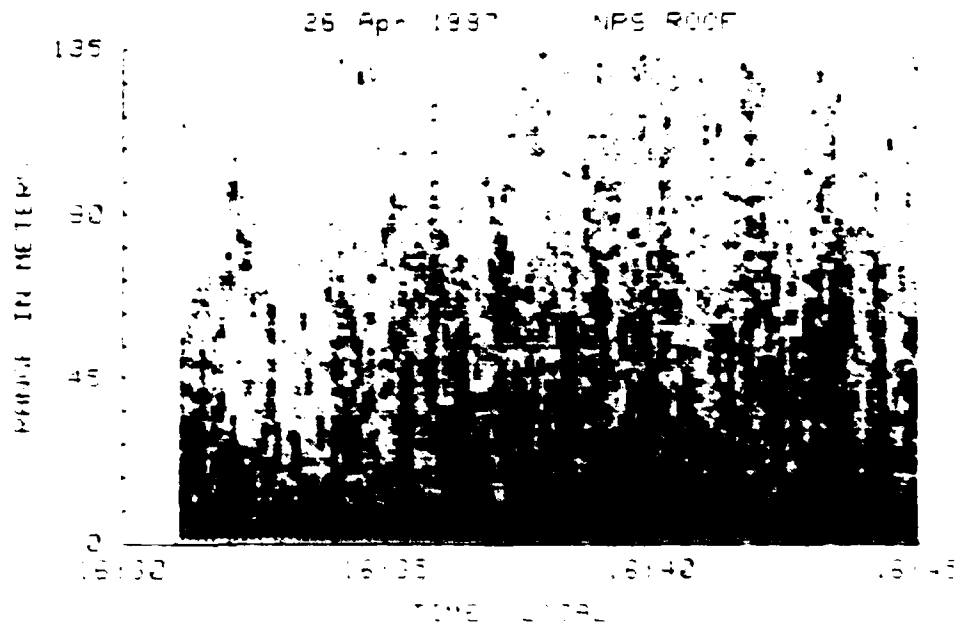
Immediately after each 15 minute interval, a report is generated. The first parameter image is printed out. At the same time the computer will use indicated parameters to determine and print out a range gate. At the end of the interval, the computer will determine the range gate and print out the range gate. The range gate is determined by the computer and printed out. The range gate is determined by the computer and printed out.

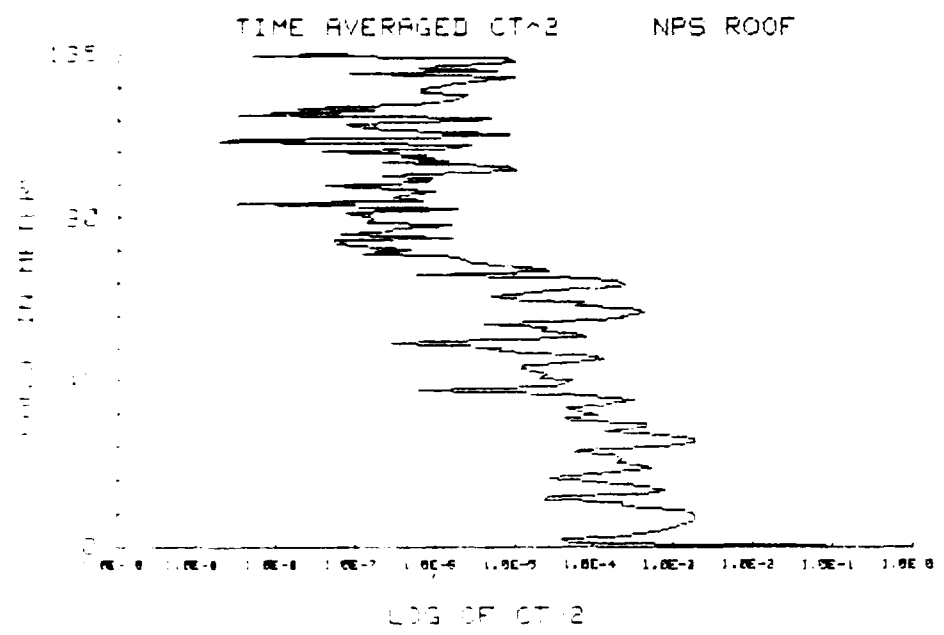
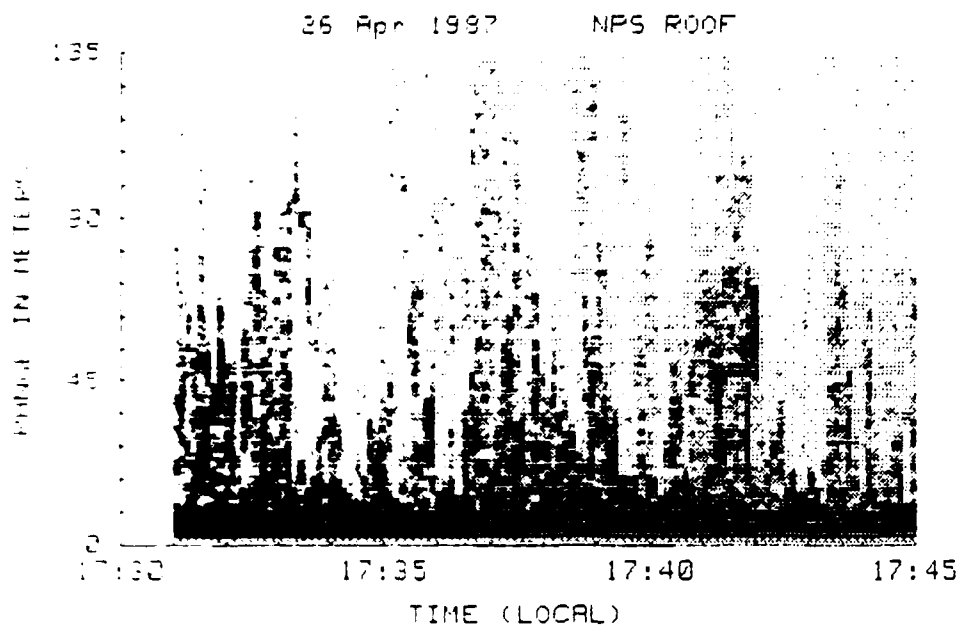
There are certain options built into the program to allow a user to change various aspects of operation. The function keys allow the user to change the local temperature, sample frequency or intensity factor during program execution. Additionally, the user can quit or restart the program, print the partial trace on the screen or elect to save a trace on a floppy disc. The save routine is invoked for the subsequent 15 minute interval after the appropriate function key is depressed. Saving a future trace may be awkward, especially if a user would like to keep an interesting trace which is presently on the terminal. This problem cannot be readily solved unless each trace is recorded to disc without user intervention. At present, this is not done because only eight traces (two hours of data) can be written to a floppy disc before it is full.

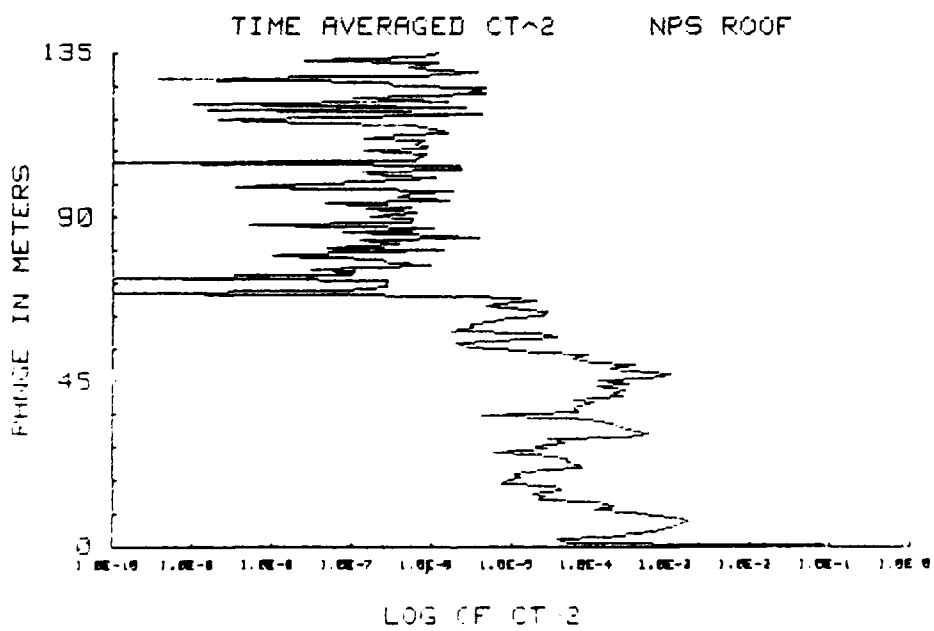
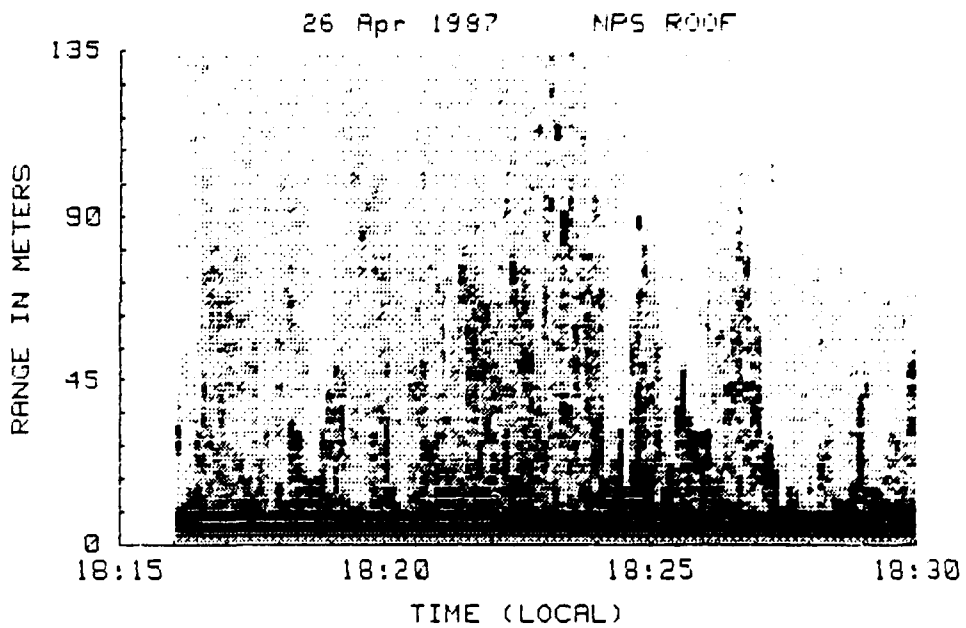
APPENDIX D
ECHOSOUNDER OUTPUT

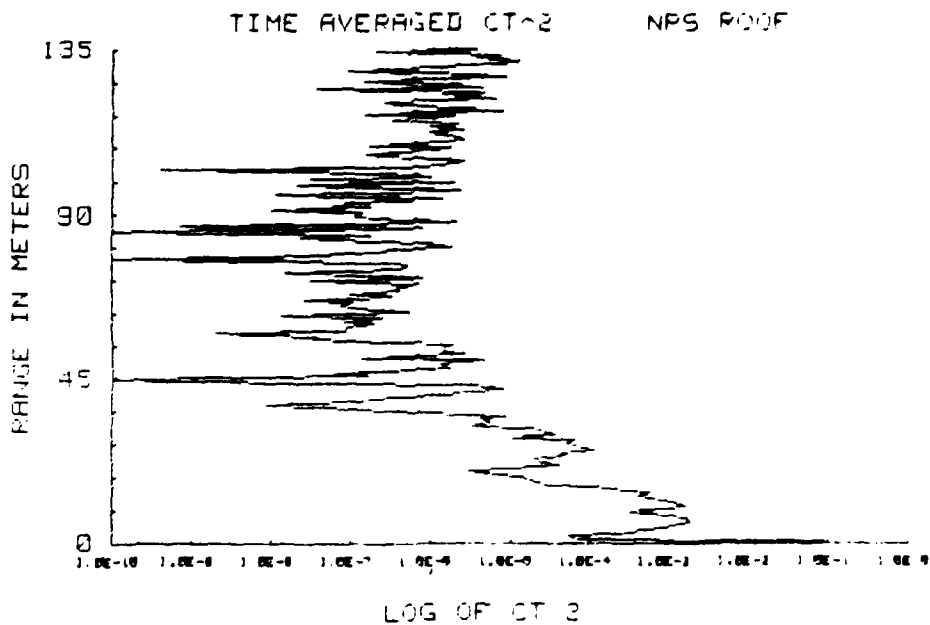
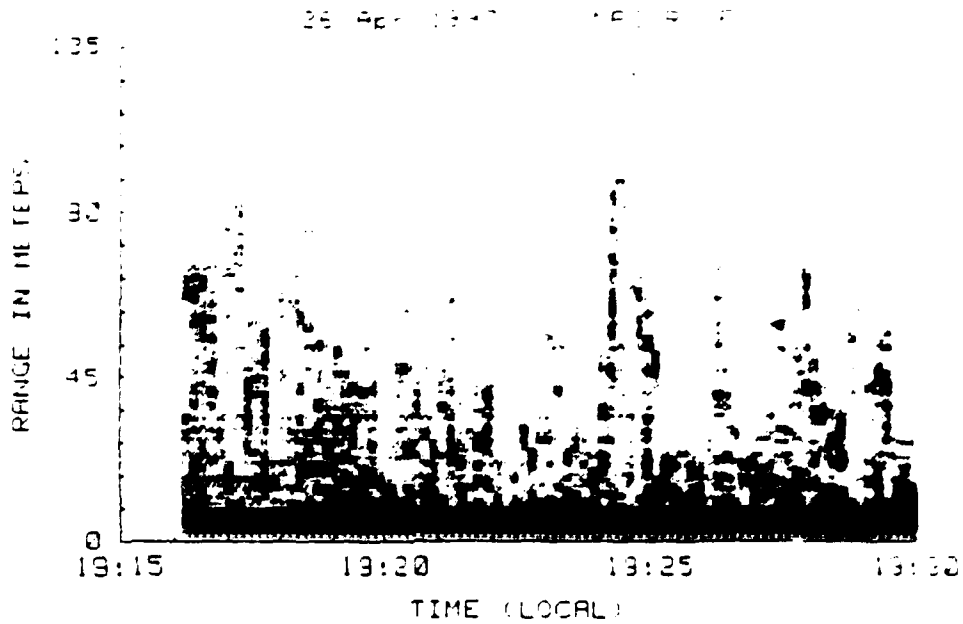


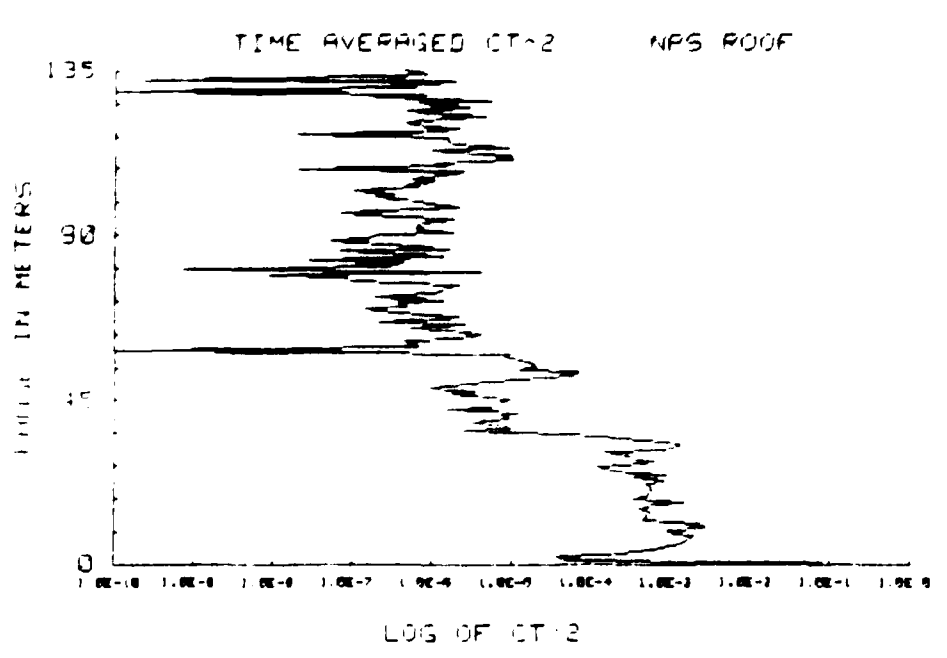
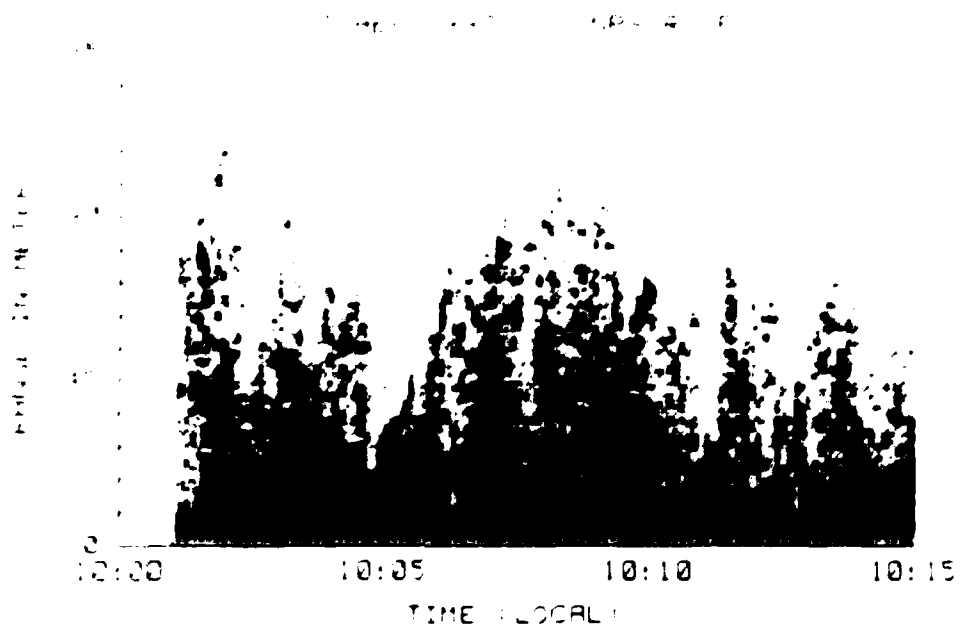


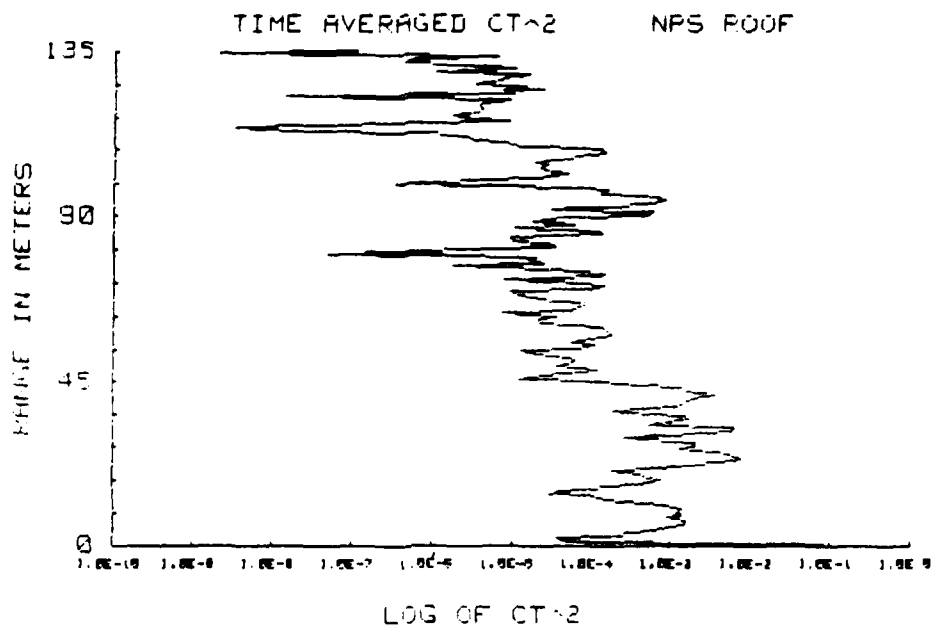
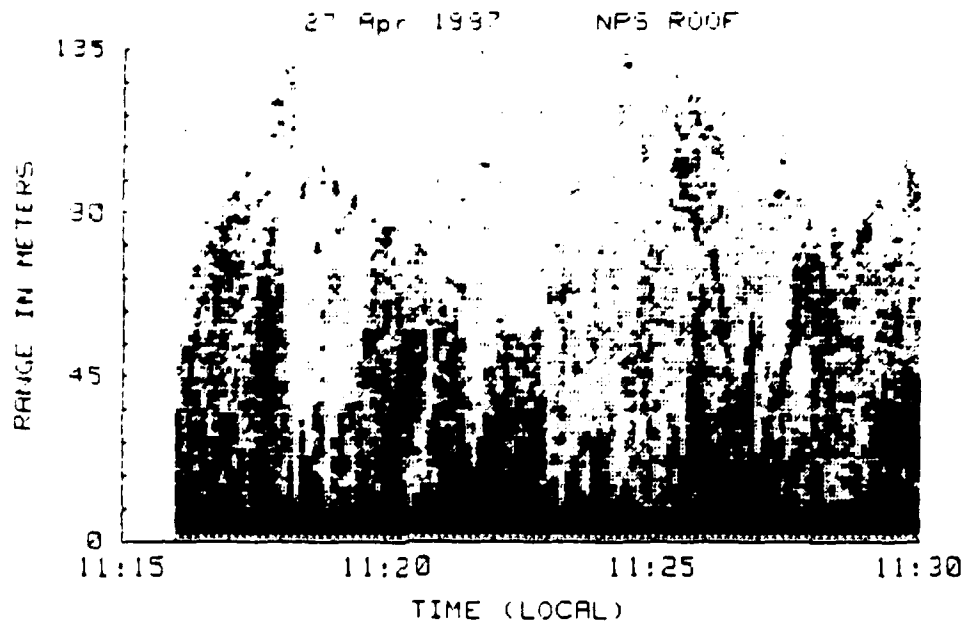


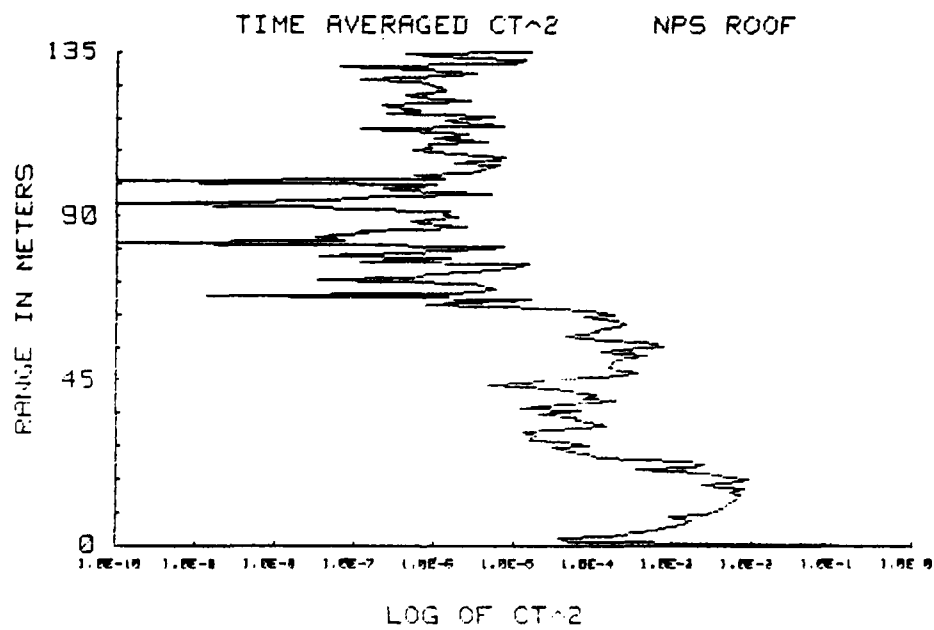
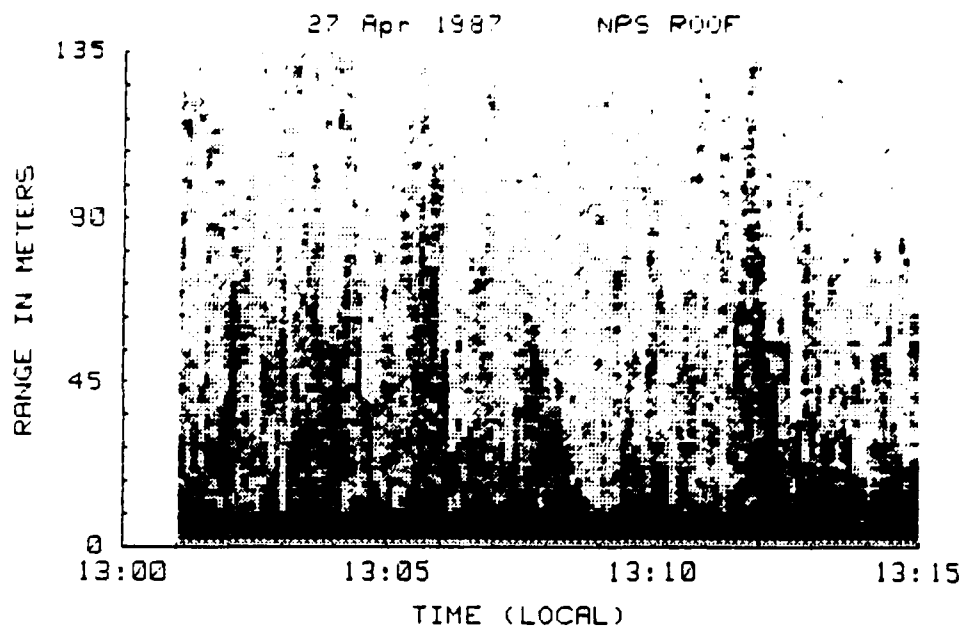


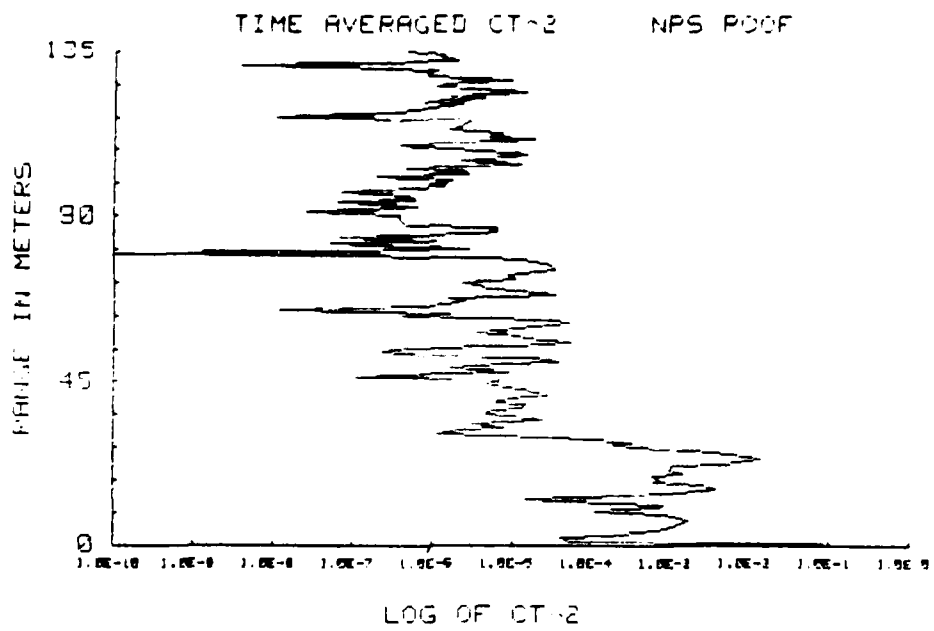
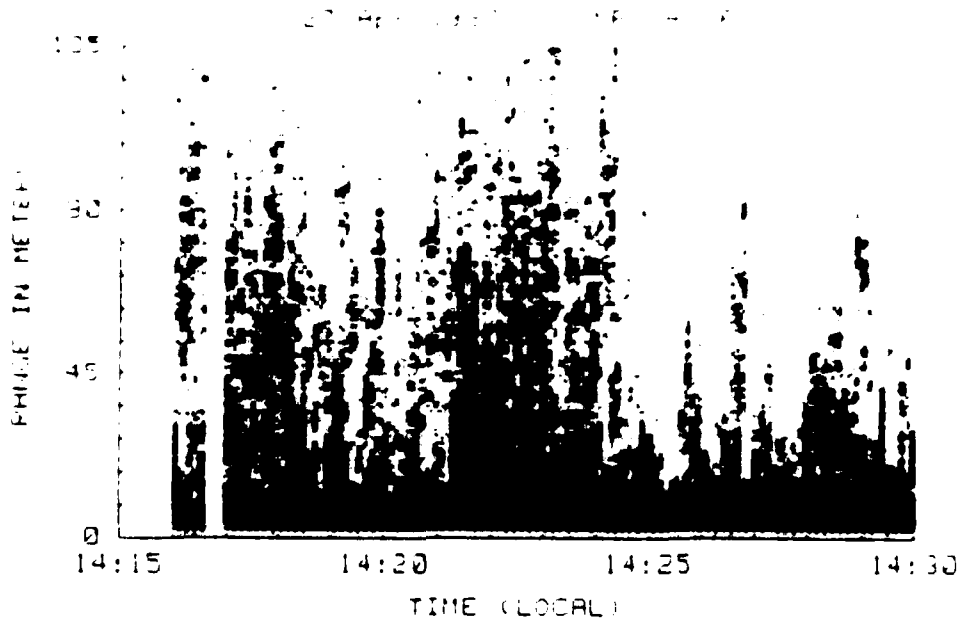


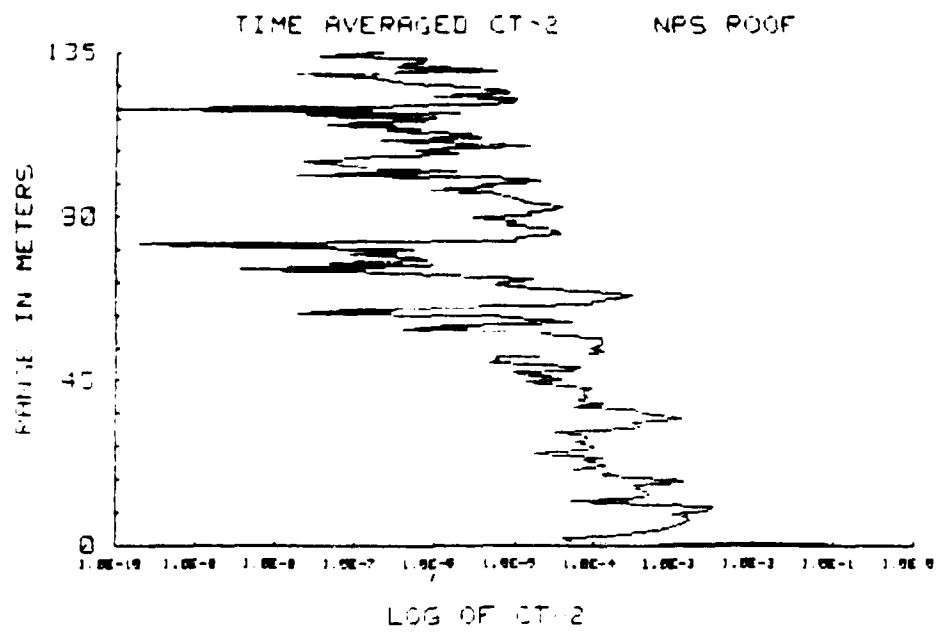
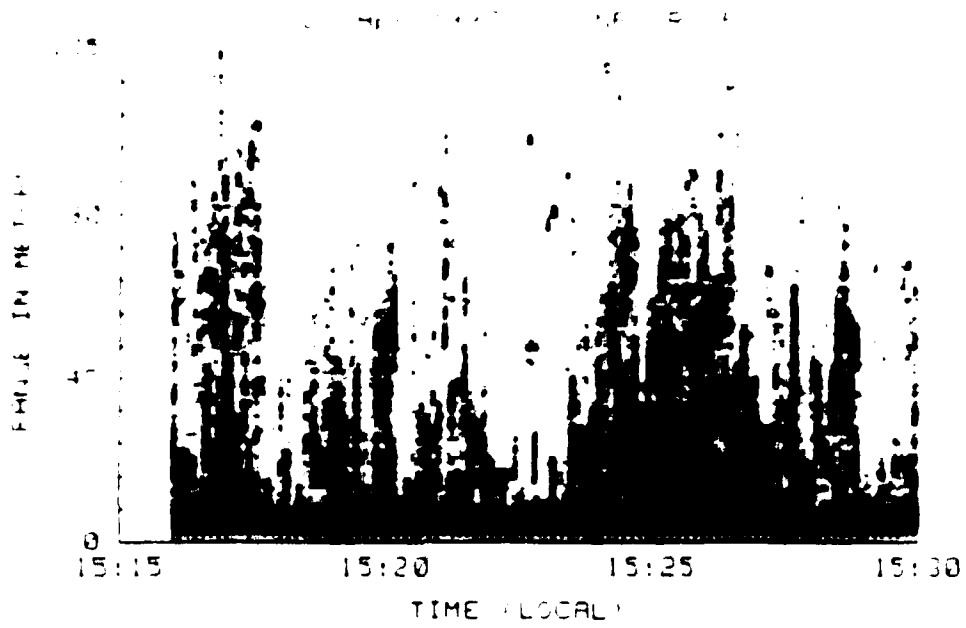


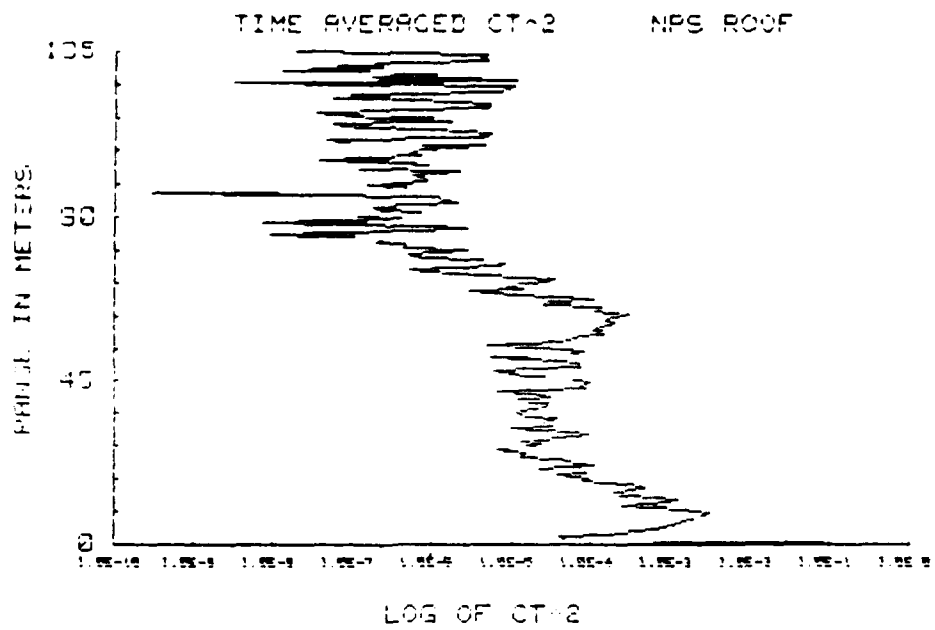
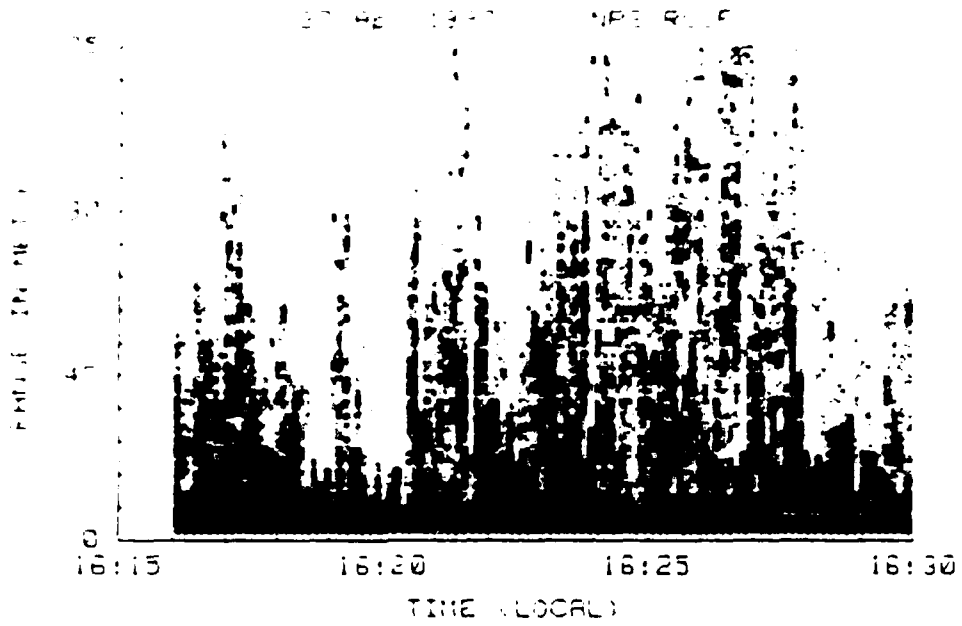


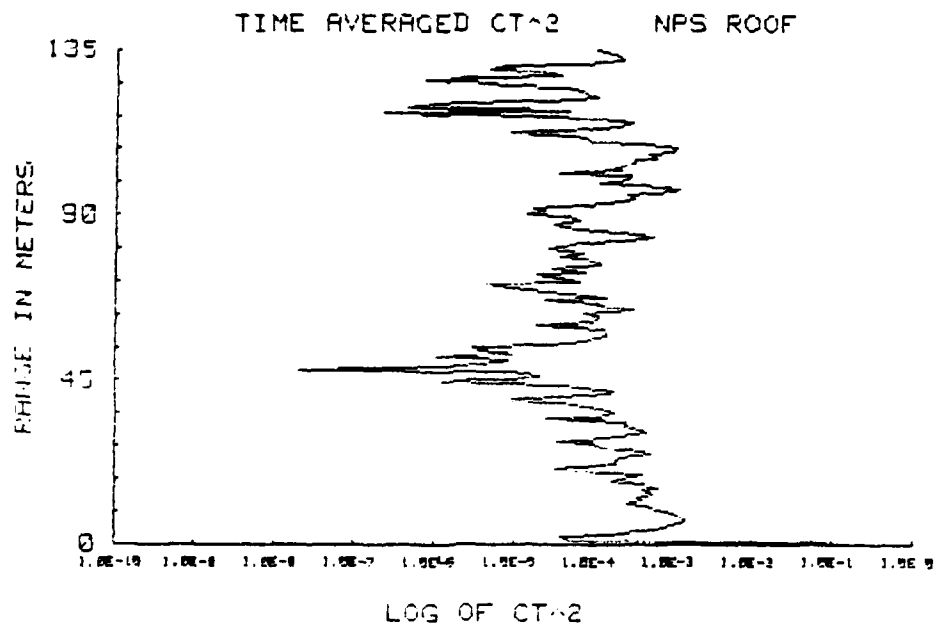
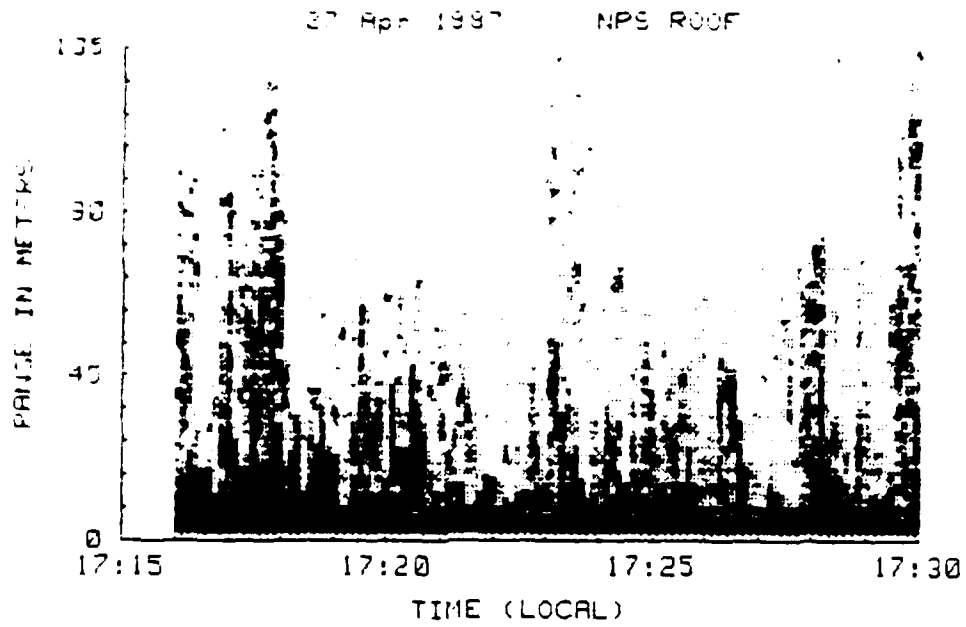


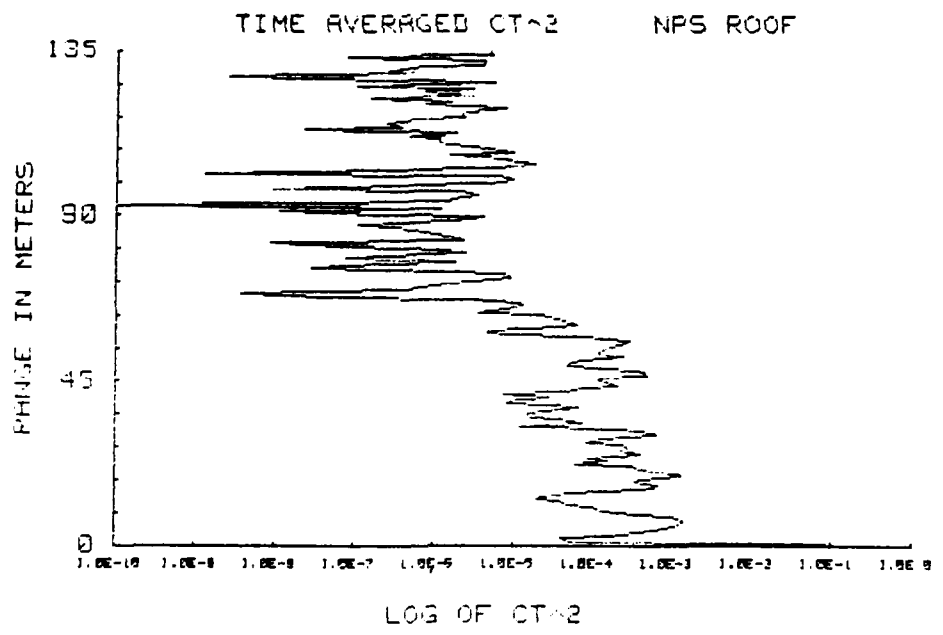
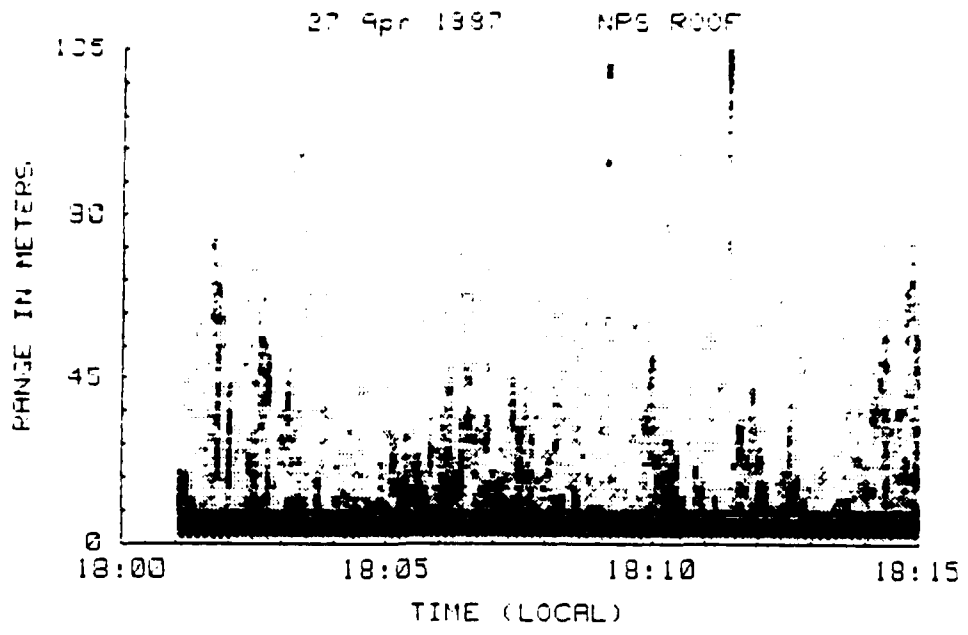


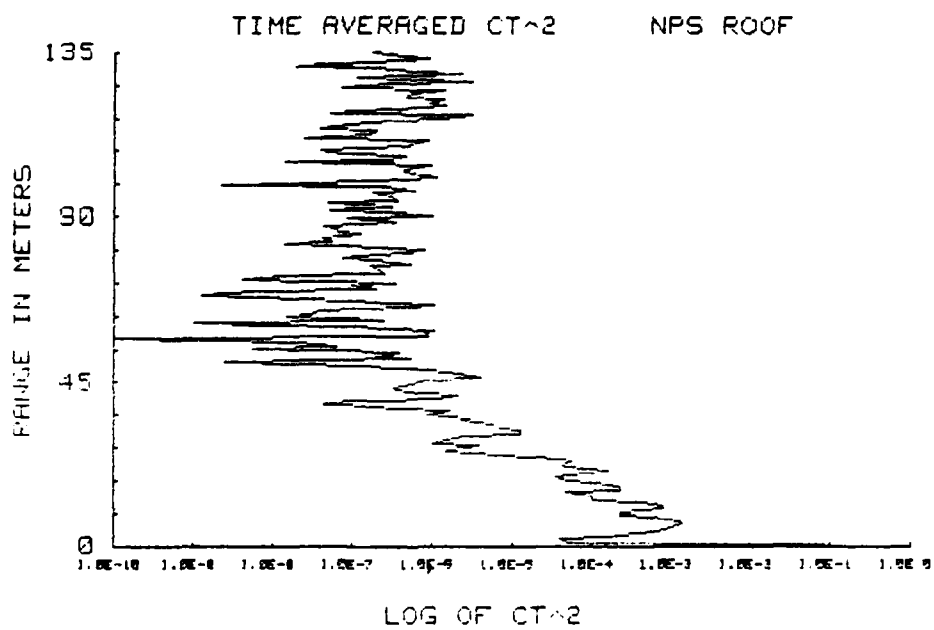
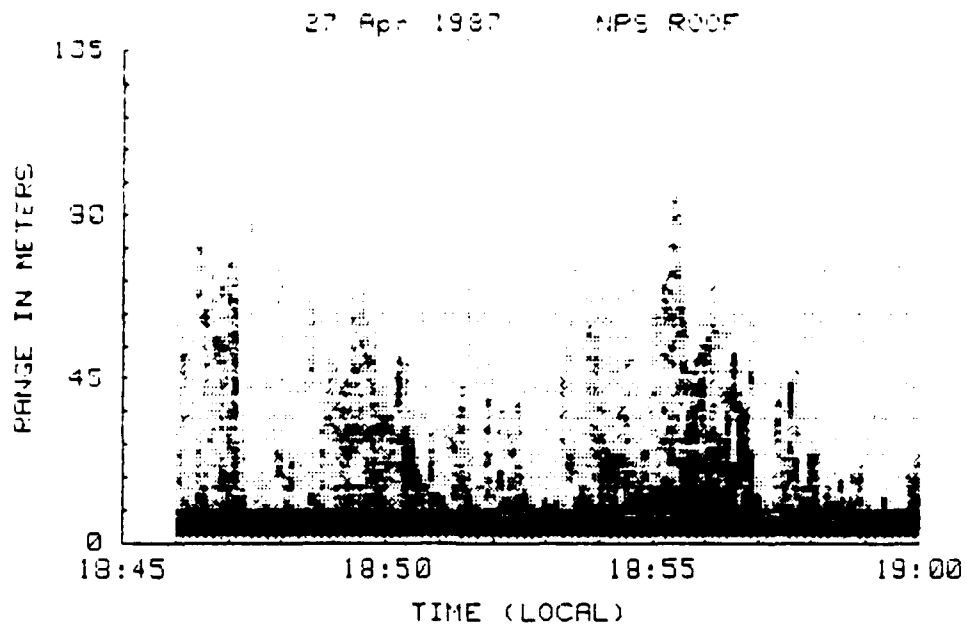


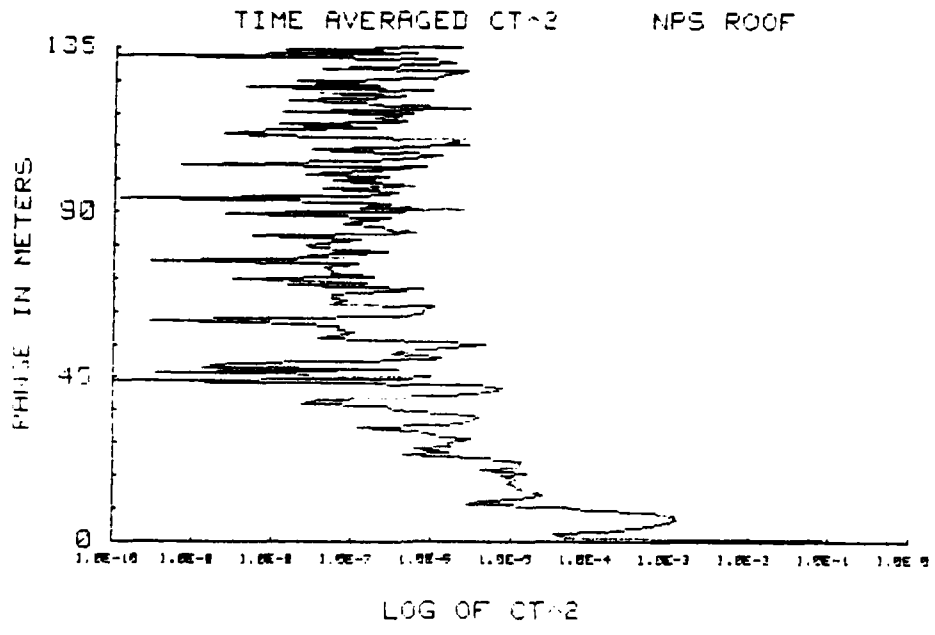
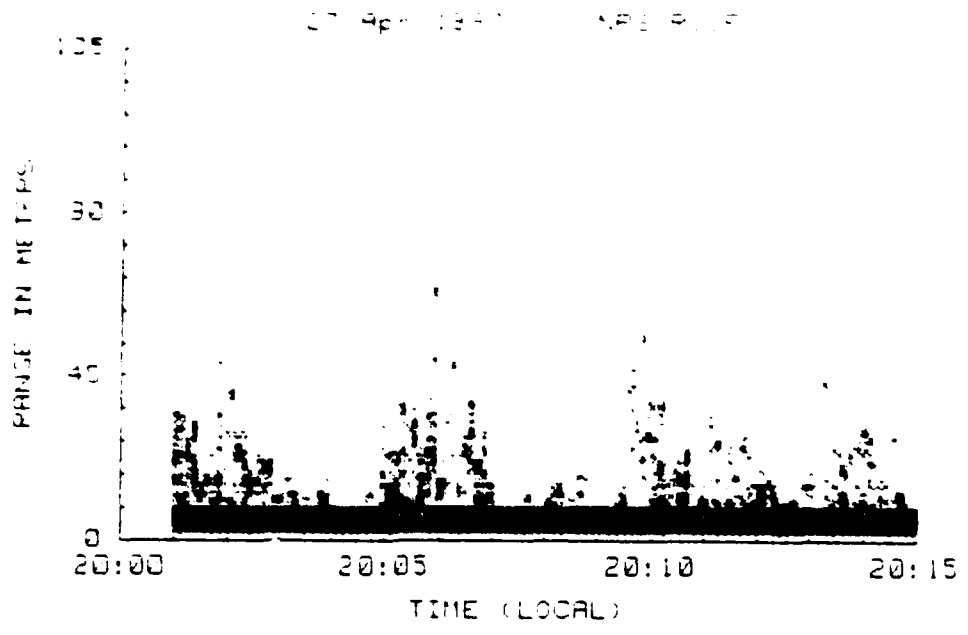












LIST OF REFERENCES

1. Walters, J. L., "Atmospheric Modulation Transfer Functions for Desert and Mountain Conditions for Measurements," Journal of Optical Society of America, Vol. 67, No. 4, pp. 464-49, April 1981.
2. Walters, J. L., "Saturation and the Length-Angle Dependence of Atmospheric Isoplanatic Angle Measurements," paper presented at the SPIE Conference, April 1988.
3. Wroblewski, Michael R., Development of a Data Analysis System for the Detection of Lower Level Atmospheric Turbulence with an Acoustic Sounder, M. S. Thesis, Naval Postgraduate School, Monterey, California, June 1987.
4. McAllister, L. G., "Acoustic Sounding of the Lower Troposphere," Journal of Atmospheric and Terrestrial Physics, Vol. 30, pp. 1439-1440, 1968.
5. Little, C. G., "Acoustic Methods for the Remote Probing of the Lower Atmosphere," Proceedings of the IEEE, Vol. 57, pp. 571-578, 1969.
6. McAllister, L. G., Pollard, J. R., Mahoney, A. R., and Shaw, P. J. R., "Acoustic Sounding - A New Approach to the Study of Atmospheric Structure," Proceedings of the IEEE, Vol. 57, pp. 579-587, 1969.
7. Beran, D. W., Little, C. G., and Willmarth, B. C., "Acoustic Doppler Measurements of Vertical Velocities in the Atmosphere," Nature, Vol. 230, pp. 160-162, 1971.
8. Mousley, T. J., Cole, R. S., Asimakopoulos, D. N., and Caughey, S. J., "Simultaneous Horizontal and Vertical Acoustic Sounding of the Atmospheric Boundary Layer," Boundary Layer Meteorology, Vol. 17, pp. 223-230, May 1979.
9. Asimakopoulos, R. S., Cole, R. S., Caughey, S. J., and Crease, B. A., "A Quantitative Comparison Between Acoustic Sounder Returns and the Direct Measurement of Atmospheric Temperature Fluctuations," Boundary Layer Meteorology, Vol. 10, pp. 137-147, 1976.

10. Neff, W. D., "Quantitative Evaluation of Acoustic Echoes from the Planetary Boundary Layer," NOAA Technical Report ERL 322-WPL 38, June 1975.
11. Tatarski, V. I., The Effects of the Turbulent Atmosphere on Wave Propagation, U. S. Department of Commerce, Washington, D. C., 1971; available from National Technical Information Service, Springfield, VA 22161.
12. Hall Jr., F. F., and Wescott, J. W., "Acoustic Antenna for Atmospheric Echo Sounding," Journal of the Acoustical Society of America, Vol. 56, No. 5, pp. 1376-1382, November 1974.
13. Motorola Piezo Ceramic Speakers Catalog, Motorola Communications Systems Division, p. R29-5-1B, 1971.
14. Kinsler, L. E., Frey, A. R., Coppens, A. F., and Sanders, J. V., Fundamentals of Acoustics, Wiley and Sons, New York, 1982.
15. Strand, O. N., "Numerical Study of the Gain Pattern of a Shielded Acoustic Antenna," Journal of the Acoustical Society of America, Vol. 49, No. 6 (Part 1), pp. 1703-1708, June 1971.
16. Adekola, S. A., "Toward a More General Formulation of the Pressure Field of an Aperture Antenna," Journal of the Acoustical Society of America, Vol. 60, No. 1, pp. 230-234, January 1976.
17. Adekola, S. A., "Concerning the Effect of Carrier Frequencies and Antenna Size on the Performance of Echosounding Antennas," Journal of the Acoustical Society of America, Vol. 60, No. 3, pp. 524-542, September 1976.
18. Adekola, S. A., and Butler, R. W., "Phase-front Distribution and Radiation Pattern of a Planar Aperture Antenna," Journal of the Acoustical Society of America, Vol. 60, No. 1, pp. 12-18, January 1976.
19. Butler, R. W., "Computer Program for the Calculation of Phase and Amplitude Distributions of a Planar Aperture Antenna," Journal of the Acoustical Society of America, Vol. 60, No. 1, pp. 19-24, January 1976.

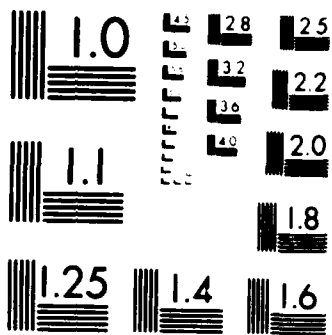
W. D. Neff
 NOAA

AD-A184 877

DEVELOPMENT OF AN ACOUSTIC ECHOSOUNDER FOR DETECTION OF 2/2
LOWER LEVEL ATMOSPHERIC TURBULENCE(U) NAVAL
POSTGRADUATE SCHOOL MONTEREY CA F J WEINGARTNER JUN 87
F/G 4/2 NL

UNCLASSIFIED





MICROCOPY RESOLUTION TEST CHART
NATIONAL BUREAU OF STANDARDS-1963-A

21. Fuller, Robert J., Parametric Analysis of Echosounder Performance, M. S. Thesis, Naval Postgraduate School, Monterey, California, September 1985.

INITIAL DISTRIBUTION LIST

	No. of Copies
1. Defense Technical Information Center Cameron Station Alexandria, VA 22304-6145	2
2. Library, Code 0142 Naval Postgraduate School Monterey, CA 93943-5002	2
3. Prof. Donald L. Walters Department of Physics (Code 61We) Naval Postgraduate School Monterey, CA 93943-5004	5
4. Prof. Steven L. Garrett Department of Physics (Code 61Gt) Naval Postgraduate School Monterey, CA 93943-5004	1
5. Prof. Karlheinz E. Woehler Department of Physics (Code 61Wh) Naval Postgraduate School Monterey, CA 93943-5004	1
6. LT Frank Weingartner 215 Baynard Road Addison, IL 60101	3

END

10-87

DTIC